Petrofacies and Paleotectonic Evolution of Permo-Carboniferous Gondwanan Sequences of the Bengal Basin, Bangladesh

by

Md. Iftekhar Alam

A thesis submitted to the Graduate Faculty of
Auburn University
in partial fulfillment of the
requirements for the Degree of
Master of Science

Auburn, Alabama
December 12, 2011

Keywords: Gondwanaland, Petrofacies, Paleotectonic,
Permo-Carboniferous, Bangladesh

Approved by

Ashraf Uddin, Chair, Professor of Geology
Charles E. Savrda, Professor of Geology
David T. King, Jr., Professor of Geology
Willis E. Hames, Professor of Geology

Abstract

The Indian subcontinent, along with Australia and Antarctica, constituted Eastern Gondwananland. Permo-Carboniferous Gondwanan sequences have been reported from several isolated basins of the Peninsular India. These siliciclastic sequences were drilled in intra-cratonic basins in northwest Bengal Basin. This ~1-km-thick sequence consists primarily of massive and trough cross-bedded sandstones and laminated mudstones, with localized conglomerate and coal layers.

Sandstone petrography, heavy mineral assemblage studies, heavy mineral geochemistry, and detrital geochronology were used in this study to decipher provenance history of Gondwanan sediments at two localities (Khalashpir and Barapukuria) from the Bengal Basin of Bangladesh.

Petrographic studies suggest that these sequences are mostly immature and poorly sorted arkosic sandstones (Khalashpir-$Qt_{58}F_{30}L_{12}$, Barapukuria-$Qt_{52}F_{31}L_{17}$), with some compositions ranging from quartzarenite to litharenite. Although monocrystalline quartz is dominant, considerable polycrystalline quartz fragments have also been found. K-feldspars dominate over plagioclase feldspars. Among lithic fragments, sedimentary types are abundant. Significant amounts of chert are observed.

Heavy minerals are volumetrically rare and of low diversity in sediments of northwest Bangladesh. However, samples from Khalashpir have higher heavy mineral concentrations than

those from Barapukuria. Garnet geochemistry suggests a metamorphic grade in the source terranes containing amphibolite and granulite facies rocks. Tourmaline chemistry suggests that the sediments were derived from aluminous and Ca-poor metapelites, metapsammites, and quartz tourmaline rocks for Khalashpir and well DOB 2 of Barapukuria. However, tourmaline samples from well DOB 4 of Barapukuria suggest Li-poor granitoid, pegmatite and aplitic sources.

Laser $^{40}Ar/^{39}Ar$ ages were determined for single crystals of detrital muscovite from Gondwanan sequences. Three samples were analyzed from Khalashpir well GDH 46 at different stratigraphic levels. The deepest sample yielded the broadest age range, with a dominant mode at circa 515 Ma and lesser clusters of ages at circa 550, 570, and 600 Ma. The other two shallower samples are dominated by ages with similar single modes at circa 495-500 Ma. The oldest samples may have been derived from the adjacent Indian craton and/or the Meghalayan craton. Younger samples were contributed from the Pinjarra orogen and proto-Himalayan orogens formed during Neoproterozoic to Early Paleozoic collision between India and Australia.

Acknowledgments

It is my pleasure to thank all those who assisted directly and indirectly with my thesis. It was a really enjoyable experience to work with Dr. Ashraf Uddin, my thesis advisor. I appreciate all his help and support that he provided to me for last two years. Also, I would like thank him for his confidence in me when he accepted me as one of his graduate students. I have matured as a student and a researcher under his supervision.

I would also like to express my heartfelt thanks to Dr. Charles E. Savrda, David T. King, Jr., and Willis E. Hames for their contributions to this research as my thesis committee members. My knowledge in sedimentary petrography improved significantly because of training from Dr. Savrda. I am grateful to Dr. King, for giving me a better handle on stratigraphy. Dr. Hames helped me understand many aspects of detrital geochronology. Dr. Savrda also did important editing that improved this thesis.

I want to thank Mr. Chris Fleisher of University of Georgia for his help with microprobe analysis. I would like to acknowledge Dr. Afia Akhter, former Director General of the Geological Survey of Bangladesh (GSB), for help in getting core samples. I am also thankful to the Chairman of Petrobangla for allowing me to obtain samples from the Barapukuria Coal Mine. I am grateful to Professor Fazlul Huq of the University of Dhaka for sharing information from his research on Gondwanan samples from northwest Bengal basin. Help from Md. Ashraful Islam, Assistant Director of GSB, also is much appreciated. I am thankful to the Managing

Director, and Mr. Badrul Alam of Barapukuria Coal Mine, Dinajpur, Bangladesh for help with samples.

Auburn University, the U.S. National Science Foundation, and the Geological Society of America provided financial assistance without which this research would not have been possible. I would also like to thank my friends and colleagues, Suraj Kumar Bajgain, Sonnet Wilson Gomes, and former Auburn graduates Raju Prasad Sitaula and Subhadip Mandal for their valuable suggestions.

I am also grateful to Ms. Eva Lilly and Ms. Sheila Arington for their support with administrative work, and to John Simms for his help related to computers, especially with printing. I thank Dr. Zeki Billor for his guidance in carrying out magnetic separation of heavy minerals and muscovite separation.

Finally, I would like to thank my parents, without whom nothing would have been possible for me, and my siblings for all their support and encouragement.

Table of Contents

List of Tables

List of Figures

List of Abbreviations

ZTR	Zircon, Tourmaline, Rutile
ANIMAL	Auburn Noble Isotope Mass Analysis Laboratory
EMP	Electron Microprobe
BSE	Back Scattered Electron

CHAPTER 1: INTRODUCTION

1.1 THE SOUTHERN SUPERCONTINENT-GONDWANALAND

Gondwanaland is defined as the southern supercontinent that existed from 550 Ma to 167 Ma. Medlicott (1873) first assigned the name Gondwanan to a suite of rocks he studied in the Satpura Basin in Madhya Pradesh, India named after the kingdom of the 'Gonds,' a pre-Aryan local tribe. In 1876, Feistmantel used this name in a paper describing fossils found in this succession of continental deposits. The term 'Gondwanaland' was first used by Suess (1885) to define a southern supercontinent comprising South America, South Africa, India, Australia, and Antarctica during the late Carboniferous to Jurassic (550 Ma to 167 Ma) and characterized by *Glossopteris* flora and coal-bearing formations.

The Indian subcontinent, along with Australia and Antarctica, constituted Eastern Gondwanaland. The South American and African continents comprised the primary components of Western Gondwanaland (Fig. 1.1). Presence of Permo-Carboniferous Gondwanan rocks have been reported from a number of isolated basins in Peninsular India (Fig. 1.2). Comparable sequences also have been found in northern India across the Indo-Gangetic plain in the western (Afganistan, Pakistan, India, etc) and eastern Himalayas (Nepal, Sikkim, Bhutan, Assam, India, etc.). These sequences are known as extra-peninsular Gondwanan sequences and are intensely folded, compressed and in many cases metamorphosed. In contrast, those in Peninsular India and Bangladesh are relatively undisturbed. The Gondwanan sequences of Bangladesh are located in several isolated basins in the northwestern Indian Platform part of Bangladesh. Unlike India and

Nepal, Gondwanan sequences of Bangladesh are not exposed. These sequences were identified from cores drilled primarily to study cyclothemic Gondwanan coal beds.

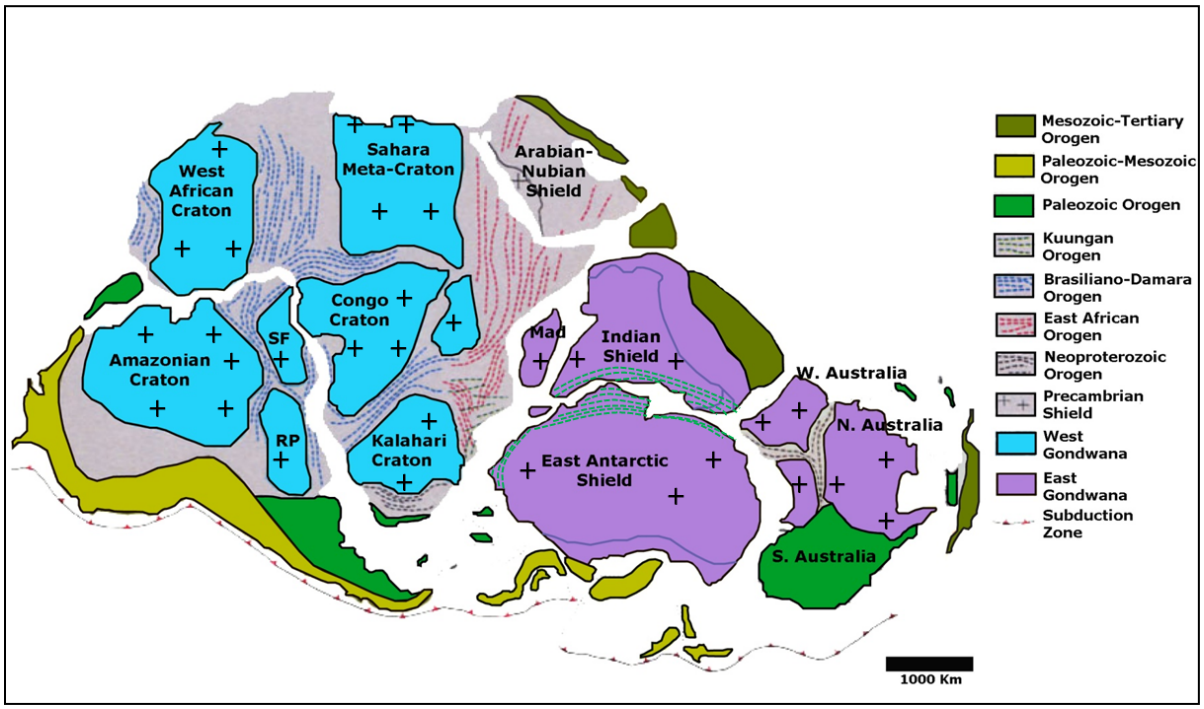

Figure 1.1 Configuration of continental masses in Gondwanaland. Mad=Madagaskar, RP= Rio La Plata, SF= Sao Francisco (after Gray et al., 2008).

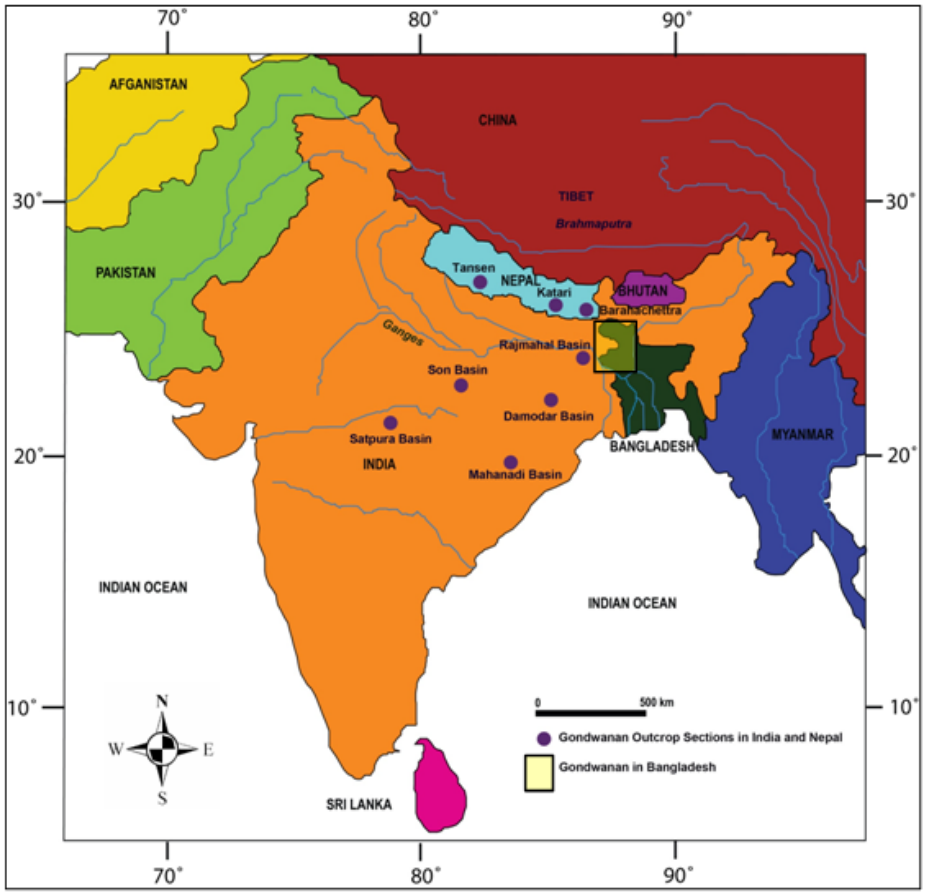

Figure 1.2 Location map of Gondwanan deposits of India, Nepal (purple dots) and northwest Bangladesh (shaded rectangle) (modified after Sitaula, 2009).

Sediment compositional studies help to reveal sediment source(s). This includes the major idea of petrofacies studies (Dickinson and Suczek, 1979). Interpretations can be made on paleogeography, paleoclimate, ancient plate tectonic settings (Graham et al., 1976; Dickinson and Suczek, 1979; Sitaula, 2009), and uplift and exhumation histories (Graham et al., 1976; Rahman, 2008) from detrital composition. In some cases, sedimentary rocks are the only source of information on deeply denuded source terranes. While the relationships between source terranes and detrital sediments and sedimentary rocks has been well demonstrated (Dickinson,

1970; Dickinson and Suczek, 1979), compositional data also requires consideration of other controlling factors such as transport distance, time, energy and climate (Suttner, 1974; Johnsson, 1993) for provenance interpretation.

Studies of sandstone composition have been a very powerful tool to evaluate provenance (Dickinson and Suczek, 1979). The Gazzi-Dickinson point-counting method (Dickinson, 1970) minimizes the control of grain size on sandstone composition. Information about source areas and associated tectonic settings can be obtained from the proportions of detrital framework grains within sandstone samples as plotted on various ternary plots (e.g., QtFL, QmFLt, etc.) (Ingersoll et al., 1995). Various factors other than source rock, such as modes of transportation, depositional environments, climate, and diagenesis (Suttner, 1974), can have significant control on composition of detrital sediments. Provenance studies focusing on detrital mineralogy is an important tool for revealing basin evolution and denudation history of orogenic belts.

Gondwanan sequences of Bangladesh are not as extensively studied as the Gondwanan sediments of Peninsular India. In Nepal, study of Gondwana sequences is still at its early stage. Sitaula (2009) studied petrofacies evolution and detrital geochronology of Gondwana sequences from both eastern and western Nepal and recognized that the provenance history was different for these two areas. Hossain et al. (2002) studied sedimentological aspects of Gondwanan sequences of Bangladesh to decipher their depositional environments. Based on palynological studies, these sequences are correlated to the middle part of the Raniganj Stage of India and the Upper Permian of the Salt Range of Pakistan (Stover, 1964; Islam, 1990). Extensive geological and geophysical investigations in northwestern Bangladesh carried out during the early 1950's revealed a number of prospective sedimentary basins. Subsequently, additional geological and

geophysical studies of these basins were conducted. As a result, many economically significant deposits have been identified in these basins. Gondwanan sequences are well known for coal deposits throughout the Indian subcontinent and also in the other Gondwanan continents. Some of these coal basins are also prospective for coal-bed methane. Besides coal, these sequences contain significant quantities of glass sand. Despite earlier studies, the sediment compositions of Gondwanan sequences from the northwestern Bengal Basin are poorly studied, and detrital ages of sediments therein have not been determined.

1.2 LOCATION OF THE SUDY AREA

The current research is focused on Gondwanan sequences of northwestern Bengal Basin in Bangladesh. Gondwanan sequences of Bangladesh are preserved in several isolated normal fault-bounded graben structures. These siliciclastic deposits were encountered in cores drilled primarily for coal exploration.

Representative core samples were collected from both Kuchma and Paharpur formations from three wells reposited by the Geological Survey of Bangladesh, Barapukuria Coal Mining Project at Dinajpur, and Petrobangla. Samples were collected from wells DOB-04 and DOB-02 at Barapukuria coal mine, and well GDH 58-01 at Khalashpir (Fig. 1.3). The Khalashpir and Barapukuria locations are approximately 50 km apart.

1.3 PREVIOUS WORKS

The Gondwanan sequences of Peninsular India have been well studied by several workers since the beginning of the twentieth century. Wadia (1919) reported basic information about Indian geology, including geology of the Peninsular India. Veevers and Tiwari (1995) modeled the Gondwanan master basin that developed between the Tethys and the Gondwanaland interior. Blakey (2008) and Yoshida et al. (2003) studied the paleogeography of Gondwanaland from its

assembly to breakup. Cawood et al. (2005) also studied the assembly of Gondwanaland, and Archbold (2004) worked on paleobiogeography. Acharyya (2000) worked on the India-Asia

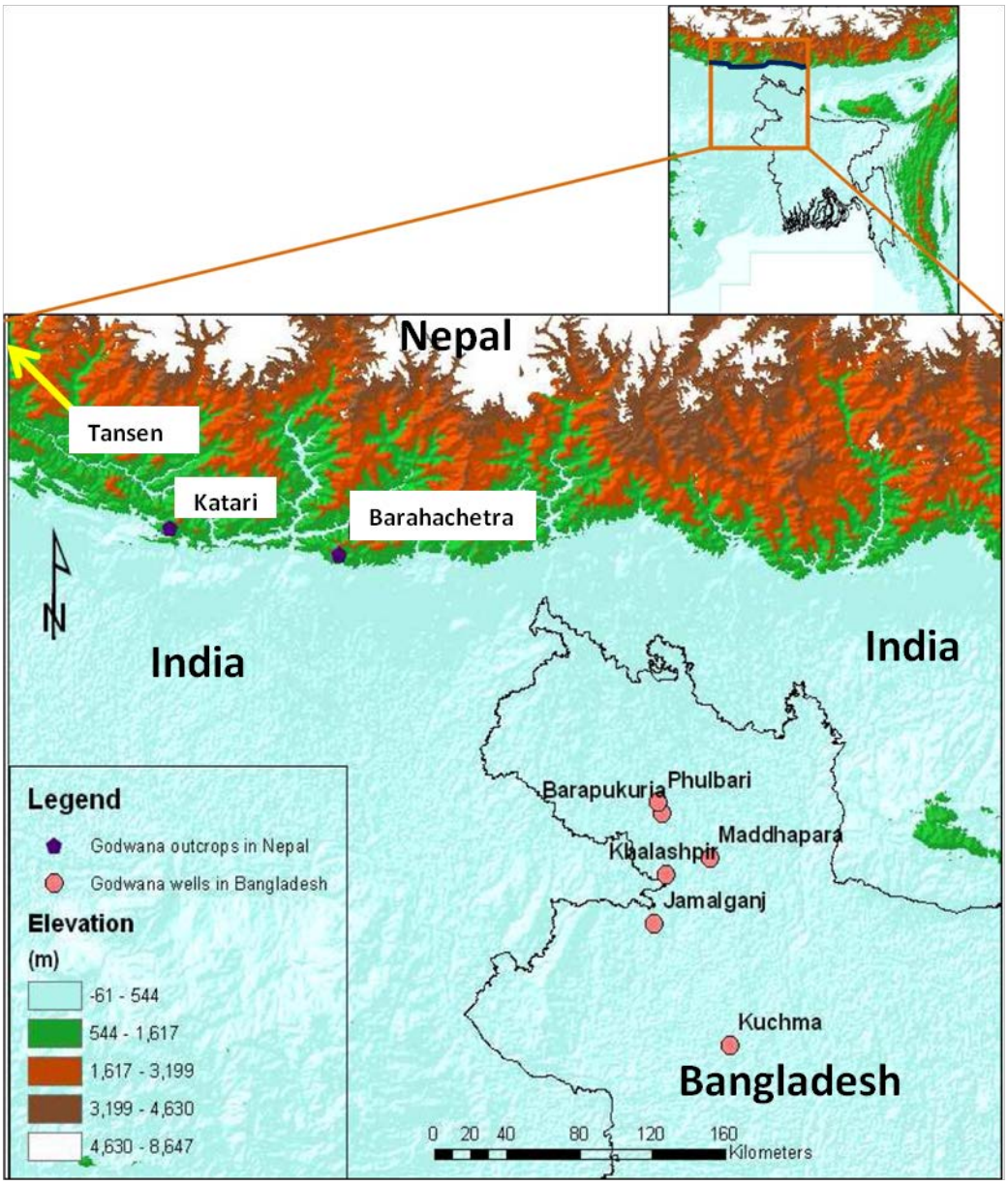

Figure 1.3 Location map of wells penetrating Gondwanan sequences in northwest Bangladesh and outcrops of such sequences in Nepal. Sitaula (2009) studied Gondwanan samples from the Katari and Barahachettra sections in Nepal which provide a basis for subsurface comparisons with the current study.

collision and resulting amalgamation of Gondwana-derived blocks in the Himalayan foreland basin. Dutta (2002) constructed a composite stratigraphic section for the Gondwanan units of Peninsular India. Kinematics of the Gondwanan basins of Peninsular India had been studied by Chakraborty et al. (2003). Chatterjee et al. (2007) worked on the geochronology of the granite and gneissic complex of Shillong Meghalayan craton.

Several works carried out on the northwestern Bengal Basin were focused mostly on coal (Bostick et al., 1991; Islam and Hayashi, 2008). Akhtar and Kosanke (2000) carried out palynomorphological studies on coal, and Akhter (2001) proposed a correlation between Gondwanan sediments of Bangladesh and other Gondwanan basins of the world based on spores and pollen. Tectonic subsidence and hydrocarbon source-rock potential were studied by Frielingsdorf et al. (2008). Uddin and Islam (1992) and Hossain et al. (2002) studied sedimentological aspects of Gondwanan sequences of Bangladesh to interpret their depositional environments. Petrographic studies of some sandstones from the Gondwanan sequences were carried out by Huque et al. (2003). Based on palynological studies, these sequences were correlated with sequences in the middle part of the Raniganj Stage of India and the Upper Permian of the Salt Range of Pakistan (Stover, 1964; Islam, 1990). The detrital history of the Permo-Carboniferous Gondwanan sequences of Bangladesh has yet to be explored. In comparison, coeval strata from India are relatively well studied (e.g., Dutta, 2002; Ghosh, 2002).

1.4 OBJECTIVES

The current study focuses on petrofacies and geochronology of Gondwanan sequences of Bangladesh in order to evaluate and reconstruct regional detrital and tectonic histories of late Paleozoic eastern Gondwanaland basins. The Gondwanan basins in Peninsular India and Bangladesh are relics of the original master basin that was disrupted during and after deposition

(Veever and Tewari, 1995). Few studies have been carried out on provenance of the deposit in these basins. Core samples were collected from three wells at two locations. Sandstone petrography was carried out to infer the degree of maturity and provenance. Conventional heavy mineral studies and heavy mineral geochemical analyses were done to evaluate source and weathering history of the sediments. Laser $^{40}Ar/^{39}Ar$ geochronology of detrital muscovite grains from three stratigraphic levels of the Gondwanan sequence in one core was performed to characterize their cooling ages that can provide additional information on source terranes.

1.5 THESIS OUTLINE

This research addressed two major components – petrofacies and paleotectonic history of Gondwanan sequences of northwestern Bengal Basin. The remaining parts of this thesis contain seven chapters. Chapter 2 provides geologic background for the area, including its tectonic setting and stratigraphy, and the general geology of Gondwanan sequences of northwestern Bengal Basin and Peninsular India. Chapter 3 describes the evolution of Gondwanan basins. Chapters 4 through 7 describe the methods and results of sandstone petrography, heavy mineral studies, geochronology, and mineral chemistry, respectively. Chapter 8 provides a summary of findings and interpretations drawn from all the results and chapter 9 concludes the thesis.

CHAPTER 2: GONDWANAN SEQUENCES OF NORTHWESTERN BENGAL BASIN

2.1 GENERAL GEOLOGICAL SETTING OF BENGAL BASIN

The Bengal basin is situated generally between 20°34′ to 26°38′ N and 88°01′ to 92°41′ E (Fig. 2.1). It lies in the northeastern part of the Indian subcontinent between the Indian shield to the west and the Indo-Burman ranges to the east. A major part of the basin area falls within the political boundary of Bangladesh with a smaller part in the West Bengal State of India. The northern boundary of the basin is delineated by the Himalayan mountain ranges and the Shillong Plateau. The basin is open to the south and extends towards the Bay of Bengal.

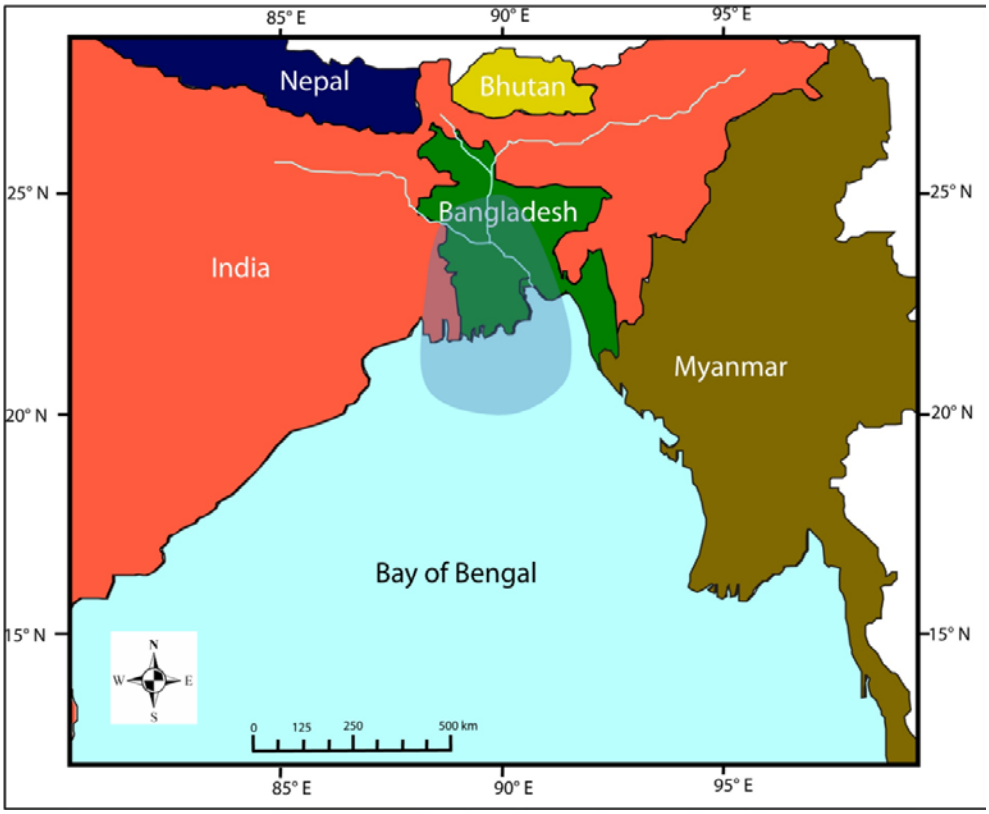

Figure 2.1 Location of the Bengal basin (shaded blue) and surrounding areas.

Bangladesh is positioned within the largest fluvial deltaic system in the world. Sediments are transported by the three major river systems (Ganges, Brahmaputra-Jamuna and Meghna) that drain the Himalayan fold belt. A huge sediment load derived from fluvial and coastal environments has been deposited in the Bengal fan system since the onset of collision between the Indian plate and the Eurasian plate.

2.2 TECTONIC SETTING OF GONDWANAN SEQUENCES IN BANGLADESH

The Bengal Basin is considered to be one of the largest depositional features in the world today (Graham et al., 1975; Salt et al., 1986; Kuehl et al., 1989; Alam et al., 2003). It is a major geotectonic element of the Assam–Himalayan region, which broadly is divided into an (1) Indian Platform flank zone in the west, (2) a deeper basin zone in the middle, and (3) the folded belt in the east (Uddin and Lundberg, 2004) (Fig. 2.2). Within Bangladesh, the Indian Platform flank zone includes numerous grabens/ half-grabens in which Gondwanan sediments were deposited **(**Fig. 2.3**)**. Different geotectonic divisions of Bengal Basin are discussed below.

1. Indian Platform flank zone: This zone occupies the Rajshahi-Bogra-Rangpur-Dinajpur areas and is characterized by limited to moderate thickness of sedimentary rocks above a Precambrian igneous and metamorphic basement (Fig. 2.2). The Gondwanan deposits of northwestern Bangladesh lie in this tectonic unit. This geotectonic element is comparatively stable relative to the other units and has not been affected by any active plate movement. Some normal fault-bounded half graben basins filled with coal-bearing siliciclastic rocks are encountered in the stable platform. On the basis of sedimentary thickness, this zone is divided into two parts:
    i. Rangpur Saddle (Khan, 1991) characterized by relatively thin (130 to 1000 m) sedimentary deposits above the Precambrian basement (Fig. 2.2); and

ii. Bogra shelf characterized by a thicker (1 to 6 km) sediment cover over Precambrian basement (Fig. 2.2). Sedimentary layers dip very gently toward the hinge zone to the southeast. In the hinge zone, dips increase abruptly to 15 to 20˚ and sedimentary units plunge to great depths into the deeper parts of the basin to the south and southeast.

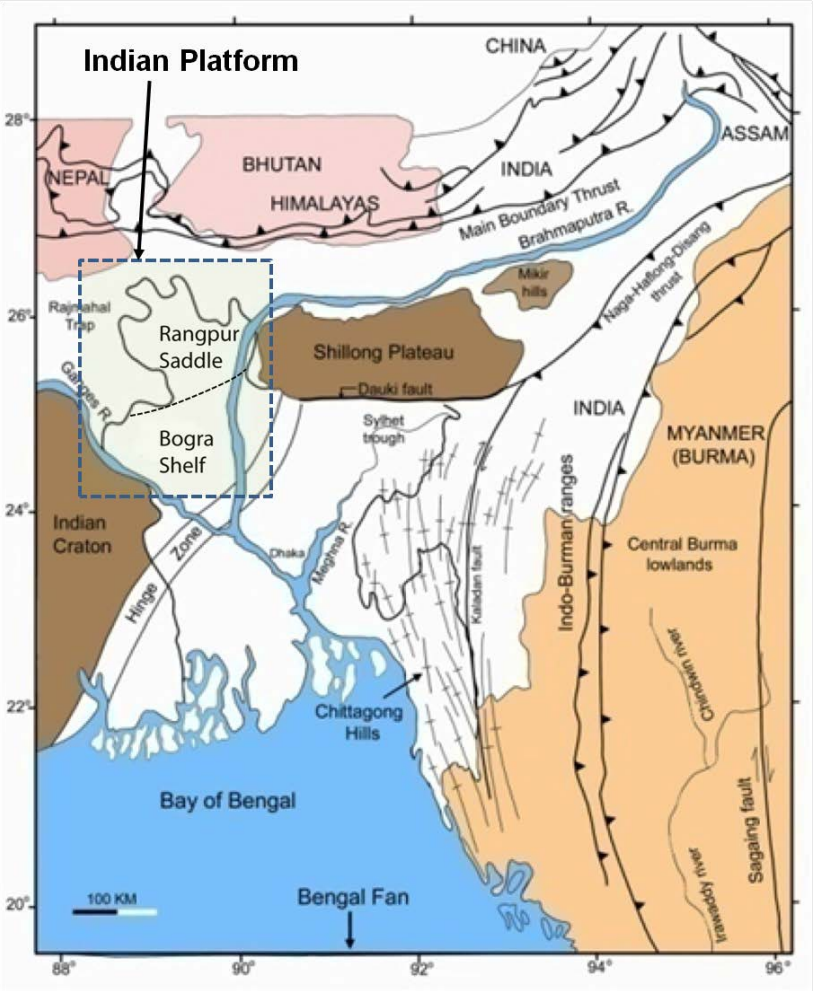

Figure 2.2 Tectonic subdivisions of Bengal Basin (modified from Uddin and Lundberg 2004).

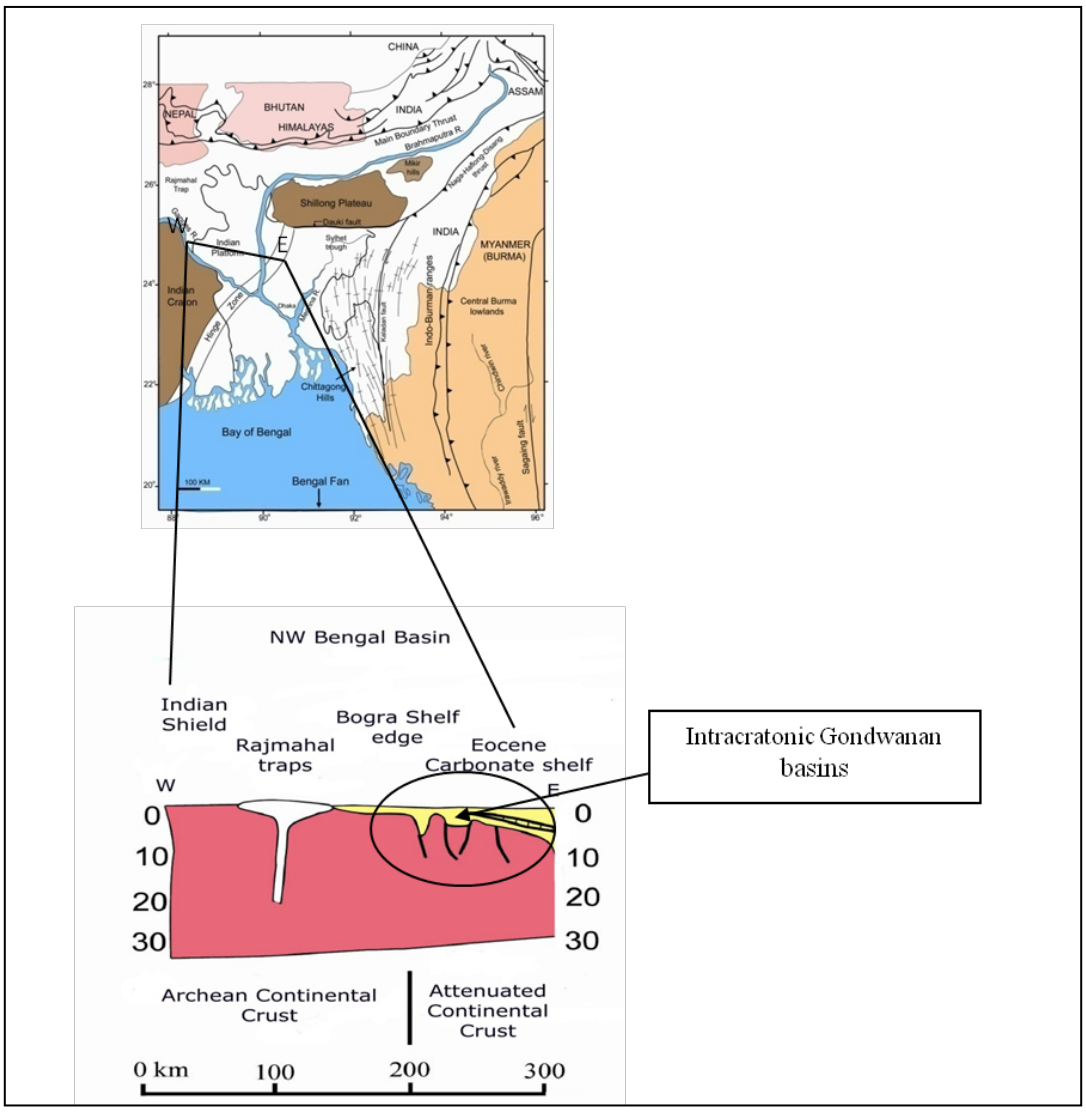

Figure 2.3 Major tectonic elements of Bangladesh with special focus on NW Bengal Basin and intracratonic Gondwanan basins (after Uddin and Lundberg, 2004).

2. Deeper basin zone: This zone, located to the south and east of the stable platform, is characterized by extremely thick sedimentary layers (maximum of about ~22 km near the basin center) (Imam and Hussain, 2002). The sedimentary rocks are mostly comprised of Cenozoic sandstones and shales. The huge thickness of sediments in the basin is a result of tectonic mobility or instability of the area, which resulted in rapid subsidence and sedimentation in relatively short

span of geologic time. The sedimentary layers of this unit are generally horizontal to sub-horizontal if not very gently folded. They merge with intensely folded rock of the folded belt to the east. This zone covers the central part of the basin and is represented by fluvial to delta-plain topography at the surface.

3. Folded belt: This area, also known as the Chittagong-Tripura fold belt (Fig. 2.2), is characterized by highly folded and faulted sedimentary layers. These layers generally are distributed into a series of anticlines and synclines. The intensity of the folding is greater towards the east, resulting in higher elevations in the eastern Chittagong Hill Tracts. Anticline and syncline axes trend NNE-SSW in the Chittagong Hill ranges and E-W in the Sylhet area.

2.3 GONDWANAN STRATIGRAPHY OF NORTHWESTERN BENGAL BASIN

Three different stratigraphic schemes (Imam and Hussain, 2002) have been employed for each of the tectonic zones described above (Fig. 2.4). The Indian Platform flank zone, characterized by the thinnest sedimentary package, includes Gondwanan Group to Recent Dupi TIla Formation (Fig. 2.5). In contrast, the deeper basin and folded belt consist of very thick Tertiary sedimentary sequences. The age of sedimentary rocks in these units ranges from Paleocene/Eocene to Recent.

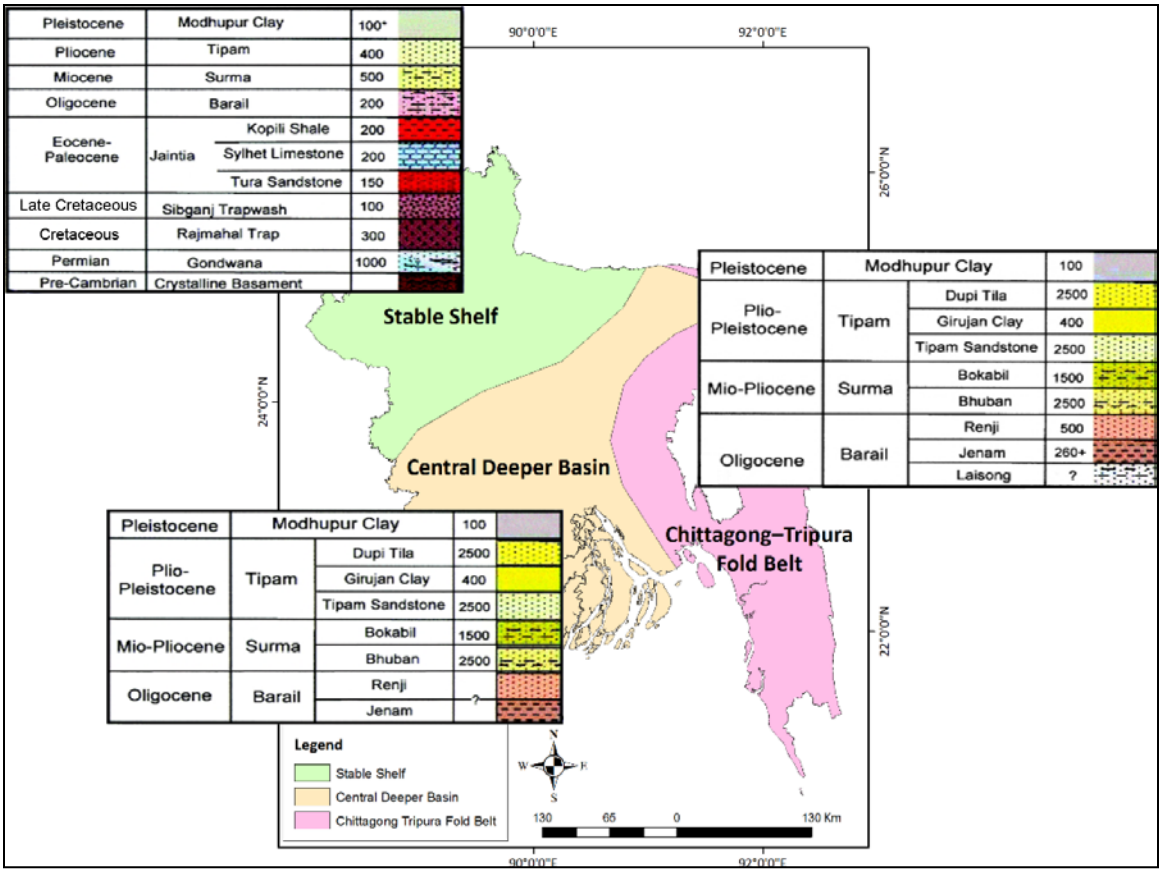

Figure 2.4 Generalized stratigraphy of three tectonic zones of the Bengal Basin (modified after Imam and Hussain, 2002).

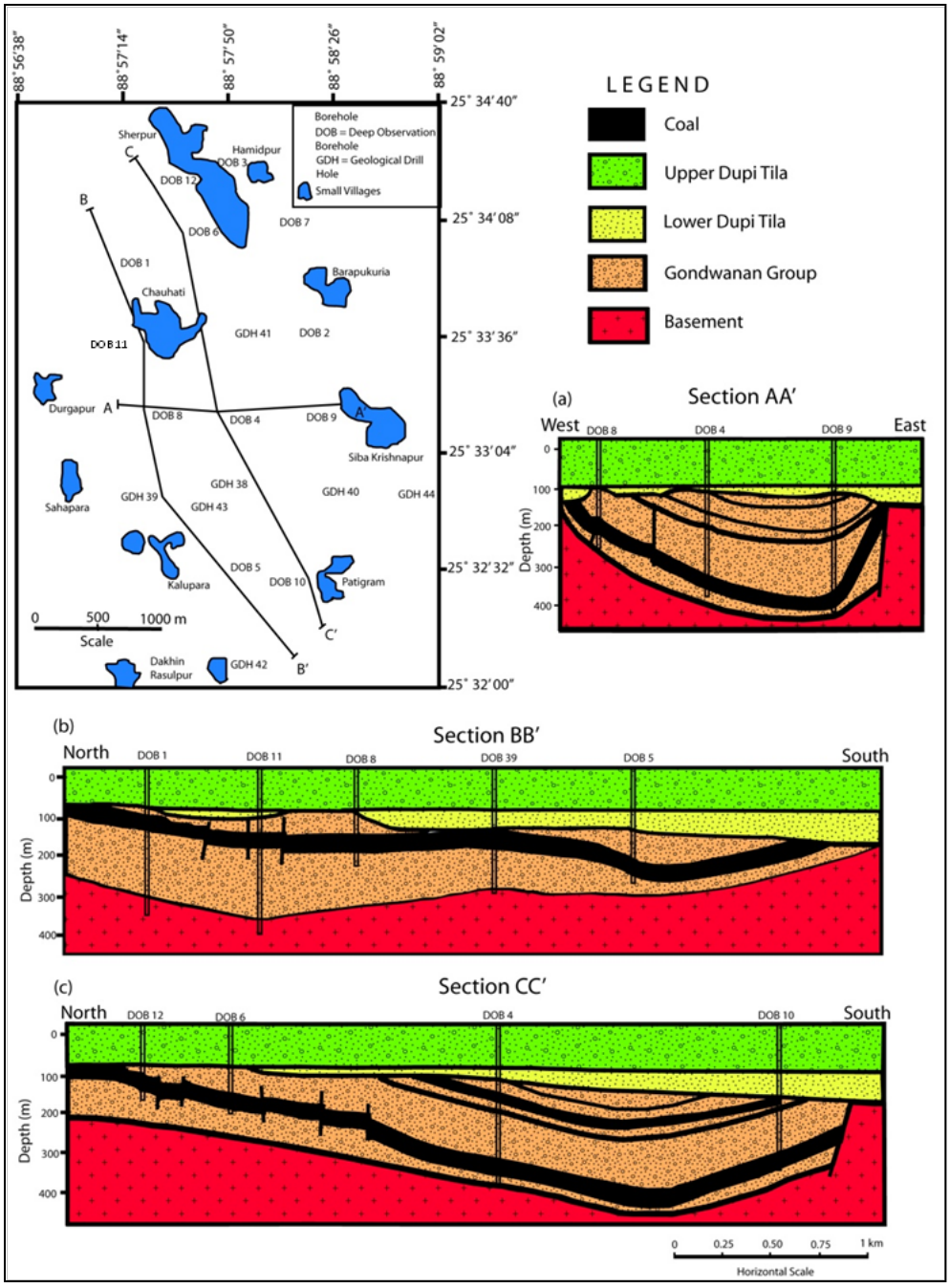

Figure 2.5 Structure and stratigraphy of Barapukuria coal basin on the Indian Platform of northwestern Bengal Basin (after Wardell, 1991).

The rock units in the stratigraphic succession of stable Indian Platform are described below.

Precambrian Crystalline Basement: The shallowest depth to the Precambrian basement complex has been reported in the Rangpur saddle, suggesting a subsurface communication between the Indian shield to the west and Shillong Plateau to the east. Khan (1991) accordingly referred to the area as the Dinajpur Shield. Basement rocks are mainly granite, granodiorite, and gneiss with occasional mafic to ultramafic intrusions. A 3-meter-thick weathered zone overlies the basement, an indication of subareal exposure in the geologic past. Precambrian basement occurs as shallow as 130 meter below the surface in the Rangpur saddle area, and to the southeast it is buried to progressively greater depths by Permian to Recent sediments. Sedimentary thickness to the southeast ranges from 1 to 6 Km.

Gondwanan Group: The oldest sedimentary unit in Bangladesh belongs to the Gondwanan Group. This unit unconformably overlies crystalline basement. The Gondwanan Group is divided into the Kuchma Formation and the Paharpur Formation. These units are predominantly composed of feldspathic sandstone with some coal layers, conglomerate and shale. The group, representing mainly fluvial environments, is about 1000 m thick and is found within normal fault-bounded half-graben basins. These sequences probably represent the preserved part of a more extensive and thicker sedimentary package that was partially lost by erosion.

Permian Gondwanan sequences of northwestern Bengal Basin are well known for their extensive coal deposits. These are similar in character and origin to the coal-bearing Gondwanan rocks of the major coal fields in the adjacent Indian states of West Bengal and Bihar.

Rajmahal Trap: The Paharpur Formation of the Gondwanan Group is overlain by Jurassic volcanic basaltic rocks known as the Rajmahal Trap (Khan and Muminullah, 1980; Khan, 1991; Reimann, 1993). This unit is named after the Rajmahal hills in adjacent India where the unit is exposed on the surface. The rocks are about 100 to 500 m thick as found in drill holes in Rajshahi-Bogra area.

Shibganj Trapwash: The Rajmahal Trap is overlain by the Cretaceous Sibganj Trapwash. This unit is a relatively thin cover of weathered products of volcanic rocks and consists of red ferruginous sandstone and mudstone.

Jaintia Group: The Paleocene-Eocene Jaintia Group overlies the Shibganj Trapwash. These Early Tertiary deposits were deposited in shallow marine, marginal marine, and continental environments.

The Jaintia Group is divided into three formations.In ascending order these are the Tura Sandstone, Sylhet Limestone and Kopili Shale. The Tura Sandstone is an upper Paleocene to lower Eocene unit, composed mainly of sandstone with minor shale and occasional thin coal beds near the top. The unit is encountered in several wells in the northwestern stable shelf area and is ~150 to 350 m thick. Only one isolated outcrop of this unit has been recorded near the Sylhet-Meghalaya border. Notably, these are the oldest exposed rocks in Bangladesh.

The Sylhet Limestone is a fossiliferous (nummulitic) limestone unit of middle Eocene age with an average thickness of 250 m. This is the most extensively developed unit in the subsurface of northwestern Bangladesh and can traced as a marker horizon in seismic sections. Scattered small outcrops of Sylhet Limestone unit are present along the northern Sylhet-Sunamganj border with Meghalaya. This formation is the most fossiliferous unit in Bangladesh. Foraminiferas include *Nummulites*, *Discocycina*, and *Alveolina*, etc.

The Kopili Shale is composed of dark gray to black fossiliferous shale with rare limestone beds. Thickness of this unit ranges from 40 to 90 m. The Kopili Shale marks the end of open marine deposition.

Bogra Formation: The Oligocene Bogra Formation, ranging from 150 to 200 m thick, is characterized by alternating sandstone, shale and siltstone with rare carbonaceous layers. This unit represents deposition under deltaic conditions. Reimann (1993) reported the palynomorph *Meyeripollis Naharkotensis.*

Jamalganj Formation: The Jamalganj Formation, consisting of ~ 400 m of interbedded sandstone, shale and siltstone, unconformably overlies the Oligocene Bogra Formation (Khan and Mominullah, 1980). This is equivalent to the undifferentiated Surma Group of the deep basin. The unit represents deposition under deltaic conditions.

Dupi Tila Formation: The Jamalganj Formation is overlain by the Pliocene Dupi Tila Formation, which is predominantly composed of commonly pebbly, medium to coarse-grained sandstone and has a thickness of about 270 m. This unit represents fluvial environments. While the Miocene-Pliocene section in the stable platform area measures about 650 m thick, the equivalent section in the deep basin area to the southeast measures more than 9000 m.

Barind Clay: Pleistocene reddish brown clay, known as the Barind Clay, overlies the Dupi Tila Formation. The Barind Clay is overlain by Holocene floodplain deposits.

Table 2.1 Generalized stratigraphy of northwest Bangladesh (after Uddin and Lundberg, 1998).

AGE	GROUP	FORMATION	THICKNESS (m)	ROCK TYPE	LITHOLOGY
Pleistocene		Barind Clay	40	Reddish clay	
Pliocene		Dupi Tilla	270	Loosely Compact Sandstone	
Miocene		Jamalganj (Undifferentiated Surma equivalent)	400	Alternating sandstone and shale	
Oligocene		Bogra	160	Sandstone and shale	
Eocene	Jaintia	Kopili Shale	170	Mostly shale	
		Sylhet Limestone	240	Nummulitic limestone	
		Cherra	370	Mostly sandstone	
Jurassic		Shibganj Trapwash	130	Basaltic volcanic rock layer	
		Rajmahal Trap	540		
Permo-Carboniferous	Upper Gondwana Lower	Paharpur	1000	Mostly hard sandstone with coal	
		Kuchma			
Precambrian Crystalline Basement				Igneous and Metamorphic rocks	

2.4 DISTRIBUTION OF GONDWANAN BASINS IN PENINSULAR INDIA

Permo-Carboniferous Gondwanan sequences of Peninsular India occur in three well-defined linear belts (Fig. 2.6; Wadia, 1919; Chakraborty et al., 2003). These include: (1) the NW-SE trending Son-Mahanadi valley with an extensive outcrop; (2) Pranhita-Godavari valley forming an elongated band of connected troughs; and (3) the east-west trending Damodar Basin. Gondwanan basins are well preserved in three belts (Fig. 2.6; Narain, 1994). Development of basins was related to crustal dynamics and mountain building. According to Dutta (2002),

development of Gondwanan basins in India was influenced by extensional forces that acted along the lineaments between the cratonic blocks of India.

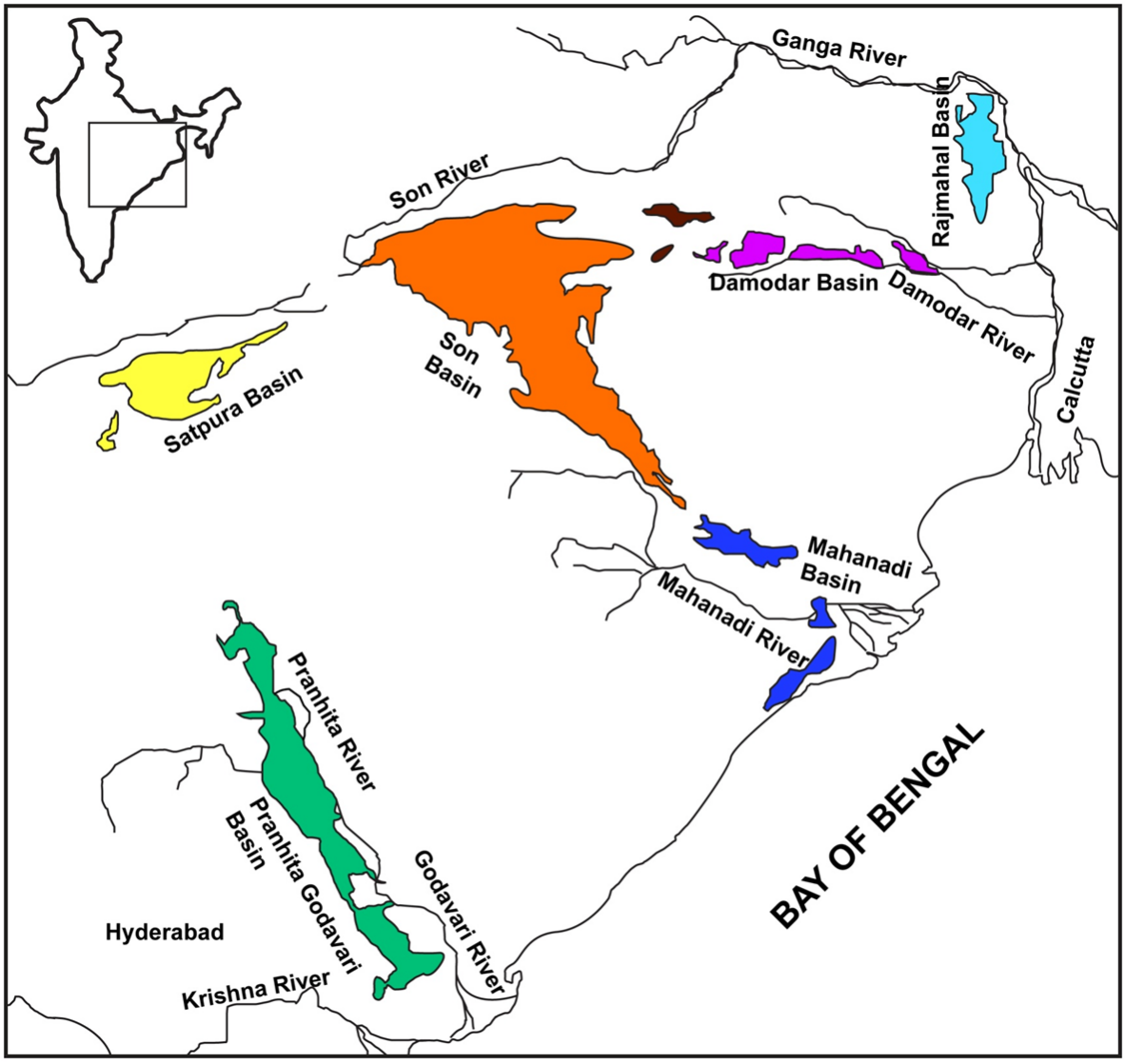

Figure 2.6 Distribution of Gondwanan basins of Peninsular India (after Dutta, 2002).

Table 2.2 Existing scheme of correlation of Gondwana Formations (after Mukhopadhyay et al., 2010)

		Damodar-Koel Valley	Rajmahal	Mahanadi		Son	Satpura	Godavari	
Cretaceous	Lower					Bansa Bed	Jalalpur	Chikiala/ Gangapur	
Jurassic	Upper		Dubrajpur				Bogra		
								Kotla	
	Middle Lower					Bandhavgarh		Dharmaram	Maleri Group
						Parsora			
Triassic	Upper	SupraPanchet		Kamthi	Kamthi	Tiki		Maleri	
	Middle					Pali	Dewna	Bhimaram	
								Yerrapalli	
	Lower						Panchamari	Upper Kamthi Middle Kamthi	Kamthi Group
		Panchet							
Permian	Upper	Raniganj		Raniganj		Raniganj	Bijuri	Lower Kamthi	
		Barren Measures		Barren Measures		Barren Measures	Motur	Barren Measures	Barak
	Lower	Barakar	Barakar	Barakar		Barakar	Barakar	Barakar	
		Talchir	Talchir	Talchir		Talchir	Talchir	Talchir	
Late Carbonifeorus									

Based on depositional age, the Gondwanan system of India is divided into three different deposits that correspond to the Lower, Middle and Upper Permian, Triassic, and Jurassic, respectively (Wadia, 1919). These individual deposits are divided into different formations,

depending on their lithologic associations. Indian Gondwanan successions, excluding the Talchir formation, have been interpreted to have been deposited in alluvial environments (Fox, 1931; Robinson, 1967; Rao, 1982, 1983, 1987; Casshyap and Tiwari, 1991; Veevers and Tiwari, 1995). The presence of marine fossils in the Talchir Formation is an indication of marine incursion during the early Permian (Fig. 2.7; Reed, 1927; Ghosh, 1954, 2003; Ahmad, 1957; Dutta, 1965; Chaudhuri, 1985; Venkatachala and Tiwari; 1987; Ahmad and Khan, 1993; Veevers and Tiwari, 1995; Biswas, 2003).

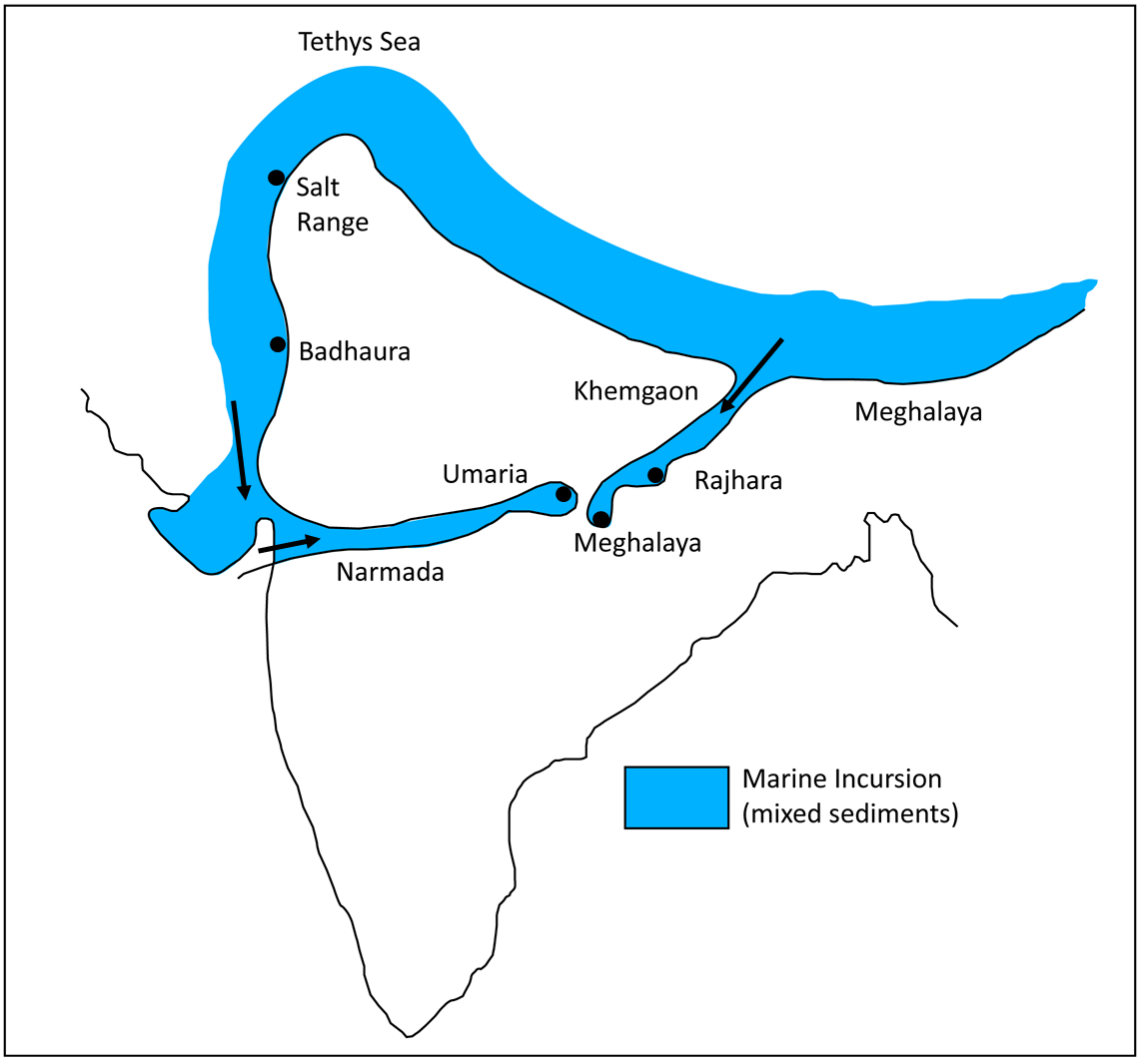

Figure 2.7 Marine incursions (shown with arrows) in Gondwanaland during the Permian (Valdiya, 1997).

The general stratigraphy of Gondwanan sequences of the Damodar Basin (DB), Penninsular India, is described below (Fig. 2.8).

Talchir Formation: The Talchir Formation consists of the lowermost beds of Gondwanan sequences that were first documented in the Talchir district of Orissa in southeast India. The formation is mainly characterized by glacial, glacio-fluvial, and glacio-lacustrine deposits (Smith, 1963; Banerjee, 1966; Veevers and Tiwari, 1995; Dasgupta, 2002). Glacial deposits are mainly matrix-supported boulder conglomerates with striated and faceted clasts. This formation is ~ 300 m thick in the Damodar basin (Dutta, 2002).

Damuda Group: This group is divided into three different formations. These are the Barakar Formation, Barren Measures, Raniganj Formation, Panchet Formation, and Mahadev Formation (Supra Panchet).

The Barakar Formation, which conformably overlies the Talchir Formation, is mostly composed of massive coarse-grained sandstone, shale, and interbedded coal layers. Sandstones are dominantly subarkosic with minor variations in composition ranging to quartz aenite (Dutta, 2002). Thick coal seams are common in this formation.

The Barren Measures is a thick sequence of carbonaceous shale, sandstone, and minor impure iron carbonates and oxides. The thickness of this unit varies among basins (Wadia, 1919). Dominance of shale and sandstone varies within the basin. In the eastern part, shale is more common, whereas sandstone is more abundant towards the west (Fig. 2.6; Dutta, 2002).

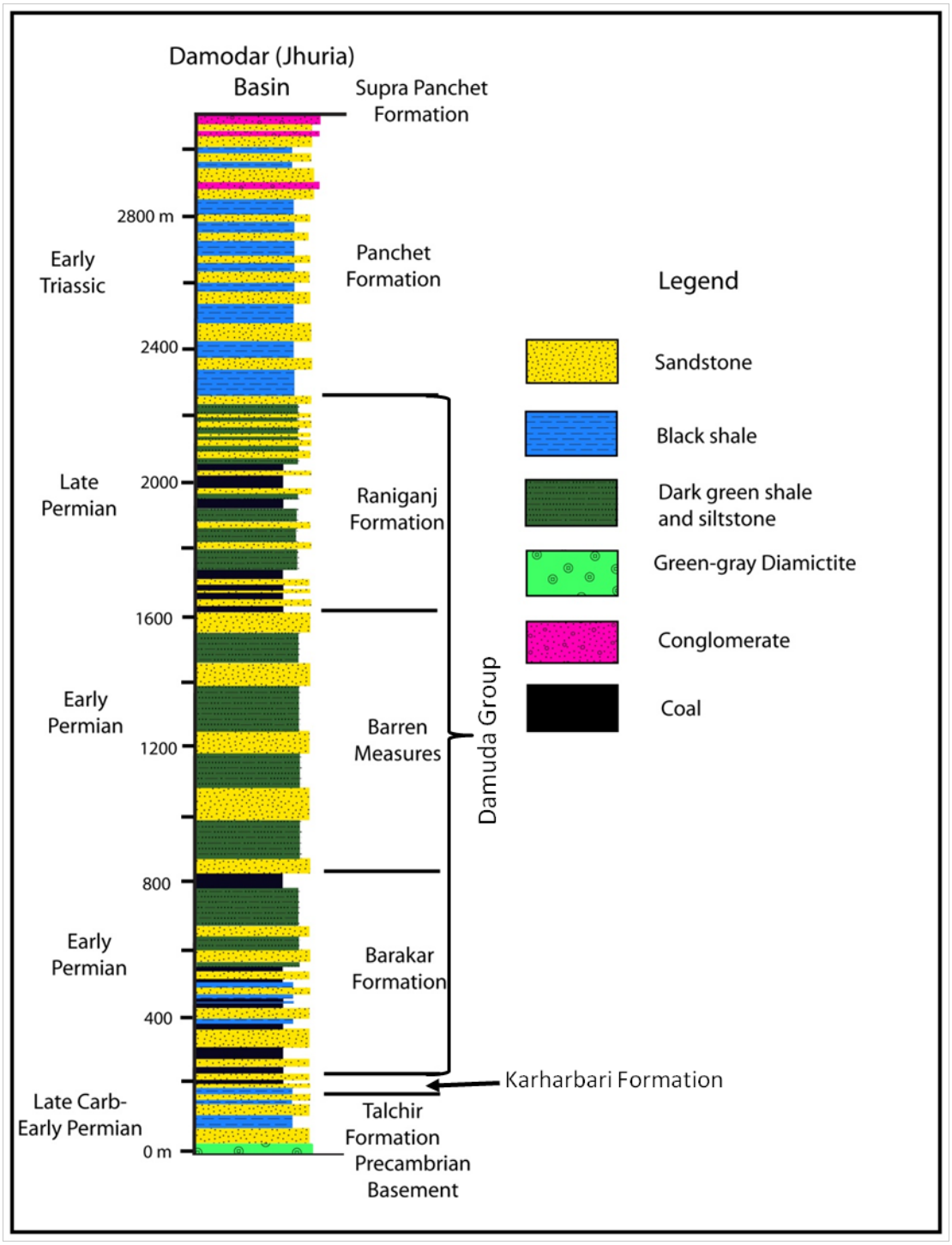

Figure 2.8 Stratigraphic column of Gondwanan sequences in the Damodar Basin (after Veveers and Tiwari, 1995).

The Raniganj Formation consists of coal, carbonaceous shale, sandstone, and siltstone. Coal layers of the Raniganj Formation are thinner than those of the Barakar Formation. Sandstones are mostly fine grained and arkosic to sub-arkosic (Dutta, 2002). Thickness of this formation varies from 700 m to 900 m.

Panchet Formation: The Panchet Formation unconformably overlies the Raniganj Formation, although locally it directly overlies the Barakar Formation. This formation is characterized by alternating red clay and coarse sandstone. However, the lower part of the formation is mostly composed of greenish shale and sandstone (Dutta, 2002).

Mahadev Formation (Supra Panchet): This formation consists of massive, variegated, coarse- to medium-grained sandstones with ferruginous and micaceous clay. Sandstones are very highly mature quartz arenites with little or no feldspar (Dutta, 2002). This formation is well developed in Madhya Pradesh (central India) and Damodar Basin. The Mahadev Formation reaches upto 1,300 m in thickness near Nagpur at Madhya Pradesh and has a thickness of about 800 m at Damodar Basin.

2.5 GONDWANAN STRATIGRAPHY OF OTHER PARTS OF EXTRAPENINSULAR INDIA AND PARTS OF GONDWANALANDS

Gondwanan sequences of Indian subcontinent are not restricted to Peninsular India. Comparable sequences also have been found in northern India across the Indo-Gangetic plain in the western Himalaya (in Afganistan, Pakistan, India, etc.) and the eastern Himalayas (in Nepal, Sikkim, Bhutan, Assam, India, etc.). These sequences are known as extra-peninsular Gondwanan sequences. Gondwanan sequences of extra-Peninsular India are intensely folded, compressed and in many cases metamorphosed. In contrast, those in the Peninsular India and Bangladesh are

relatively undisturbed and well preserved. The identification and age evaluation of Gondwanan sequences of extra-peninsular India have been a major problem.

The eastward extension of Gondwanan basins stretched to the Yilgarn craton of Western Australia, as indicated by gravity data (Khan et al., 1994). This is considered to be the northernmost Gondwanan subbasin, which was separated from a southern subbasin by a northeast-southwest trending intra-cratonic high. Shillong Plateau and Chhotangpur gneissic terrain are connected by this cratonic high. The southern Gondwanan subbasin extended to the western periphery of the Shillong plateau through Ghatal-Behrampur (Fig. 2.9).

Gondwanan basins were widely distributed on all the Gondwanan continents including India, Africa, Antarctica, Australia and South America. The distribution of these deposits was controlled by paleotopography. According to Veevers (2006), the Gondwanan sequences of the Indian subcontinent are contemporaneous with those in the Australian Collie Basin and South African Karoo Basin. These two basins are described below (Fig. 2.10).

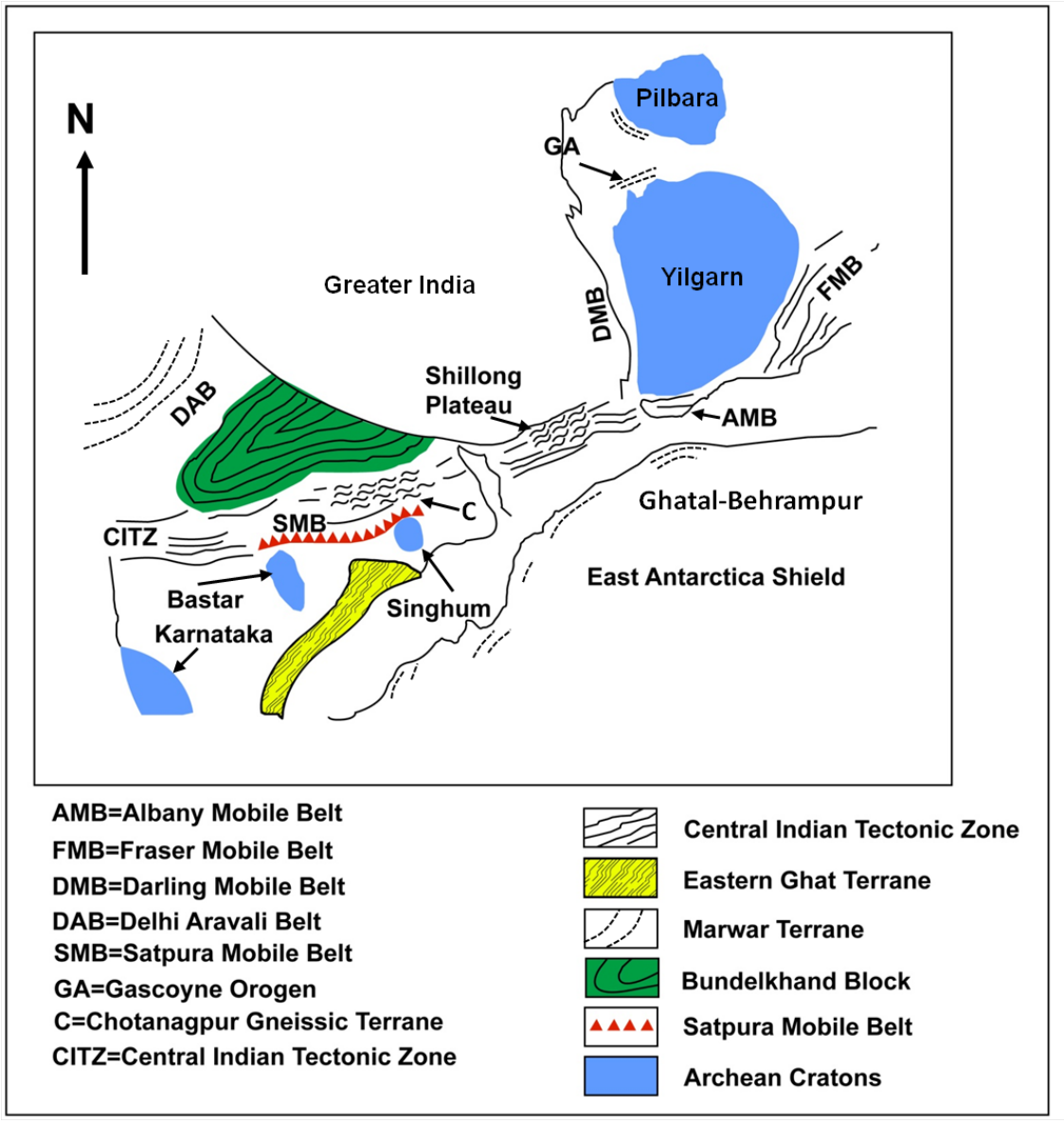

Figure 2.9 Different tectonic subdivisions and relation of Indian Precambrian shield (after Khan et al., 1994).

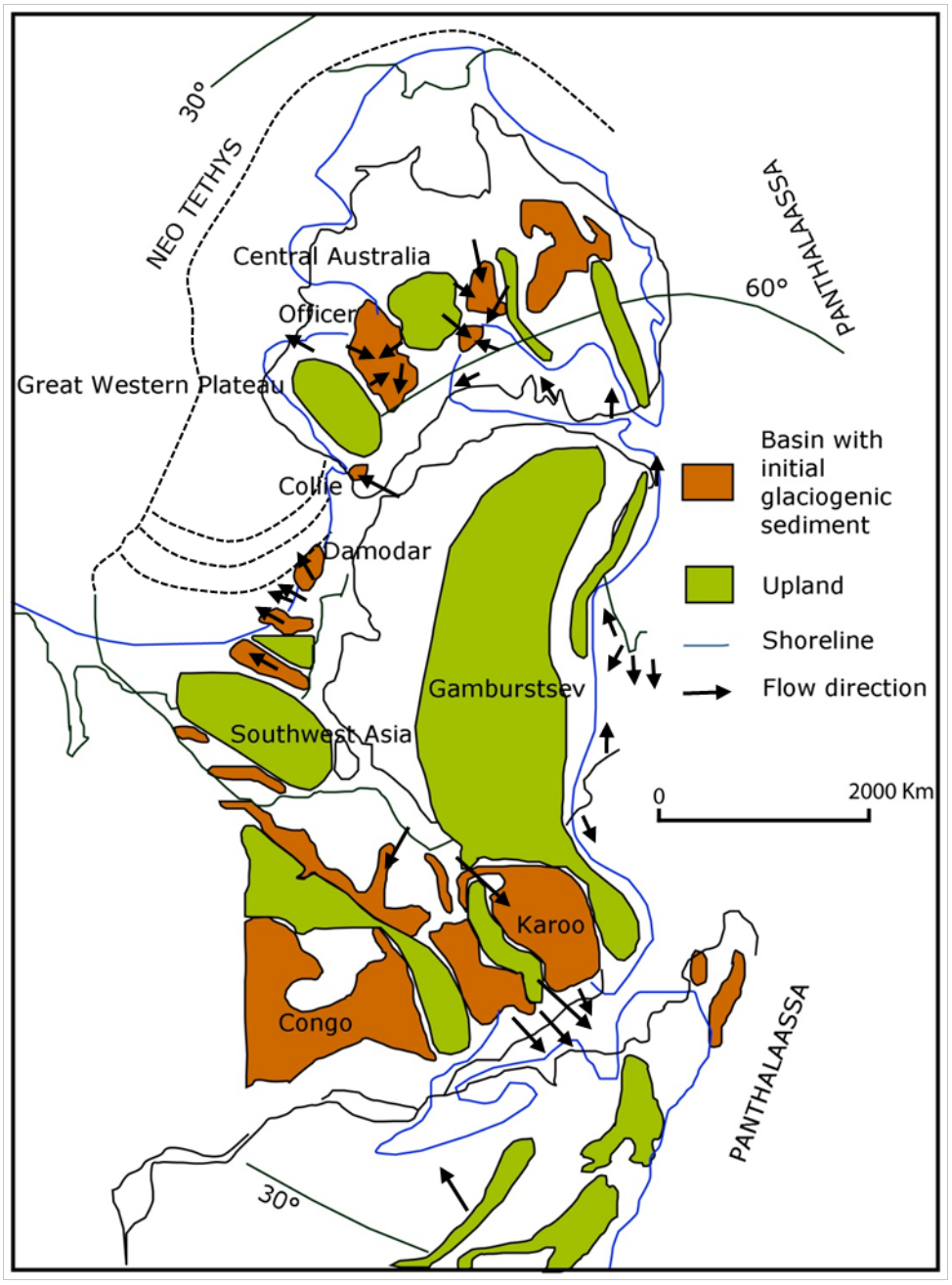

Figure 2.10 Distribution of Gondwanan basins in Gondwanaland during Early Permian (after Veevers and Tiwari, 1995).

Collie Basin: The Permian coal-rich Collie Basin is situated within the Yilgarn craton (Veevers, 2006). The Stockton Formation, the oldest unit of the Collie Basin, is composed of sandstone, shale, and diamictite. Three coal measures overly the Stockton Formation; the Ewington, Premier and Muja (Veevers, 2006) measures. Sandstones of the Cretaceous Nakina Formation overlie the coal-bearing Stockton Formation.

Karoo Basin: The South African Karoo Basin developed between the Carboniferous and Jurassic. It consists of several isolated or connected basins. The western part of the system was associated with extensional settings (Catuneau et al., 2005). The total thickness of strata in the Main Karoo basin is approximately 1100 m. Several formations have been delineated in this basin. The lowermost Dwyka Formation consists of glacial till. The overlying Volksrust Formation predominantly consists of shale with sandstone. The Belmont, Estcourt, Elliot, Mol Teno and Ottenburn are predominantly composed of sandstone and shale. The Estcourt Formation is well known for its coal deposits.

CHAPTER 3: PALEOHISTORY OF GONDWANAN BASINS

3.1 CONTINENTAL BREAK-UP OF GONDWANALAND

Gondwanaland, also known as Gondwana (Veevers, 2004), represents the southern supercontinent comprising all of the southern continents during the late Proterozoic. Rifting events throughout Phanerozoic led to the break-up of this supercontinent (Blakey, 2008). Some of the Gondwanan continents are currently partly or wholly situated in the northern hemisphere. However, Gondwanaland was situated in the southern hemisphere during its existence. Li and Powell (2001) and Veevers (2004) established the general Gondwanan history, whereas Scotese (1998) proposed a general plate configuration. A Paleozoic terrane rifting model was developed by Stampfli et al. (2002) (Fig. 3.1).

Several margins of Gondwanan continents were affected by early stage rifting and sea floor spreading (Li and Powell, 2001; Stampfli and Borel, 2002; Veevers, 2004). The initial break-up of Gondwanaland was associated with rifting along East Africa and Arabia during the Permian (Stampfli and Borel, 2002) and associated extrusion of Early to Middle Jurassic flood basalts (Veevers, 2004) extending from Tasmania to South Africa. Rifting of the Indian subcontinent started with Rajmahal volcanic activity (~110 Ma) (McDougal and McElhinny, 1970; Reimann, 1993) during Cretaceous at the eastern Indian margin (Baksi et al., 1987). Several models have been proposed to explain the possible mechanisms of

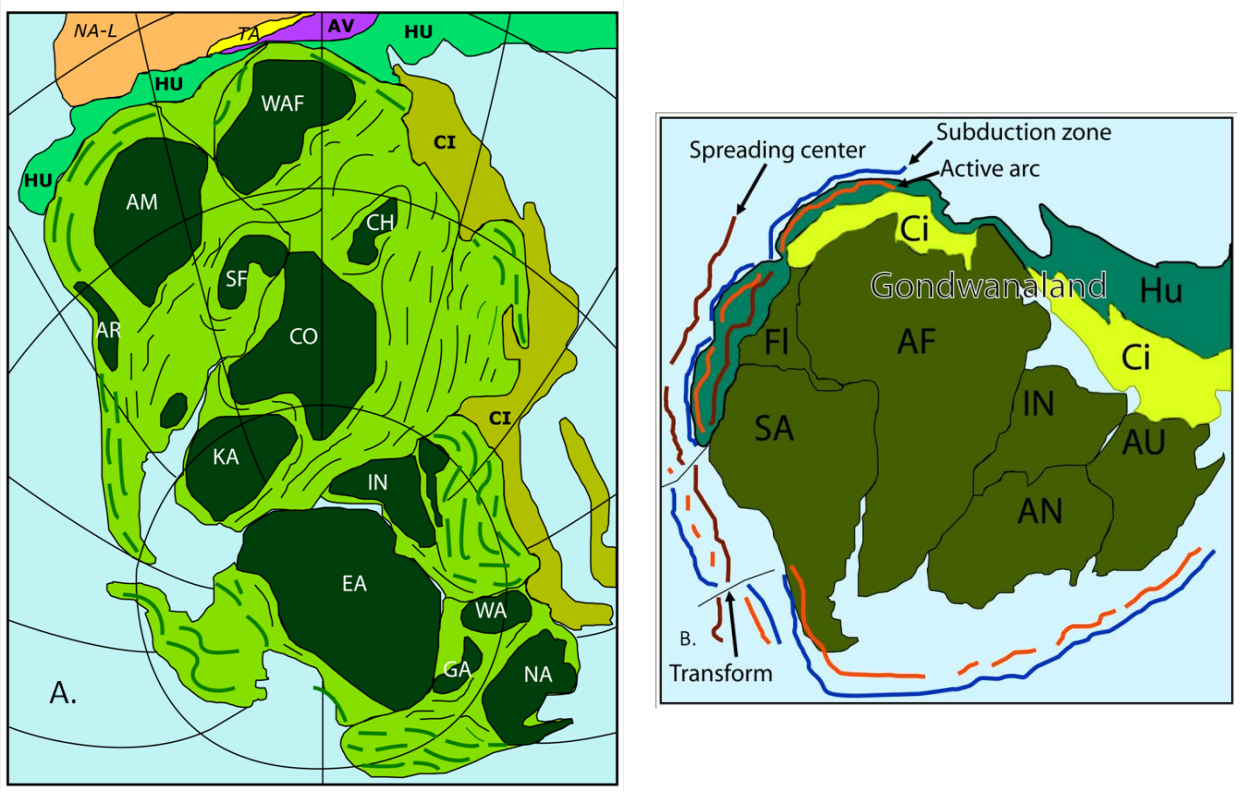

Figure 3.1 Elements of Gonwanan (A) Late Paleozoic South Polar projection of Pangea (after Dickerson, 2004) showing Gondwanan cratons (green areas, white letters) sandwiched between Middle and Late-Proterozoic Pan-African fold belts (light green areas with thin dashes; dashes show general structural trends) and superimposed Phanerozoic fold belts (thick dashes), peri-Gondwanan terranes (bold letters) and western Laurasia (Italic letters); (B) Key to colors and symbols used on tectonic maps; Gondwanan elements are shown in green, oceans are shown in blue. Here, Gondwanan cratons are-AM=Amazon, Ar=Arequina Massif, CH=Chad, CO=Congo, EA=East Antarctica, GA=Gawler, IN=Indian, Ka=Kalahari, NA=North Australia, RL=Rio La Plata, SF=Sao Francisco, WAF=West Africa, WA=Western Australia; Continents, continental blocks, other terranes, orogenic belts are-AF=Africa, AN=Antarctica, AU=Australia, FL=Florida, IN=India, KA=Kazakhstan (Kipchak arc), NA-L=North America/Laurentia, SA=South America, TA=Taconic/Taconia, WA=West Antarctica; Peri-Gondwanan terranes are-AV=Avalonia, Ci=Cimmeria, and HU=Hun (Hunic) (after Blakey, 2008).

Gondwanaland break-up. However, none of those can satisfy every aspect of the break up.

Among these mechanisms, mantle upwelling seems most convincing (Segev, 2002). The formation of the Gondwanan basins in India and other parts of the continents resulted from a major tectonic event. The Carboniferous Variscan (Hercynian) orogeny of the Carboniferous was a result of collision among several Gondwanan plates and Laurasia during the final assembly of

the Pangaean supercontinent. This collision was followed by post-convergent extension by crustal thinning, lowering of crustal viscosity, formation of numerous sedimentary basins and widespread alkaline magmatism between 320-240 Ma (Segev, 2002). The well-known normal fault-bounded half graben type structures in Gondwanan basins are the result of crustal loading caused by widespread magmatism.

The southern limit of Gondwanaland was characterized by a subduction zone that led to the formation of orogenic belts in South Africa, South America, and southwest Antarctica (Segev, 2002). Rifting between East Gondwanaland (India, Antarctica, and Australia) and West Gondwanaland (Africa and South America) took place during the Jurassic with the initiation of Karoo uplift followed by Karoo plume activity (Segev, 2002).

The evolution of the Bengal Basin of Bangladesh began with the separation of the Indian continent from the Gondwanan supercontinent during the Late Jurassic to Early Cretaceous (Reimann, 1993). After the breakup of Gondwanaland, the combined Indo-Australian plate moved southeasterly by ~ 1750 km in 135 Ma from Rodrigues triple junction of (RRR) at a drift rate of 6 cm/yr (Reimann, 1993). The space created between India and Antarctica due to this drifting was filled up Kerguelen Plateau basalts (Segev, 2002).

The break-up between India and Western Australia took place about 132 to 130 Ma (Segev, 2002). India broke apart from Australia when the Ninety East Ridge megashear, Broken ridge, and Diamantina fracture zone formed (Fig. 3.2). After the break-up, the Indian continent drifted northward. Its drift was acommodated by the Chagos-Laccadive Ridge and Ninety East Ridge megashears. Drift at this time was synchronous with the extrusion of the Deccan volcanics, dated ~ 65-67 Ma (Courtillot and Renne, 2003). Rifting between Madagascar and

Seychelles-India took place during late Cretaceous, along with gabbroic intrusion in India and basaltic volcanism in Madagascar and Seychelles.

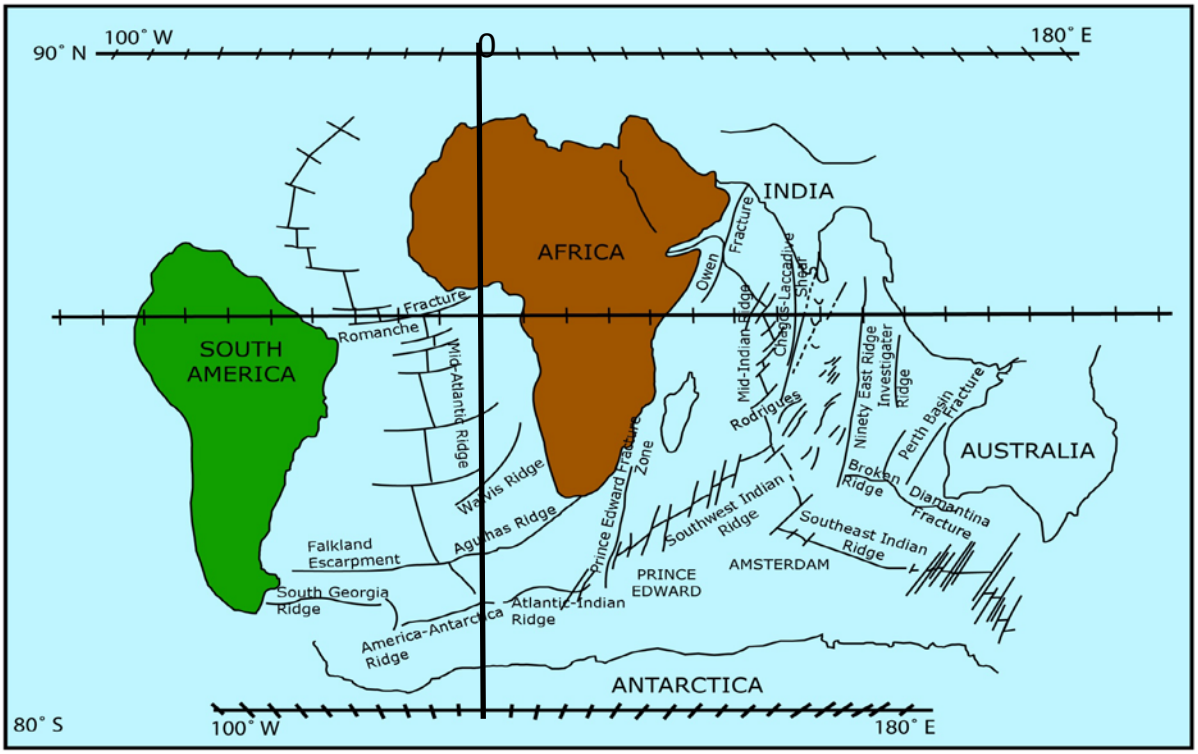

Figure 3.2 Orogenic map of Indian Ocean (after Condie, 1982).

3.2 EVOLUTION OF PASSIVE MARGIN ALONG THE NORTHERN BOUNDARY OF PENINSULAR INDIA

The nature of the northern margin of Peninsular India prior to collision with India has been a subject of debate (Brookfield, 1993) and requires further study. Several studies had been carried out and a range of few kilometers to 2800 km of collisional margin was proposed, which was based on the concept of ‘Greater India’. The Indian plate remained as a passive margin while travelling northeast from Cretaceous to Eocene before the collision with Eurasia

(Brookfield, 1993). The initial collision between India and Asia did occur until the Eocene (Fig. 3.3).

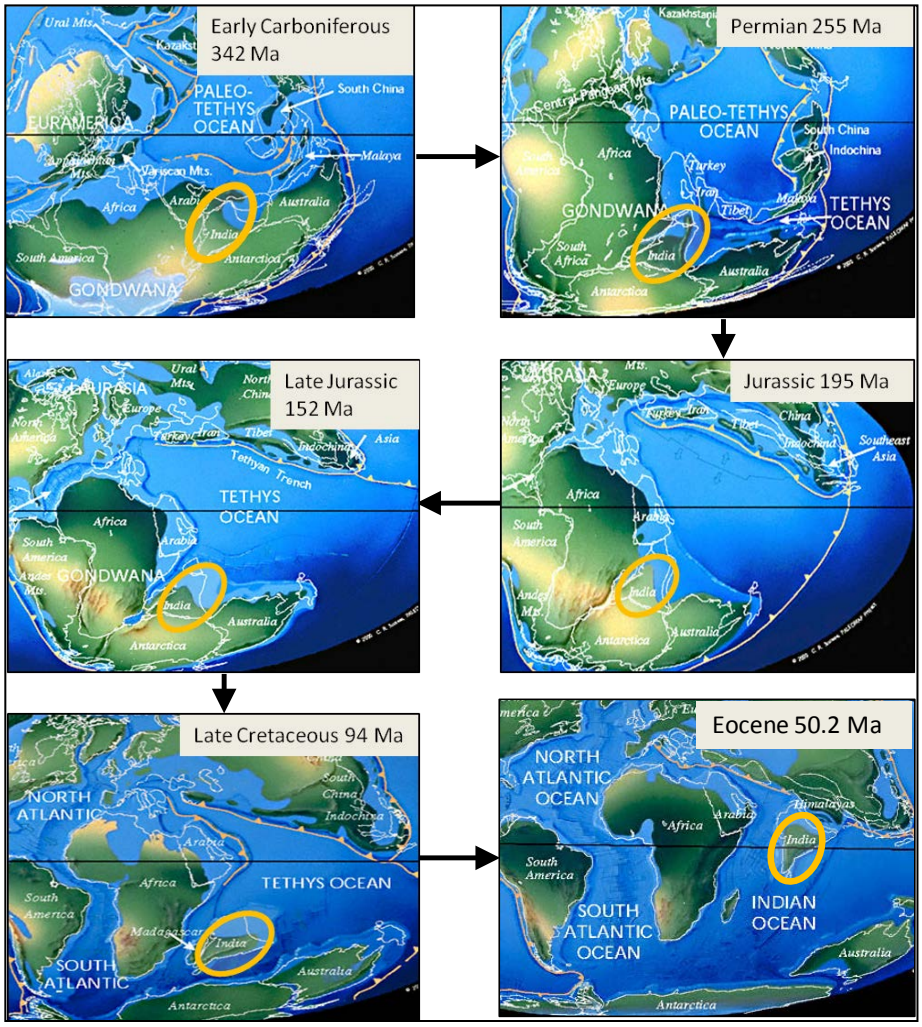

Figure 3.3 Paleogeography of Gondwanaland at different stages (from http://www.scotese.com/earth.htm) (Orange circles represent positions of India with time).

3.3 FACIES AND CLIMATES DURING DEPOSITION OF GONDWANAN SEQUENCES

Paleoclimatic changes played an important role in controlling sedimentation patterns in Gondwanan basins. Several studies have documented the importance of climate and source rock

composition (Mann and Cavarock, 1973; Basu, 1975; Young, 1976; Suttner et al., 1981; Fluteau et al., 2001). Climatic change has an effect on variables such as source rock composition, depositional environment, and distance of transportation, which control the composition of sediments (e.g., sand, and shale) and the presence of coal, etc. (Basu, 1975; Young, 1976; Ray and Chakraborty, 2002). Changes in paleoaltitude due to ongoing tectonic activity also may influence sedimentation in a particular basin.

Initial sedimentation in Gondwanan basins was in glacial and pro-glacial environments. Tillite, glacio-fluvial sandstone-conglomerate, and glacio-lacustrine mudstone represent the glaciogene succession (Pascoe, 1959). Dutta (2002) also postulated that meandering channel and flood plain deposits were laid down as outwash from glaciers and glacial lakes. Channels were filled by fluviatile sandstone-conglomerate (Ghosh and Mitra, 1975), and lakes were filled with argillaceous sediments (varved mudstone or as turbidites) (Banerjee, 1966; Ghosh and Mitra, 1975). Presence of multiple sedimentary cycles with coarse sandstone and/or lag conglomerate and at their bases and with fine-grained clastics (shale) or coal at tops indicate that the depositional basin was shallow and subject to episodic subsidence (Dutta, 2002). During the Triassic, coal-bearing facies were replaced by red-bed sequences (Dutta, 2002) characterized by alternating red shale and feldspathic sandstone. Red bed sequences are generally very thick, although they are absent in extra-peninsular Gondwanan sequences (Dutta, 2002).

Following the Triassic, the entire source area was uplifted. Tectonic uplift together with climatic changes resulted in a change from a predominantly arid regime to a warm humid one. Climatic changes resulted in deposition of very mature sediments, while tectonic uplift caused river systems to change from meandering to braided (Dutta, 2002). Thus, coarse-grained conglomerates, pebbly sandstones, and sandstones were deposited. The maturation of sand

composition increases with decreasing relief and increasing current energy (Sweet et al., 1971; Flores, 1972; Ethridge, 1977; Mack, 1984).

CHAPTER 4: SANDSTONE PETROGRAPHY

4.1 INTRODUCTION

Sandstone petrography is a widely used and well established tool to evaluate the provenance of sediments. Sandstone composition is primarily controlled by provenance, nature of depositional basins, and travel path, which are closely linked to plate tectonic settings (Dickinson and Suczek, 1979). The relative abundance of major framework grains (e.g., quartz, feldspar and lithic fragments) can be plotted on various ternary diagrams with provenance fields (Dickinson and Suczek, 1979; Ingersoll and Suczek, 1979; Dickinson, 1985). For example an overwhelming abundance of quartz generally indicates a passive tectonic setting, whereas limited quartz and abundant volcanic lithic fragments suggest a magmatic provenance (Crook, 1974). These relationships enable interpretation of paleogeography, paleoclimate, ancient plate tectonic settings (Graham et al., 1976; Dickinson and Suczek, 1979; Sitaula, 2009), and uplift and exhumation histories (Graham et al., 1976; Peavy, 2008) from the sedimentary record.

Detailed studies of provenance based on petrography are based on the assumption that detrital mineralogy was not altered significantly by sedimentary processes such as transportation, depositional environment, climate, and diagenesis (Basu, 1975). Hence, interpretation of sediment compositional data requires that these factors be considered (Suttner, 1974; Johnsson, 1993). Mixing of sediments from different sources complicates the interpretation of provenance (Velbel, 1985). Multiple source identification requires multiple basin analytical techniques such

as mineral chemistry, bulk-rock chemistry, traditional modal analysis and thermochronology (Morton and Hallsworth, 1999; Peavy, 2008).

Gondwanan sequences have been encountered at several locations in northwestern Bangladesh (Fig. 1.3). Except for one (Maddhapara), all of these localities are well known for their coal deposits. Representative well logs from five localities (Singra, Kuchma, Jamalganj, Barapukuria, and Khalahspir) are presented in figure 4.1 to show the general vertical distribution of Gondwanan deposits.

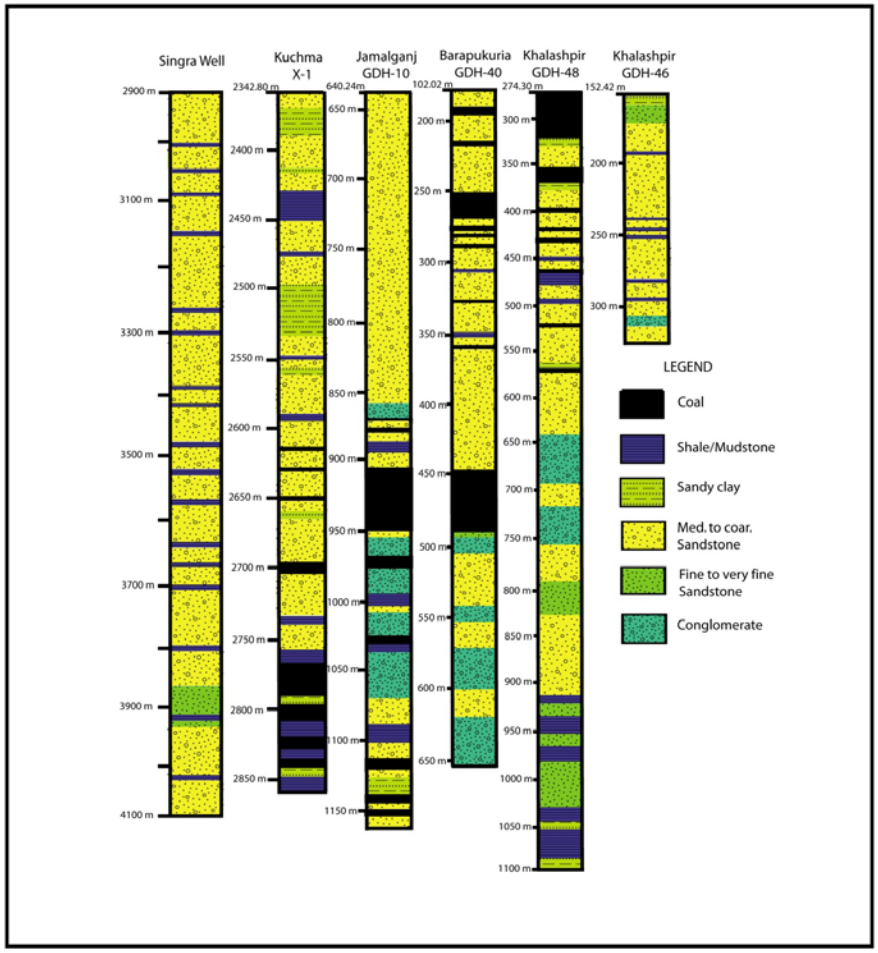

Figure 4.1 Lithologic logs (Gondwanan portion) of wells drilled in different basins in northwestern Bengal basin (depth below ground level; after Uddin and Islam, 1992; Singra well from Reimann, 1993).

4.2 METHODS

A total of thirty-nine sandstone samples from different stratigraphic levels within both the Kuchma and Paharpur formations were collected from three cores reposited by the Geological Survey of Bangladesh and Barapukuria Coal Mining Project in Dinajpur. Samples were collected from well GDH 46 at Khalashpir (Figure 1.3) at depths ranging from ~270 to 450 m (Figure 4.2), and well DOB-02 and DOB-04 at the Barapukuria (Figure 1.3) coal mine at depths ranging from ~130 to 360 m and ~135 to 385 m, respectively (Figure 4.3). The samples were prepared in the rock preparation lab in the Department of Geology and Geography at Auburn University and sent to Spectrum Laboratories to prepare petrographic thin sections. Half of each sample was stained with Alizarin red and barium sulphate in order to facilitate identification of feldspars. Compositional analyses were carried out using the Gazzi-Dickinson point count method (Dickinson, 1970; Ingersoll et al., 1984). This method is used because it minimizes the effects of differences in grain size. A minimum of 300 framework grains were counted in each of the samples. Then these framework grains are normalized to 100% using all the end members using quartz, feldspar, and lithic fragments. The following compositional parameters (Table 4.1) were calculated: Qt = Total Quartz; Qm = monocrystalline quartzose grains; Qp = polycrystalline quartz grains, including chert grains; F = total feldspar grains; P = plagioclase feldspar grains; K = potassium feldspar grains; L = lithic fragments; Lt = total lithic fragments; Ls = sedimentary lithic fragments; Lv = volcanic lithic fragments; Lm =metamorphic lithic fragments. Data were plotted on different ternary diagrams (QtFL, QmFLt) to evaluate out the tectonic settings (Dickinson, 1970; Dorsey, 1988; Uddin and Lundberg, 1998a).

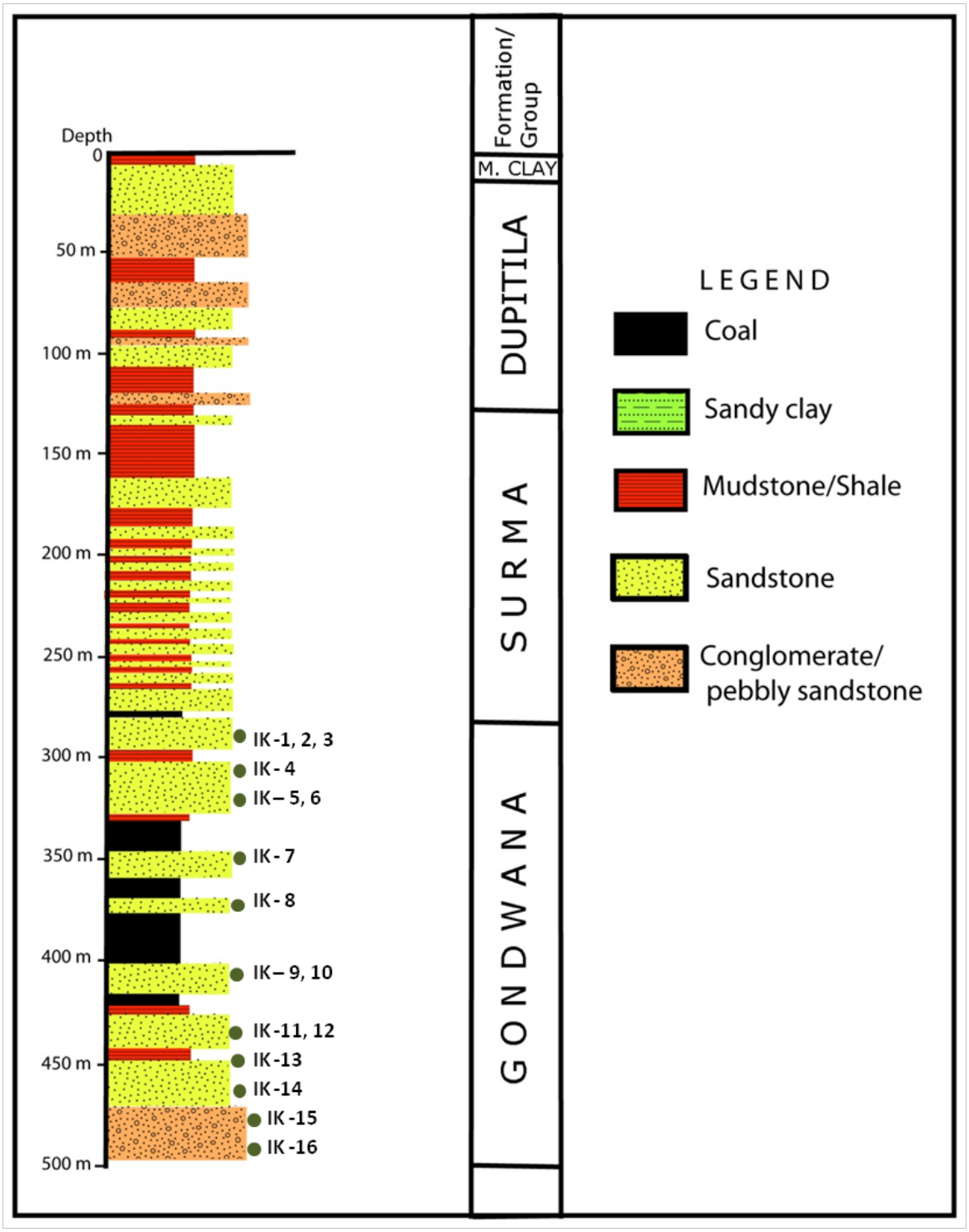

Figure 4.2 Stratigraphy of GDH 46 well of the Khalashpir basin (green dots represent sample location; after Islam et al., 1992).

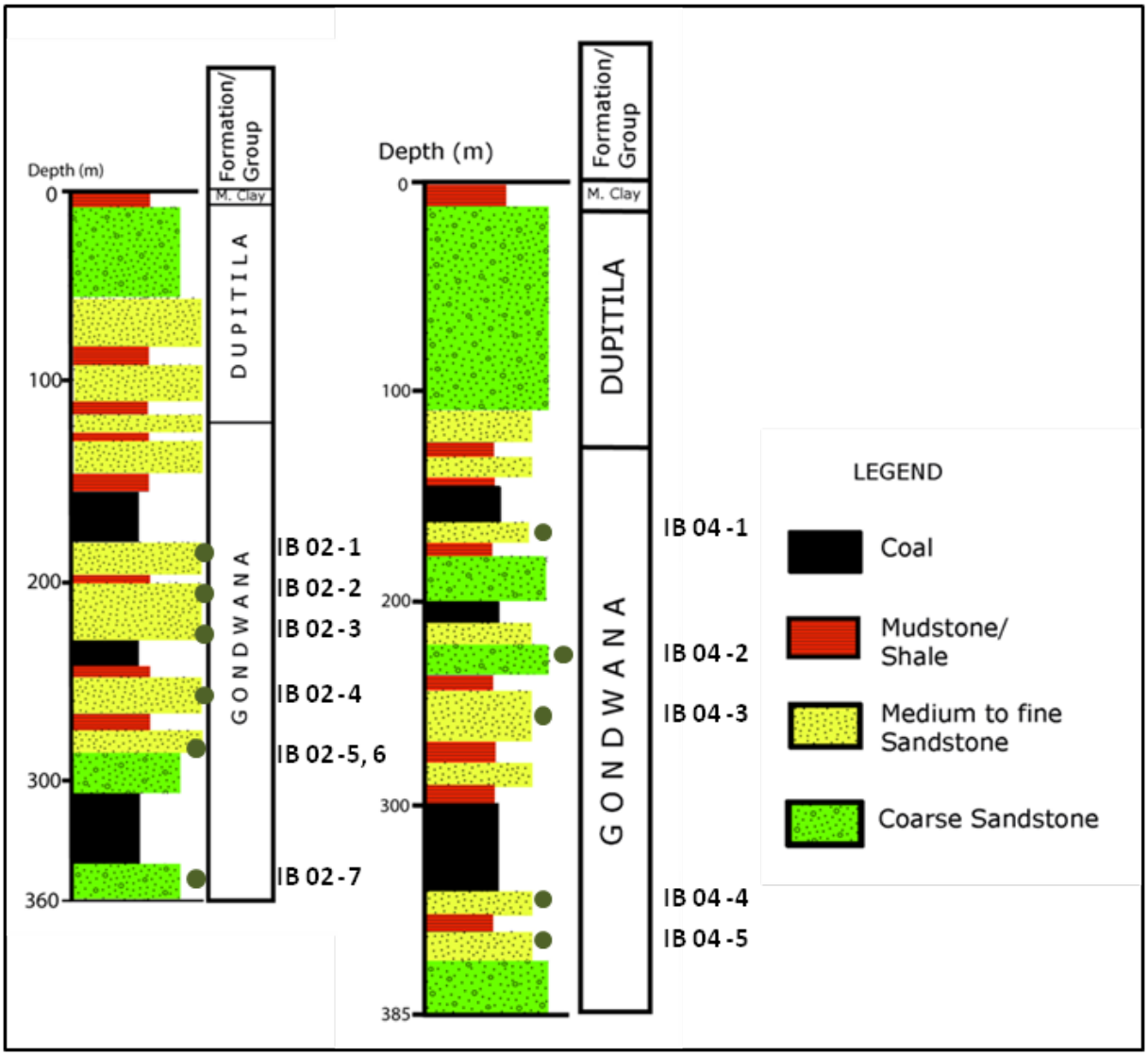

Figure 4.3 Stratigraphy of DOB 02 (left) and DOB 04 (right) well of the Barapukuria coal basin (green dots represent sample location; after Bakr et al., 1996).

All quartz grains are plotted at the Qt end member for QtFL plot. However, polycrystalline quartz and chert are included in the Lt end-member for QmFLt plots. For all major framework grains, normalized sandstone modal compositions are given in Table 4.2.

Table 4.1 Recalculated modal parameters of sand and sandstone.

Primary parameters (after Graham et al., 1976; Dickinson and Suczek, 1979; Dorsey, 1988; Uddin and Lundberg, 1998a)
Qt = Qm + Qp, Where, Qt = total quartzose grains Qm = monocrystalline quartz (> 0.625 mm) Qp = polycrystalline quartz (including chert)
Feldspar Grains (F=P+K), where F = total feldspar grains P = plagioclase feldspar grains K = potassium feldspar grains
Unstable Lithic Fragments (Lt = Ls + Lv + Lm), where Lt = total unstable lithic fragments and chert grains Lv = volcanic/metavolcanic lithic fragments Ls = sedimentary/metasedimentary lithic fragments Lm_1 = very low- to low-grade metamorphic lithic fragments Lm_2 = low- to intermediate-grade metamorphic lithic fragments

4.3 PETROGRAPHY

Gondwanan sequences record the history of pre-Himalayan orogenesis and of dispersal and distribution of Gondwanaland. The Gondwanan Group of northwestern Bengal Basin, which consists of the Kuchma and Paharpur formations, records sedimentation during the early Permian that is equivalent to Lower Gondwanan (Islam et al., 1992). These sediments are continental and deposited in cold climatic conditions. Sediments of these Gondwanan basins are primarily glacial in origin but also include fluvial sandstone and shale or mudstone (Dutta, 2002). The presence of coarse conglomerate beds of braided river systems indicates channel and/or lag deposits (Sengupta, 1970) with coal.

The petrography of Gondwanan sequences of northwestern Bengal Basin are discussed below.

4.3.1 PETROGRAPHY OF KHALASHPIR COAL BASIN

Rocks of the Gondwanan group of Khalashpir Basin have not been assigned to any particular formation. However, the lithological character and thick coal beds with characteristic *Glossopteris and Gangamopteris* flora suggest that these strata might be equivalent to Lower Gondwanan rocks found in India and other parts of the world (Islam et al., 1992). Based on lithology and coal geochemistry, the Paharpur Formation and Kuchma Formation in the Khalshpir basin are considered to be equivalent to the Raniganj Group and Barakar Group in India Group (Zaher and Rahman, 1980).

The depositional sequences of the Gondwanan Group in the Khalashpir basin consist of alternating sandstone and mudstone with coal layers of variable thickness. The grain size decreases upward. The bottom parts of the sequences are characterized by pebbly sandstone and conglomerate.

Twenty-two (22) core samples were collected from the GDH-46 well at Khalashpir from different stratigraphic levels for petrographic studies. Abundance of framework grains in the sandstones from this core are, in a descending order, quartz, feldspar, mica, organic matter, and lithic fragments. The modal composition of the Khalashpir core sandstones is $Qt_{58}F_{30}L_{12.}$ Quartz grains are sub-angular to rounded, and monocrystalline quartz is dominant over polycrystalline quartz. Coarser of polycrystalline quartz grains are observed locally (Fig. 4.4).

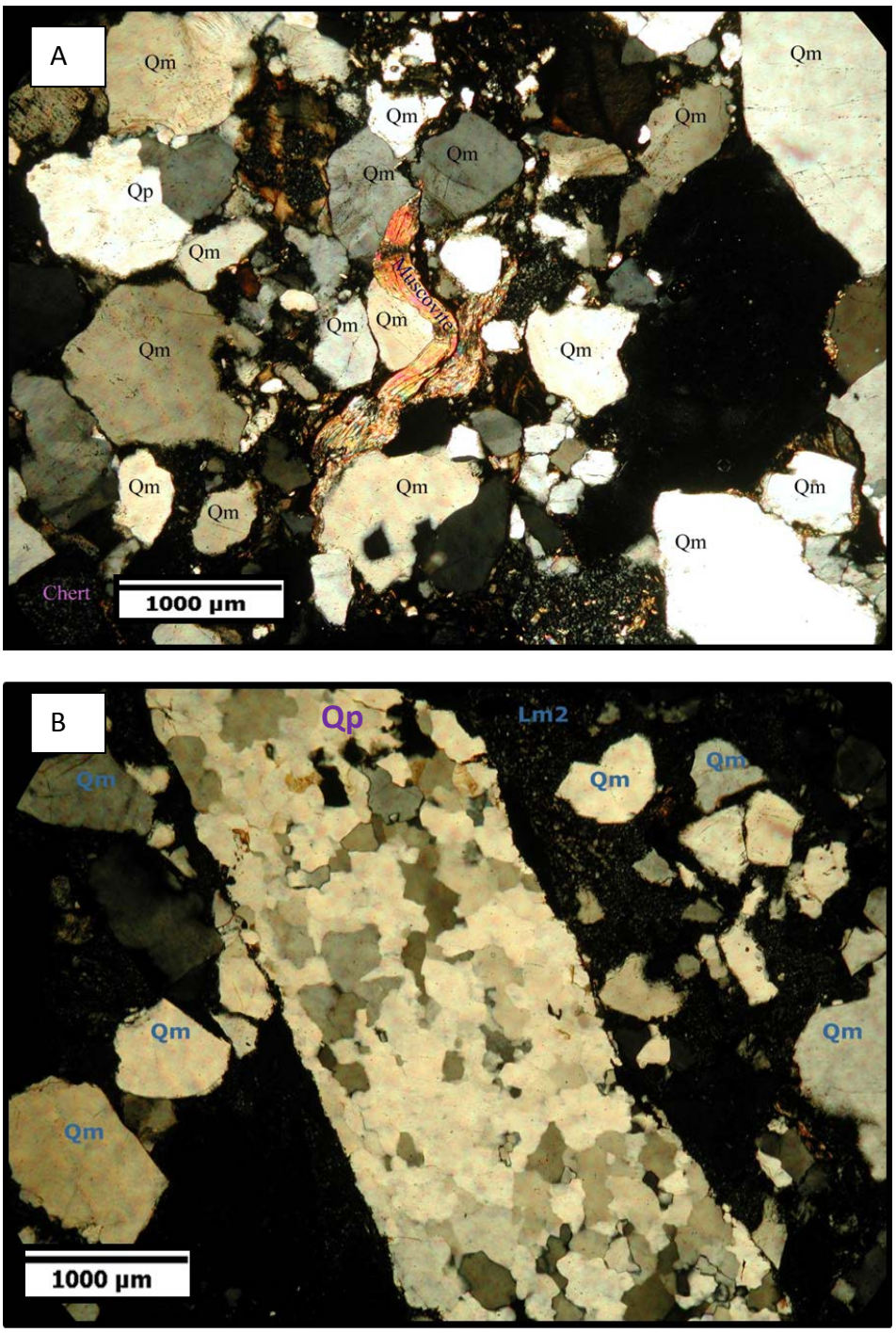

Figure 4.4 (A-B) Representative photomicrographs of Gondwanan sandstones of northwestern Bengal Basin from Khalashpir coal basin (Qm = monocrystalline quartz, Qp = polycrystalline quartz, Lm_2=upper grade metamorphic lithic fragments); Photomicrograph A shows ductility deformed muscovite as well as dominance of monocrystalline quarts grains, and B includes a clast of polycrystalline quartz.

Both plagioclase and K-feldspar are observed in significant amounts. Feldspar grains are variably alterated to sericite or clay minerals. Muscovite and biotite are also present. Organic matter is also present. Lithic fragments are the least abundant framework grains present in these sandstones. Sedimentary lithic fragments are dominant, although some volcanic and metamorphic lithic grains are observed. Chert is dominant among all the sedimentary lithic fragments (Fig 4.5-A). Some mudstone lithics were identified. Mudclasts are reddish because of leaching of iron rich solutions which eventually developed iron encrustations. Grain contacts are mostly line and point throughout the sequence although some concavo-convex contacts were found. Matrix is more common than cements (siliceous).

Quartz grains from some horizons exhibit Boehm lamellae (Fig 4.5-B). Thses represented by warped, sub-parallel lines of very small bubble inclusions. Such features in quartz crystals are caused by intense strain and deformation of grains (Scholle, 1979).

Probable mud injections were observed in four different stratigraphic levels of Khalashpir well (Fig 4.6). This may be related to tectonic instability such as a combination of high rates of sedimentation and tectonic compression. The mud injections may have formed by rise of fluidized sediments along faults (Milkov, 2000).

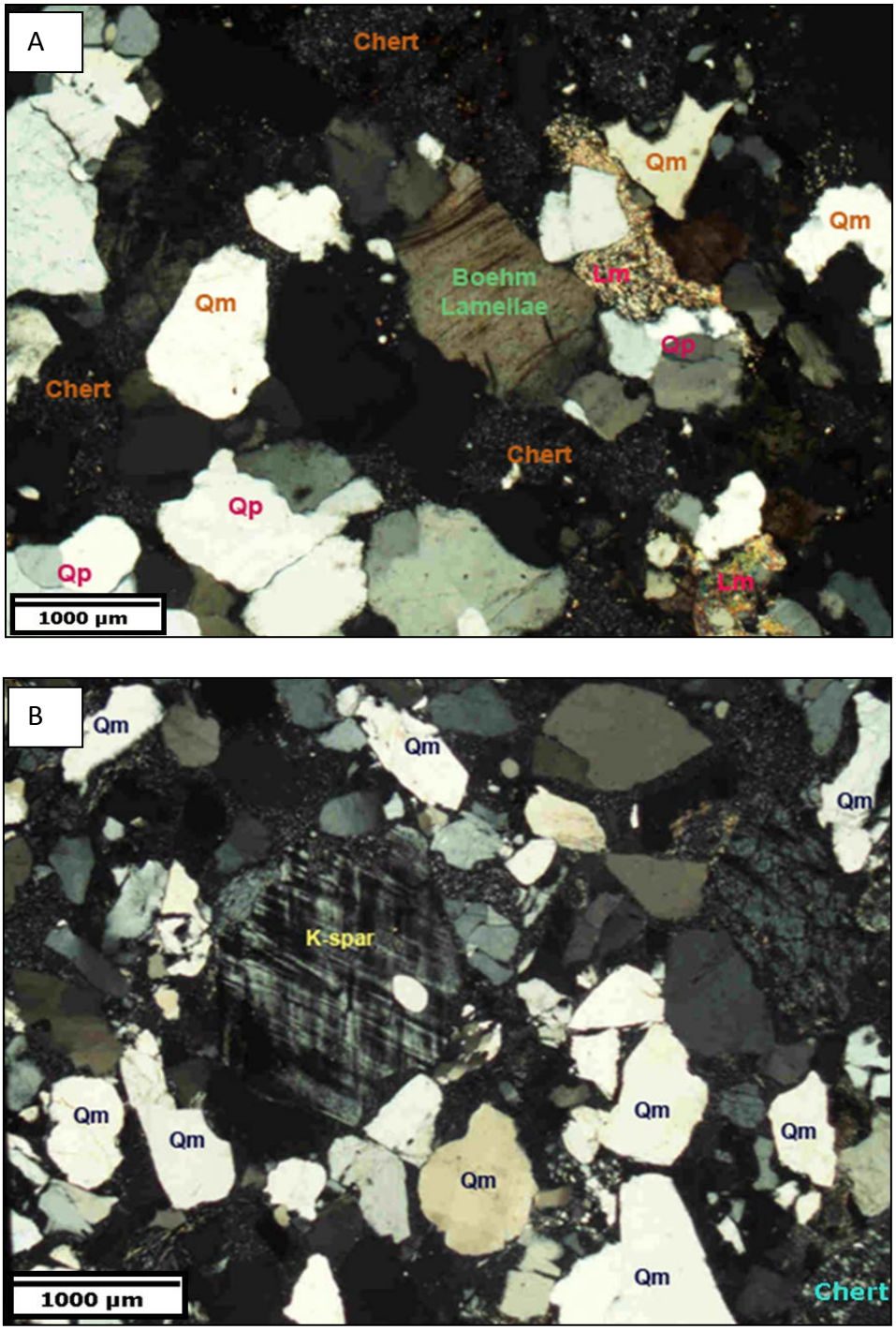

Figure 4.5 (A-B) Representative photomicrographs of Gondwanan sandstones of northwestern Bengal Basin from (A) Khalashpir coal basin and (B) Barapukuria coal basin (Qm = monocrystalline quartz, Qp = polycrystalline quartz, Lm = metamorphic lithic fragment).

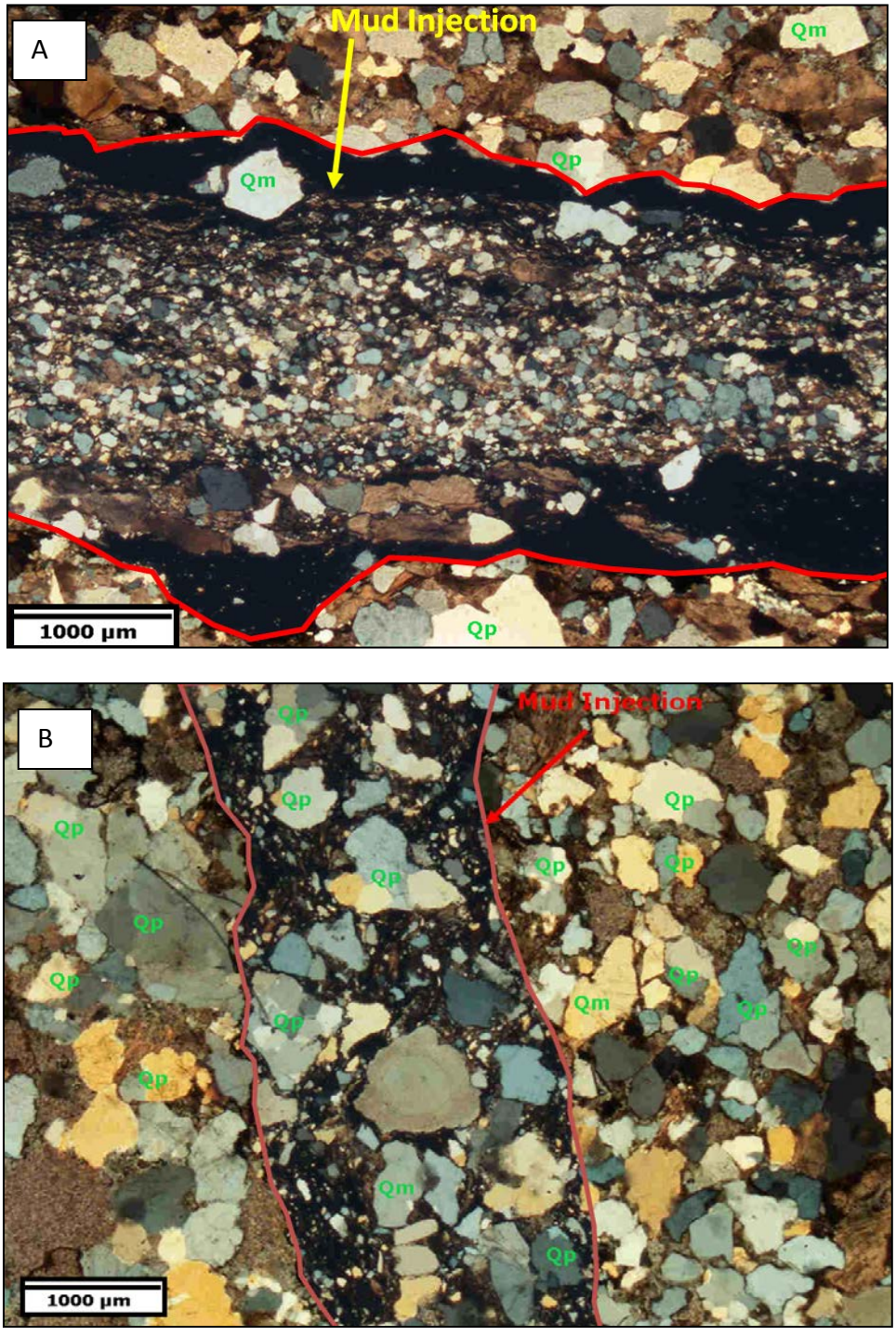

Figure 4.6 (A-B) Representative photomicrographs of Gondwanan sandstones of northwestern Bengal Basin from Khalashpir coal basin (Qm = monocrystalline quartz, Qp = polycrystalline quartz). Both photomicrographs show mud injections from different stratigraphic levels.

4.3.2 PETROGRAPHY OF BARAPUKURIA COAL BASIN

The Barapukuria basin area is covered with Holocene alluvium and Pleistocene Barind Clay. The stratigraphic succession of this basin has been established on the basis of borehole data (Bakr et al., 1986; Islam et al., 1987). The sedimentary units encountered in boreholes include the Gondwanan Group (Permian), Dupi Tila Formation (Pliocene), Barind Clay (Pleistocene), and Holocene Alluvium.

The Barapukuria coal mine is located about 80 km north of Khalashpir. A total of fifteen core samples were collected from two exploratory drill wells (DOB 2 and DOB 4) representing different stratigraphic levels. Eight samples were taken from DOB 2 and seven were from DOB 4.

Grain size generally decreases with height in the Gondwanan sequence. The lower part of the group is characterized by conglomerates that unconformably overlie the Archean basement complex. Clasts are mostly angular to subrounded granules, pebbles, and cobbles (Bakr et al., 1986). Sandstone and carbonaceous material locally are present between the conglomerate beds.

The samples studied from Barapukuria coal mine are mostly arkosic, although some samples are quartz arenitic and litharenitic. Core samples are quartz-rich but also include, in descending order, feldspar, mica, organic matter and lithic fragments. Lithic fragments are more abundant in Barapukuria samples than in Khalashpir samples. Sedimentary lithics are dominant. The sandstones are overall very poorly sorted, angular to sub-angular and immature. Samples studied from Barapukuria are more poorly sorted than the samples from Khalashpir. Average modal composition of Barapukuria sandstones is $Qt_{52}F_{31}L_{17;}$ samples from wells DOB 2 and DOB 4 have modal compositions of $Qt_{49}F_{33}L_{18}$ and $Qt_{55}F_{29}L_{16}$ respectively. Monocrystalline quartz crystals are more abundant than polycrystalline quartz. K-feldspar is dominant over

plagioclase feldspars. Plagioclase is more common in Barapukuria samples than in Khalashpir samples (Figs. 4.7 and 4.8).

Feldspars are weathered but not as intensely as those observed in Khalshpir samples. The appearance of feldspar crystals vary from fresh to highly altered. This again may be due to compositional differences among feldspar grains. In some samples, feldspar grains were very large and could be seen without the aid of a microscope.

4.4 SANDSTONE MODES

Vertical changes in sandstone modal composition in each of the three studied cores are shown in Figure 4.9 (Table 4.2). Sandstones are mostly arkosic, although composition does vary. Sandstone modes from all the samples from the three cores are plotted in Figure 4.10 (McBride, 1963). All plots show that the average sandstone falls in the lithic arkose field. However, sandstone mode for the Khalashpir sample falls closer to the boundary of the arkose field. Of the two Barapukuria cores, DOB-02 samples are slightly more feldspathic.

Overall quartz percentage is higher in Khalashpir samples than Barapukuria samples. However, Barapukuria DOB 4 samples are more quartzose than those in core DOB 2. The samples from the Barapukuria coal mine area contain more lithic fragments than those from the Khalashpir area.

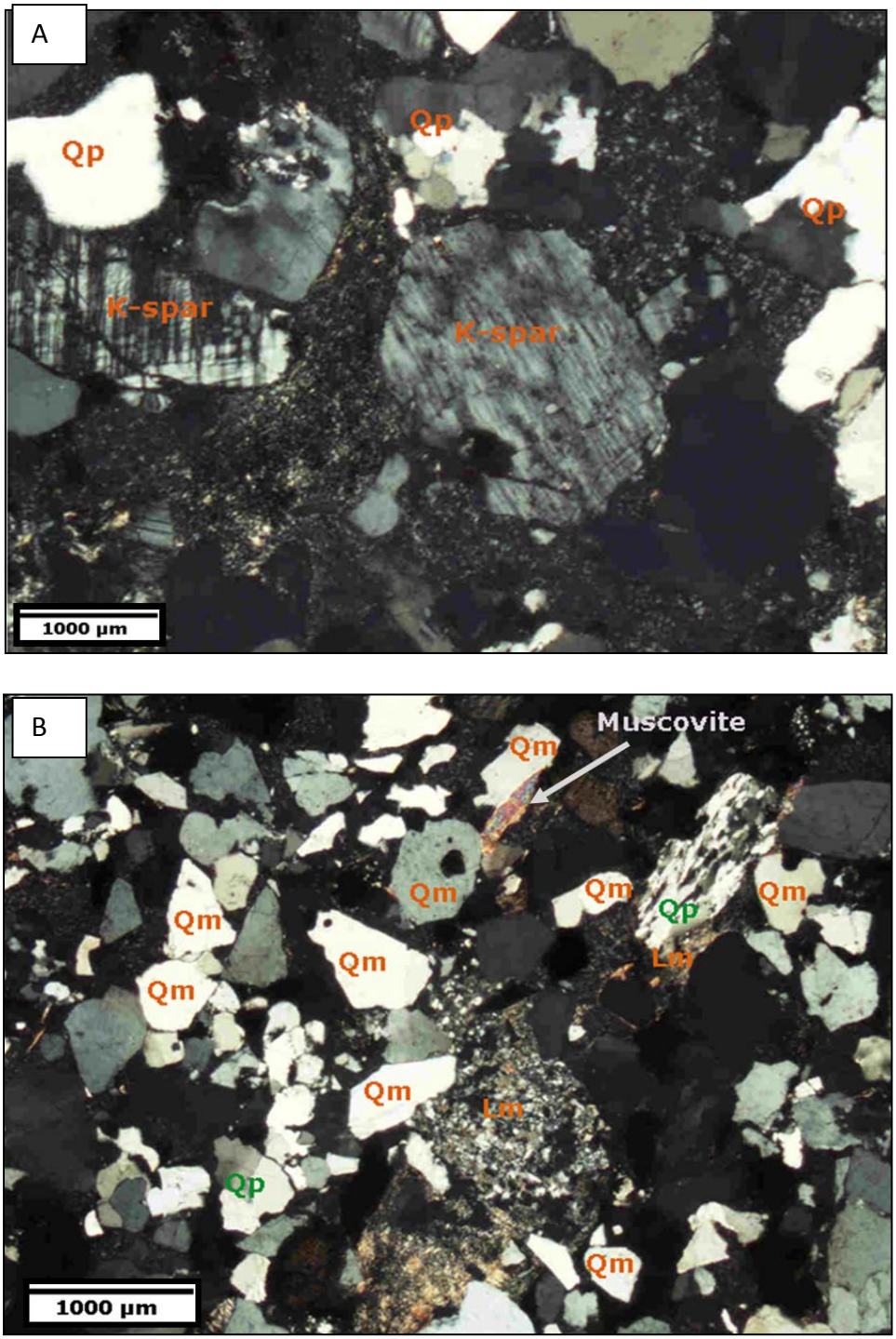

Figure 4.7 (A-B) Representative photomicrographs of Gondwanan sandstones of northwestern Bengal Basin from Barapukuria (Qm = monocrystalline quartz, Qp = polycrystalline quartz, K-spar = potassium feldspar, Lm = metamorphic lithic fragment).

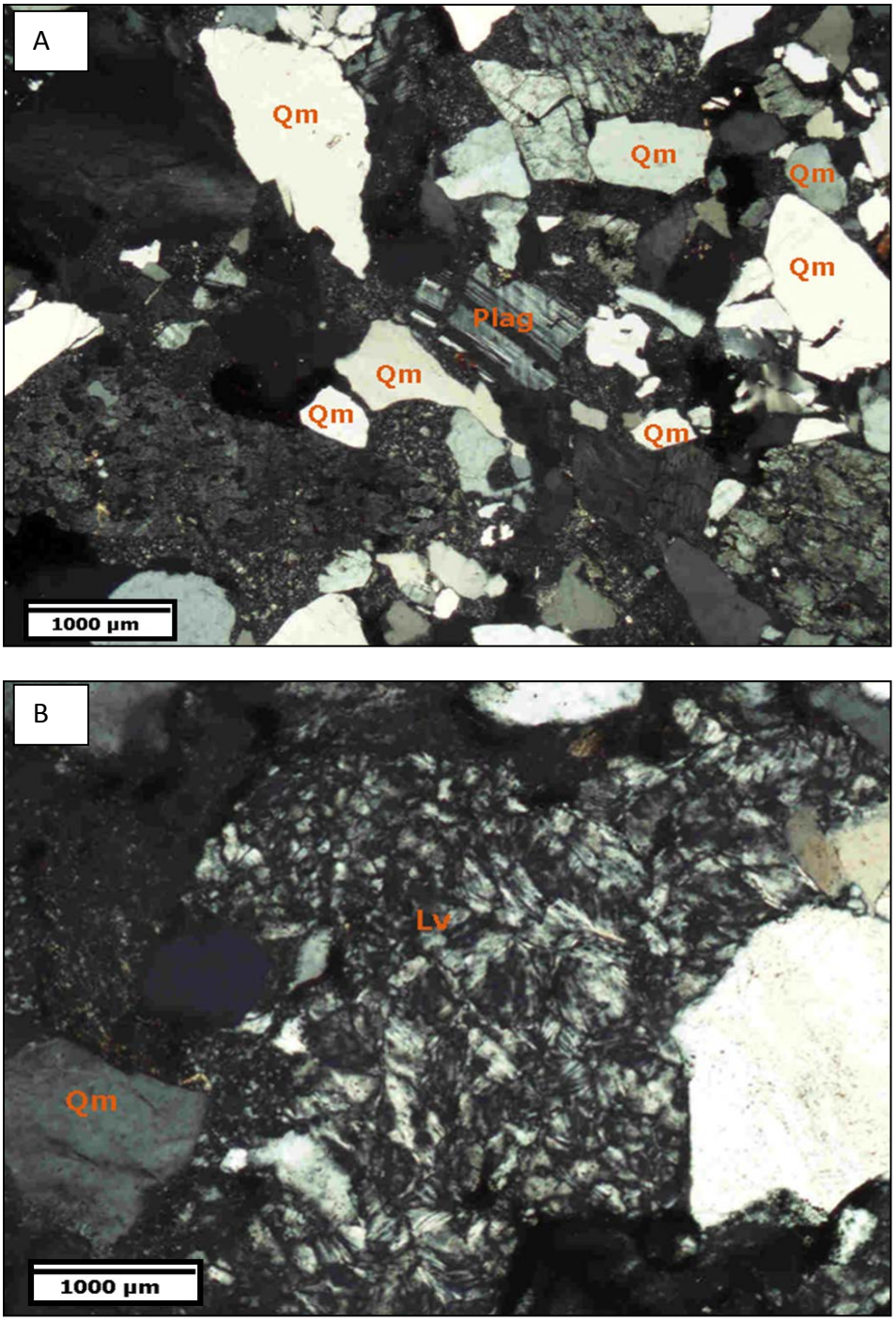

Figure 4.8 (A-B) Representative photomicrographs of Gondwanan sandstones of northwestern Bengal Basin from Barapukuria (Qm = monocrystalline quartz, Qp = polycrystalline quartz, Plag = plagioclase feldspar, Lv = volcanic lithic fragment).

Table 4.2 Normalized modal compositions of Gondwanan sandstones in Bengal basin from Khalashpie and Barapukuria.

Sample Location	Core Name	Core Depth (m)	Sample No.		Qt	F	L		Qm	F	Lt		Qm	P	K
		276.81	IK-1		54	26	20		47	26	27		64	33	3
		285.55	IK-2		75	15	10		68	15	17		82	1	17
		295.48	IK-3		71	17	12		55	17	28		76	1	23
		310	IK-4		68	12	20		61	12	27		83	1	16
		317	IK-5		70	18	12		58	18	24		76	5	19
		325.77	IK-6		48	36	16		40	36	24		52	45	3
		351.61	IK-7		55	29	16		40	29	31		58	3	39
Khalashpir	GDH 46	370.39	IK-8		51	30	19		39	30	31		39	26	35
		410.06	IK-9		48	41	12		33	41	26		45	25	30
		415	IK-10		53	42	5		33	42	25		44	24	32
		435	IK-11		50	44	6		30	44	26		40	26	34
		445	IK-12		64	34	2		44	34	22		55	35	10
		450	IK-13		60	22	18		51	22	27		70	26	4
		465	IK-14		71	10	19		58	10	32		86	0	14
		480	IK-15		65	25	10		54	25	21		45	40	15
		494	IK-16		60	27	13		28	27	45		52	10	38
			Average		60	27	13		46	27	27		60	19	21
		182	IB 02-1		43	50	7		31	50	19		39	39	22
		201.68	IB 02-2		44	41	15		38	41	21		48	39	13
		240	IB 02-3		40	46	14		33	46	21		42	9	49
	DOB 02	265	IB 02-4		63	11	26		58	11	31		84	13	3
		283	IB 02-5		32	46	22		26	46	28		36	12	52
Barapukuria		289	IB 02-6		68	7	25		60	8	32		89	4	7
		351	IB 02-7		49	31	20		38	31	31		55	5	40
			Average		49	33	18		41	33	26		56	17	27
		163	IB 04-1		86	0	14		71	0	29		100	0	0
		239	IB 04-2		37	43	20		31	44	25		42	10	48
	DOB 04	255	IB 04-3		28	52	20		23	52	25		31	40	29
		351	IB 04-4		72	5	23		65	5	30		94	0	6
		360	IB 04-5		54	43	3		44	43	13		50	48	2
			Average		55	29	16		47	29	24		63	20	17

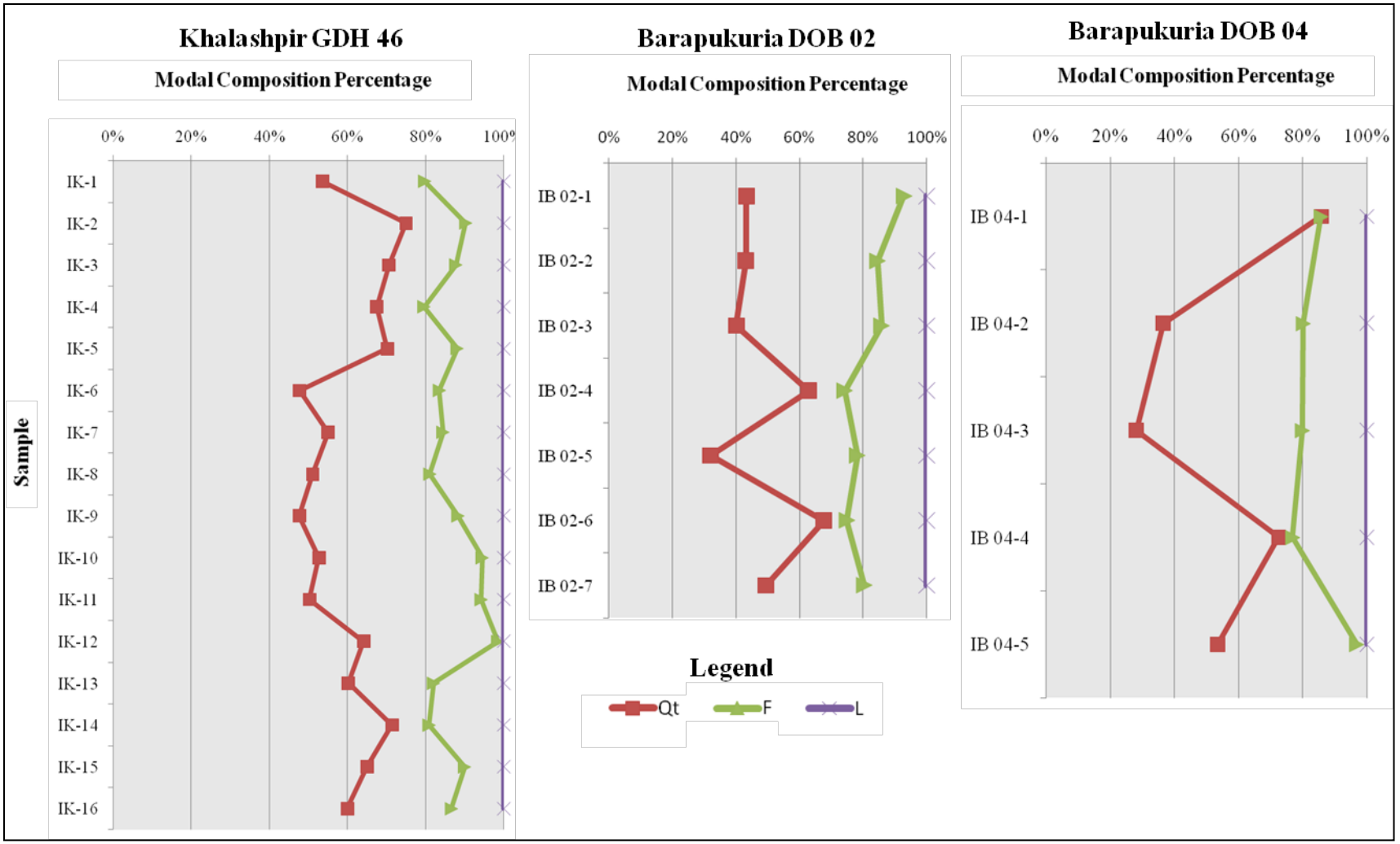

Figure 4.9 Vertical variation of modal composition of the Gondwanan sandstones in the three cores.

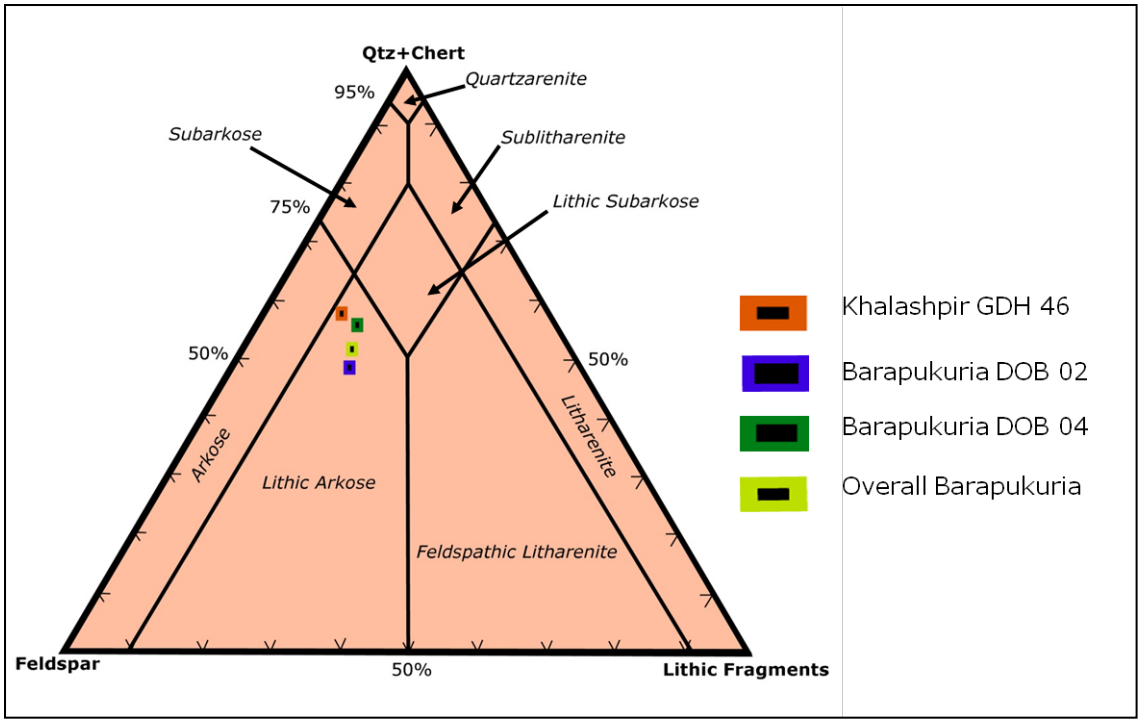

Figure 4.10 Average modal compositions of the Gondwanan sandstones from the three cores (after McBride, 1963).

4.5 PETROFACIES EVALUATION

Additional ternary plots were prepared in order to discriminate the possible tectonic settings from which siliciclastic sediments were derived. Sandstone modes from the three different cores are used. Since both DOB 02 and DOB 04 are from the same area, an overall mode of sandstone composition is used for the Barapukuria area. The QtFL plots suggest contribution of sediments from multiple sources (Fig. 4.11). These include craton interior, transitional continent, basement uplift, dissected arc, and recycled orogen provenance fields (Dickinson, 1985).

The QtFL plot shows that the Gondwanan sandstones from Khalashpir GDH-46, Barapukuria DOB 02, and DOB 04 represent mostly recycled orogen. However, some samples fall within transitional continental and dissected arc areas. There are several tectonic settings

from which orogenic sediments could be derived. These include subduction zones, backarc thrustbelts, and suture belts (Dickinson, 1985). Major river systems that are contemporaneous with orogenesis also can transport sediments from adjacent continental blocks to the basin (Potter, 1978).

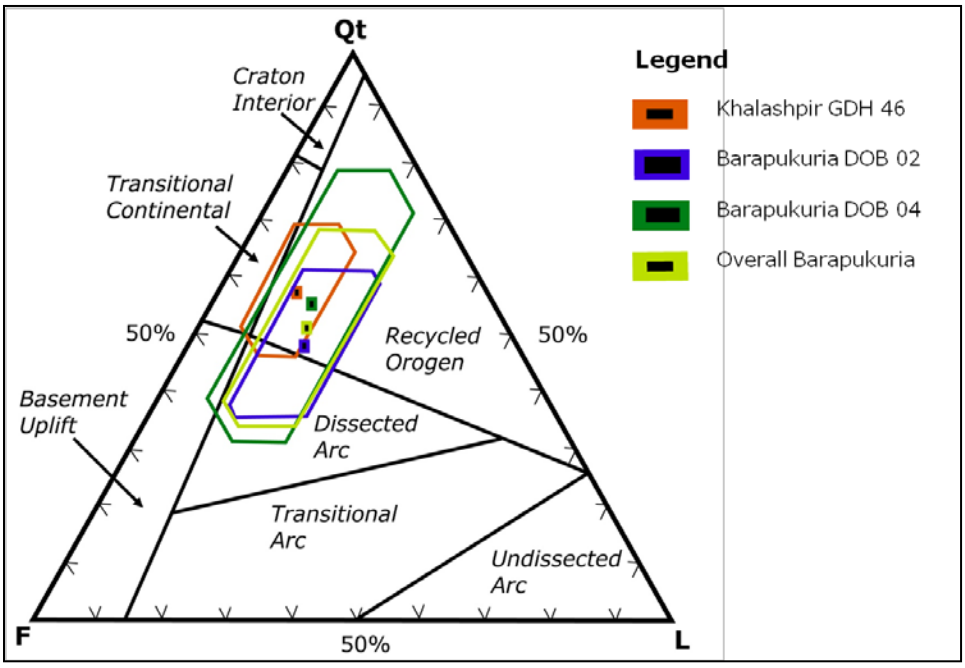

Figure 4.11 QtFL plot of Gondwanan sandstone samples showing mean and standard deviation polygons (provenance fields from Dickinson, 1985).

The QmFLt triangular plots using sandstone modes for all the wells show similar type distribution (Fig. 4.12). These are dominantly quartzose recycled, mixed recycled, and dissected arc. However, sandstones from well DOB-4 falls partially within basement uplift zone.

QmPK triangular plot suggests that potassium feldspar is dominant over plagioclase feldspar (Fig. 4.13). But the ratio between the two types of feldspars varies from well to well. Overall Barapukuria has more potassium feldspar than Khalashpir.

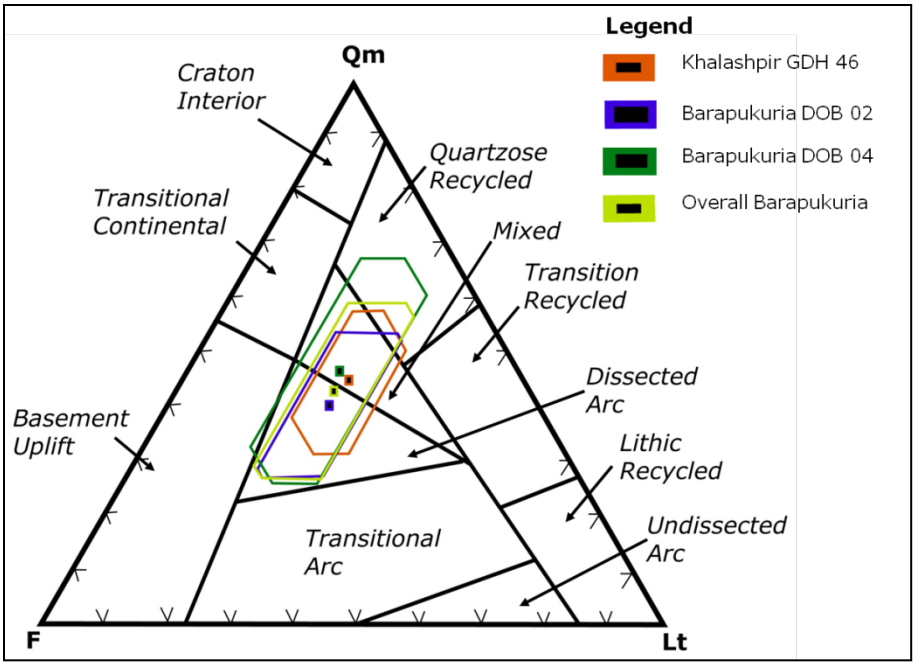

Figure 4.12 QmFLt plot of Gondwanan sandstone samples showing mean and standard deviation polygons (provenance fields from Dickinson, 1985).

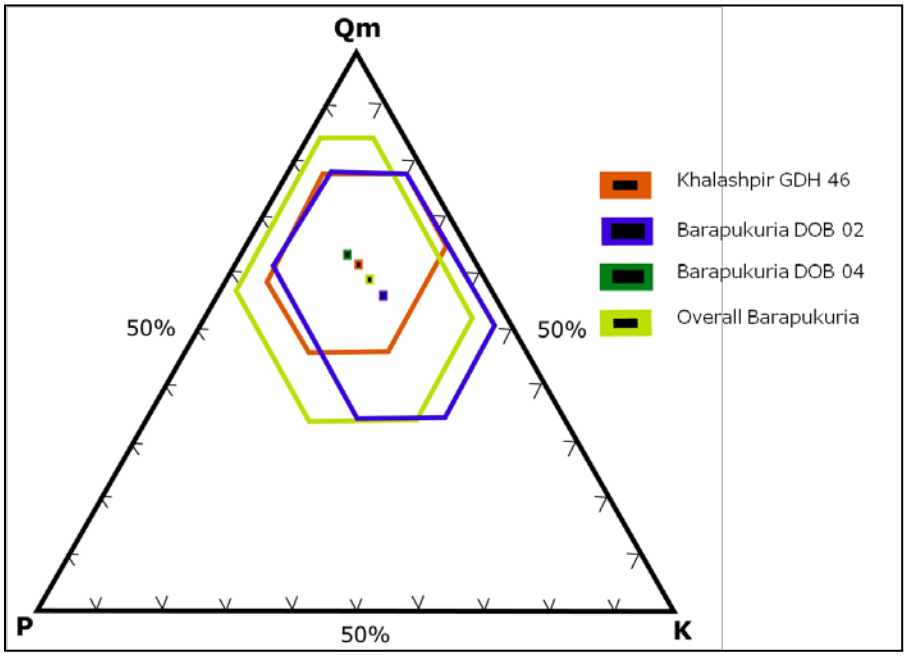

Figure 4.13 QmPK plot of Gondwanan sandstone samples showing mean and standard deviation polygons.

The sandstones from both Khalashpir and Barapukuria coal mines also reflect sediments sources from transitional continental, basement uplift, and dissected arc (Fig. 4.12 and 4.13). Sediment sources from the continental blocks are either on stable shields and platforms or from uplift along plate boundaries. The basement uplift tectonic setting is characterized by the onset of rifting, transform ruptures, deepseated thrusts, and wrench tectonism. These settings yield mostly quarztofeldspathic, lithic poor sands. The transitional continental setting forms the intermediate area between craton interior and basement uplift. The transitional continental group is mostly associated with feldspathic sands derived from basement uplifts (Dickinson, 1982). In the study area, these sediments may have been derived from adjacent Indian craton. However the Meghalayan craton located to northeast of the study area also could have contributed sediments to the Gondwanan sediments of northwest Bangladesh.

Several orogenies have been inferred for Neoproterozoic to Late Paleozoic time. These are collectively known as Terra-Australis Orogen (Cawood, 2005). This orogen had a length of ~18,000 km and was about 1600 km wide along the margin of Gondwanan continental blocks. This orogen includes the Tasman, Ross, and Tuhua orogens of Australia, Antarctica, and New Zealand, respectively, as well as the Andean Cordillera of South America. The Terra-Australis Orogen as a whole consisted of numerous basement blocks of both continental and oceanic origin (Cawood, 2005). These orogens can be further subdivided on the basis of pre-orogenic geographic affinity (Laurentia versus Gondwanan) and proximity to inferred continental margin sequences (peri-Gondwanan versus intra-oceanic). Orogenesis began around 570 Ma along the Gondwanan margin with initiation of subduction of the Pacific Ocean. This represents a time of major global plate reorganization associated with the final assembly of Gondwanan continents

and opening of the Iapetus Ocean. The Terra Australis orogenesis terminated around 300 – 250 Ma, associated with assembly of the Pangea.

Assembly of the various continental blocks of East and West Gondwanan into a coherent Gondwanan supercontinent along the East African, Pinjarra, Damara, and Braziliano orogens ("Pan-African") by the early Paleozoic resulted in propagation of the Terra Australis Orogen along the entire Pacific/Iapetus margin of Gondwana. However, the Gondwanan sediments of northwestern Bengal Basin were not in close proximity to any of the Terra Australis Orogenic belts. In the global plate reorganization, India and the Terra Australis Orogen were positioned on oposite sides of Antarctica and Australia. However, the Pinjarra Orogen, which was located between Western Australia and eastern India, could have been a possible source of sediments in the study area (Collins, 2003; Cawood, 2005; and Collins and Pisarevsky, 2005).

Early Paleozoic tectonism in the proto-Himalayas was inferred by Gehrels et al. (2003). Along the northern margin of Indian craton in the Lesser Himalaya, strata overlain by the Main Boundary Thrust (MBT) are mainly of Proterozoic age. Lesser Himalayan rocks are overlain by crystalline thrust sheets along the Mahabharat thrust in the lower portions of the Himalayas. These are mostly composed of Neoproterozoic to Lower Paleozoic metamorphic rocks and granite bodies, overlain by Ordovician and younger strata (Gehrel et al., 2003). These Neoproterozoic to Lower Paleozoic rocks could have been sources of sediments to the Gondwanan sequences of Bangladesh.

CHAPTER 5: HEAVY MINERAL ANALYSIS

5.1 INTRODUCTION

Heavy minerals are powerful tools for provenance analysis. Studies of heavy minerals can even help distinguish sources within the same tectonic setting (Morton, 1985; Najman and Garzanti, 2000; Garzanti et al., 2007). A wide variety of heavy minerals are found in sandstones. Approximately thirty non-opaque heavy minerals are considered to be useful in source-rock studies (Morton, 1985; Mange and Maurer, 1992). Heavy minerals are generally resistant enough to endure transport, and heavy mineral assemblages can be used for high resolution provenance studies (Uddin and Lundberg, 1998b; Morton and Hallsworth, 1999; Uddin et al., 2007).

According to Tucker (1988), heavy minerals are those having specific gravities of 2.9 or more, and they are present in sandstones normally in proportions of less than 1%. Analyses of heavy minerals are most helpful for synorogenic sediments that have not traveled very far from source areas. Several sedimentary processes, including weathering of source rock, mechanical breakdown and hydraulic processing during transport, alluvial storage, and burial diagenesis can modify original heavy mineral assemblages (Morton and Hallsworth, 1994, 1999). However, Morton and Hallsworth (1999) recognized that some heavy minerals are relatively more stable (Table 5.1).

Table 5.1 Relative stability of minerals with similar hydraulic and diagenetic behaviors.

Stability in weathering profiles (Grimm, 1973; Bateman & Catt, 1985; Dryden & Dryden, 1946) #	Mechanical stability during transport (Freise, 1931)#	Burial persistence North Sea (Morton, 1984, 1986)	Chemical weathering (Pettijohn, 1941)
Zircon, Rutile Tourmaline, Andalusite, Kyanite, Staurolite Epidote Garnet Calcic Amphibole Clinopyroxene Orthopyroxene Apatite	Tourmaline Corundum Chrome-spinel Spinel Rutile Staurolite Augite Topaz Garnet Epidote Apatite Zircon Kyanite Olivine Andalusite Diopside Monazite	Apatite, Monazite, Spinel, TiO_2 minerals, Tourmaline, Zircon Chloritoid, Garnet Staurolite Kyanite Titanite Epidote Calcic Amphibole Andalusite Sillimanite Pyroxene Olivine	TiO_2 minerals Zircon Tourmaline Sillimanite Andalusite Kyanite Staurolite Topaz Titanite Monazite Garnet Epidote Calcic amphibole Orthopyroxene Clinopyroxene Olivine Apatite

Provenance studies using heavy mineral analysis have been applied to strata in Peninsular India as well as extra-peninsular India. Several studies that employed heavy mineral assemblages have been carried out in Bengal Basin, Bangladesh. Aslam et al. (1991) studied heavy mineral suites from the Barakar sandstone of the Gondwanan sequence of the Moher sub-basin in peninsular India. These studies of heavy mineral assemblages have proven to be quite useful in revealing source rock and unroofing histories and reconstructing paleo-drainage patterns associated with the Himalayas and Indo-Burman Ranges.

Morton and Hallsworth (1994) proposed several mineral ratios, pairs and indices for heavy minerals with similar hydraulic properties (e.g., index ATi with mineral pair apatite and

tourmaline, GZi with mineral pair Garnet and Zircon, CZi with mineral pair chrome-spinel and zircon). It is not always possible to extract a full suite of heavy minerals for study. In such cases, analyses focus on the dominant heavy mineral species and their relative abundance in each stratigraphic unit. Key heavy mineral species can help determine metamorphic grades, evaluating associations or paragenesis of specific heavy minerals, and establishing index minerals from stratigraphic levels in selected sections (Rahman, 2008).

5.2 METHODS

Nineteen samples were used for heavy mineral separation. Samples were crushed with a hammer and disintegrated carefully so that individual grains were not broken. Samples were then treated with HCl to remove carbonate and dried in an oven. Dry samples were sieved to obtain the size fraction between 0-4 phi. Heavy minerals were separated from other framework grains using heavy liquid gravity-settling methods. For this study, the liquid used for heavy mineral separation was tetrabromoethane ($C_2B_2Br_4$, density 2.89-2.96 gm/cm^3). Samples were weighed and put into the heavy liquid in a funnel for separation. The liquid-sediment mixture was stirred at regular intervals to make sure grains were thoroughly wet and not adhering to one another. Heavier fractions were allowed to settle to the bottom of the funnel for 24 hours. Heavy minerals at the base of the funnel were retrieved by opening the stopcock and collecting grains on filter paper. The heavy fractions were washed with acetone and dried, first in open air and then in an oven for few hours. The lighter fractions were also washed, dried and saved for future studies.

The heavy mineral fractions of samples were weighed, and magnetic separation was carried out using a Frantz magnetic separator at the Department of Geology and Geography at Auburn University. Four groups of heavy mineral fractions were separated based on different

magnetic susceptibilities by adjusting side slope angle and current values in the magnetic separator (Table 5.2; Hess, 1966).

The groups are as follows:

i. Group 1: Strongly Magnetic (SM)

ii. Group 2: Moderately Magnetic (MW)

iii. Group 3: Weekly Magnetic (WM)

iv. Group 4: Poorly Magnetic (PM)

Table 5.2 Four different groups of minerals based on magnetic susceptibility (Hess, 1966)

Side slope 15˚				Side slope 5˚	
Strongly magnetic	Moderately magnetic		Weakly magnetic	Poorly magnetic	
Hand magnet	0.4 Amps	0.8 Amps	1.2 Amps	1.2 Amps	
Magnetite Pyrrhotite Fe-oxides	Illmenite Garnet Olivine Chromite Chloritoid	Hornblende Hypersthene Augite Actinolite Staurolite Epidote Biotite Chlorite Tourmaline (dark)	Diopside Tremolite Enstatite Spinel Staurolite (light) Muscovite Zoisite Clinozoisite Tourmaline (light)	Sphene Leucoxene Apatite Andalusite Monazite Xenotine	Zircon Rutile Anatase Brookite Pyrite Corundum Topaz Fluorite Kyanite Silimanite Anhydrite Beryl
Group 1	Group 2A	Group 2B	Group 3	Group 4	

Group 1 comprises strongly magnetic minerals such as magnetite, pyrrhotite, and Fe-oxides. However, this group was not separated using a hand magnet. It was grouped together with Group 2A minerals, which include illmenite, garnet, olivine, chromite and chloritoid using a 15º side slope and a 0.4-Amp current.

Group 2B minerals include hornblende, hypersthene, augite, actinolite, staurolite, epidote, biotite, chlorite, and tourmaline. This fraction separated from weakly to poorly magnetic minerals using a 0.8-Amp current and a 15º side slope.

Weakly magnetic Group 3 minerals include diopside, tremolite, enstatite, spinel, staurolite (light), muscovite, zoisite, clinozoisite, and tourmaline (light). These were separated from Group 4 minerals using a 1.2-Amp current and a 15º side slope.

The remainder of the heavy minerals belongs to the poorly magnetic fraction that comprises Group 4. This group includes minerals such as sphene, leucoxene, apatite, andalusite, monazite, and xenotine, and other non-magnetic minerals like zircon, rutile, pyrite, corundum, fluorite, kyanite, sillimanite and beryl. Due to the absence of certain groups of minerals in certain samples, it was not possible to obtain all four magnetic fractions from each sample.

Out of nineteen samples, only ten were sent to Spectrum Petrographics in Vancouver, WA to prepare polished thin sections (due to budget constraints). Each of the magnetically separated heavy mineral fractions was put into the holes made in each thin section. Heavy minerals were identified with a petrographic microscope using the modified Fleet method (Fleet, 1926). Heavy minerals were counted in each magnetic fraction and added together to determine the relative abundance of each heavy minerals species in the bulk sample.

5.3 RESULTS

Gondwanan sandstones of northwestern Bengal Basin contain low-diversity suites of heavy minerals. Only three to four dominant heavy mineral species occur (Tables 5.3, 5.4). Heavy minerals are overall more abundant in sandstones from Barapukuria coal basin than at Khalashpir.

Table 5.3 Heavy mineral data for Gondwanan sandstones from well GDH 46, Khalashpir.

Sample No.	IK-01		IK-02		IK-06		IK-08	
Heavy Minerals	No. of Grains	Percentage	No. of Grains	Percentage	No. of Grains	Percentage	No. of Grains	Percentage
Zircon	0.00	0.00	12.00	4.36	3.00	0.82	0.00	0.00
Tourmaline	3.00	0.93	2.00	0.73	3.00	0.82	3.00	2.01
Rutile	0.00	0.00	0.00	0.00	0.00	0.00	0.00	0.00
Chrome-Spinel	0.00	0.00	0.00	0.00	0.00	0.00	0.00	0.00
Garnet	127.00	39.56	178.00	64.73	56.00	15.34	128.00	85.91
Biotite	4.00	1.25	0.00	0.00	1.00	0.27	0.00	0.00
Chlorite	0.00	0.00	2.00	0.73	0.00	0.00	0.00	0.00
Chloritoid	5.00	1.56	0.00	0.00	0.00	0.00	0.00	0.00
Opaque	173.00	53.89	60.00	21.82	289.00	79.18	10.00	6.71
Others	10.00	3.12	21.00	7.64	13.00	3.56	8.00	5.37
Total	321.00	100.00	275.00	100.00	365	100.00	149.00	100.00
ZTR	3.00	0.93	14.00	5.09	6.00	1.64	3.00	2.01

Table 5.4 Heavy mineral data for Gondwanan sandstones from well DOB 02, Barapukuria.

Sample No.	IB 2-01		IB 2-03		IB 2-05		IB 4-01		IB 4-03	
Heavy Minerals	No. of Grains	Percentage	No. of Grains	Percentage	No. of Grains	Percentage	No. of Grains	Percentage	No. of Grains	Percentage
Zircon	30.00	8.75	0.00	0.00	0.00	0.00	11.00	3.22	9.00	4.57
Tourmaline	3.00	0.87	1.00	2.70	0.00	0.00	3.00	0.88	4.00	2.03
Rutile	10.00	2.92	0.00	0.00	0.00	0.00	9.00	2.63	5.00	2.54
Chrome-Spinel	0.00	0.00	0.00	0.00	0.00	0.00	0.00	0.00	0.00	0.00
Garnet	82.00	23.91	0.00	0.00	19.00	51.35	137.00	40.06	23.00	11.68
Biotite	0.00	0.00	0.00	0.00	0.00	0.00	2.00	0.58	1.00	0.51
Chlorite	1.00	0.29	0.00	0.00	0.00	0.00	2.00	0.58	3.00	1.52
Chloritoid	2.00	0.58	0.00	0.00	0.00	0.00	1.00	0.29	0.00	0.00
Opaque	192.00	55.98	33.00	89.19	9.00	24.32	171.00	50.00	132.00	67.01
Others	23.00	6.71	3.00	8.11	9.00	24.32	6.00	1.75	20.00	10.15
Total	343.00	100.00	37.00	100.00	37.00	100.00	342.00	100.00	197.00	100.00
ZTR	43.00	12.54	1.00	2.70	0.00	0.00	23.00	6.73	18.00	9.14

All samples from Khalashpir contain abundant garnet (~86% to ~15%; average of ~51%). These grains are mostly irregular, highly fractured, and contain abundant inclusions (Fig. 5.1, 5.2, and 5.3). Highly stable grains—zircon, tourmaline, and rutile (ZTR)—are relatively rare. Among ZTR, zircon is the most abundant, ranging from 0% to ~4% (average = 1.12%; Fig. 5.4 and 5.5). Tourmaline grains are highly fractured (Fig. 5.6 and 5.7). The percentage of opaque grains (including some pyrite and magnetite) is high in all samples. Changes in abundance of opaque minerals may be caused by the change in source terranes. Opaque grains may be derived from mafic source rocks or caused by iron-oxide coating of grains after deposition. Opaques are the most abundant, and garnets are common in almost all samples. Chlorite, chloritoid, biotite, and staurolite also observed.

Three samples from Barapukuria cores (DOB 02 and DOB 04) were used for heavy mineral counts. A sharp contrast in abundance of heavy minerals is observed between samples from Khalashpir and Barapukuria. The abundance of garnet is significantly lower in Barapukuria samples than in Khalashpir samples, which average ~25.40% (range = 0 to 51.35%) (Fig. 8). Highly stable minerals (ZTR) are more abundant in Barapukuria samples, ranging from ~0% to ~12.5% with an average of ~6%. Among ZTR, zircon is the most abundant followed by rutile and tourmaline. Differences in abundance of rutile between the two areas are significant; none of the samples from Khalashpir contained rutile, while rutile is the second most dominant mineral among ZTR in the Barapukuria samples, averaging ~1.62% (range = 0-5%) (Fig. 9). Opaques are also another dominant group here. Opaque grains are more abundant in Barapukuria samples than in Khalashpir samples.

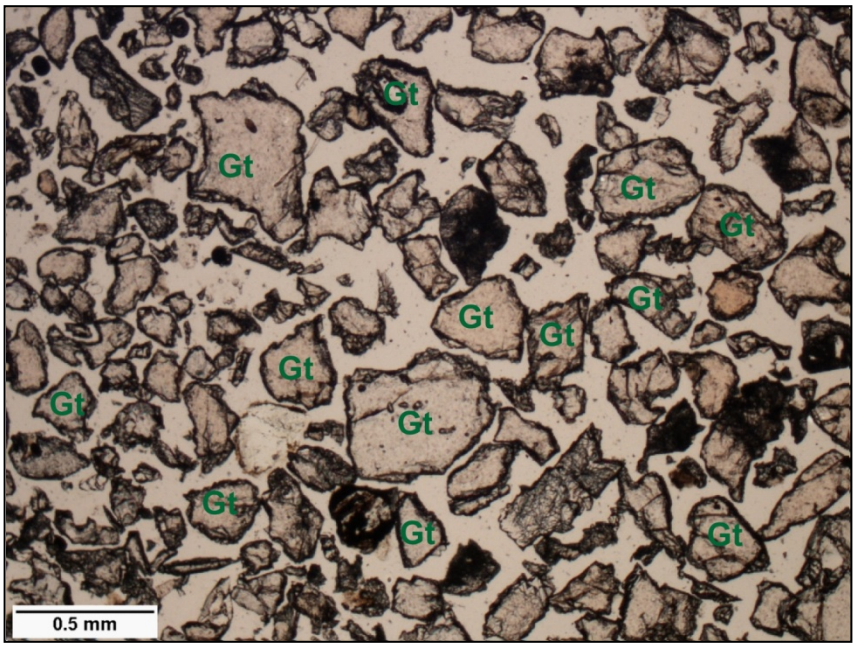

Figure 5.1 Representative photomicrograph of heavy mineral assemblage in a sandstone from Khalashpir (sample IK-01), northwestern Bengal Basin (Gt- Garnet).

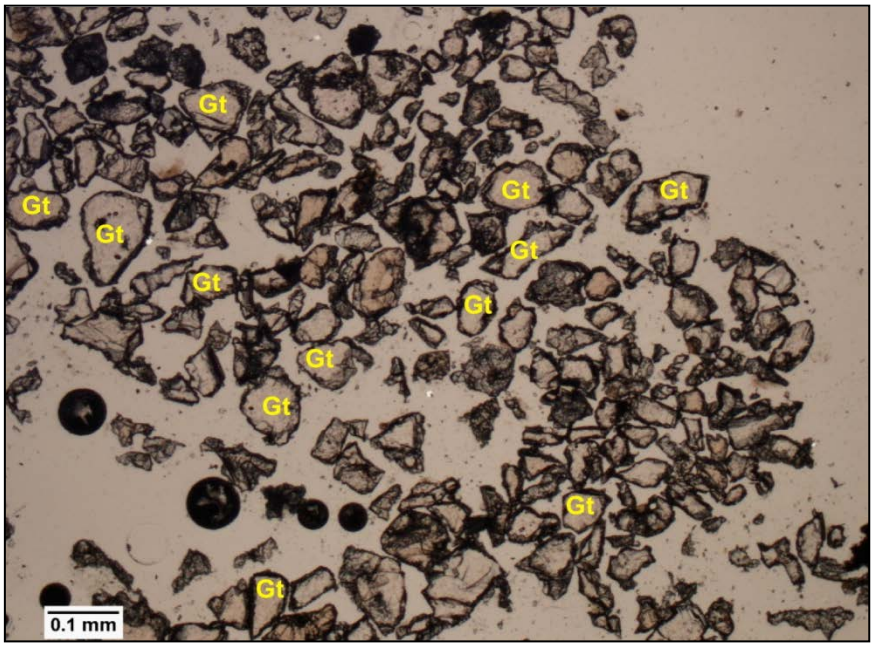

Figure 5.2 Representative photomicrograph of heavy mineral assemblage in a sandstone from Khalashpir (sample IK-02), northwestern Bengal Basin (Gt- Garnet).

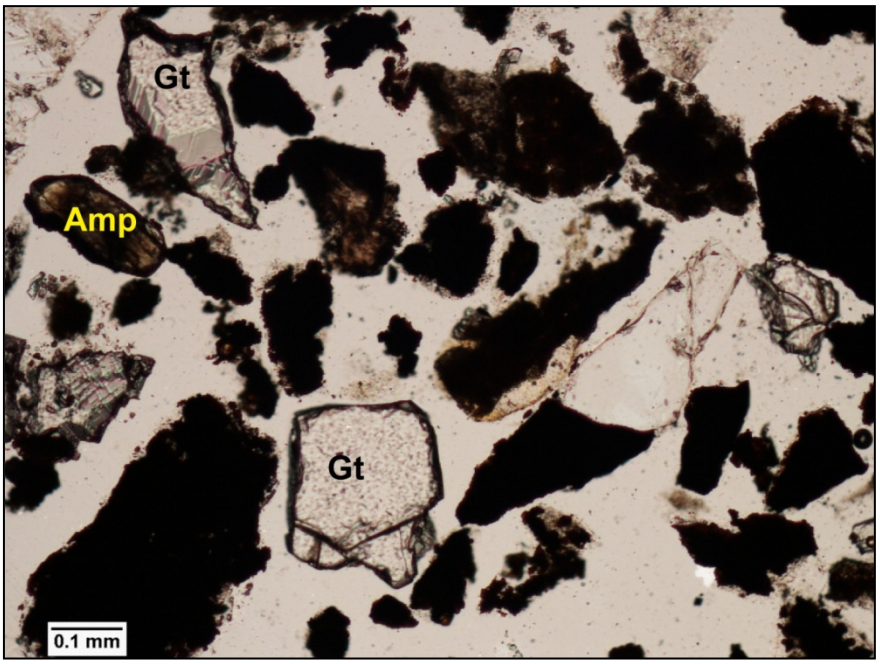

Figure 5.3 Representative photomicrograph of heavy mineral assemblage in a sandstone from Khalashpir (sample IB 4-01), northwestern Bengal Basin (Gt- Garnet, Amp- Amphibole).

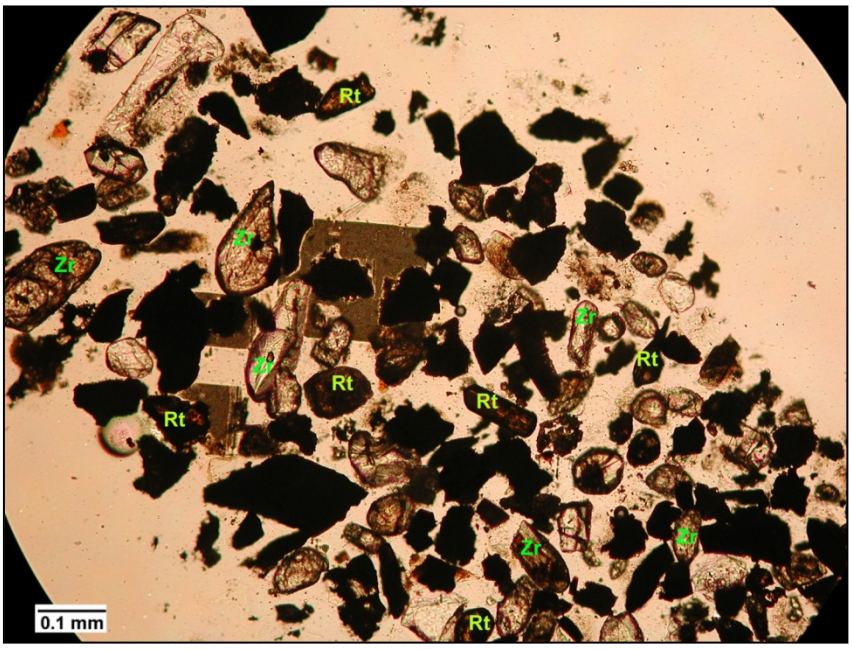

Figure 5.4 Representative photomicrograph of heavy mineral assemblage in a sandstone from Barapukuria (sample IB 2-05), northwestern Bengal Basin (Zr- Zircon, Rt- Rutile).

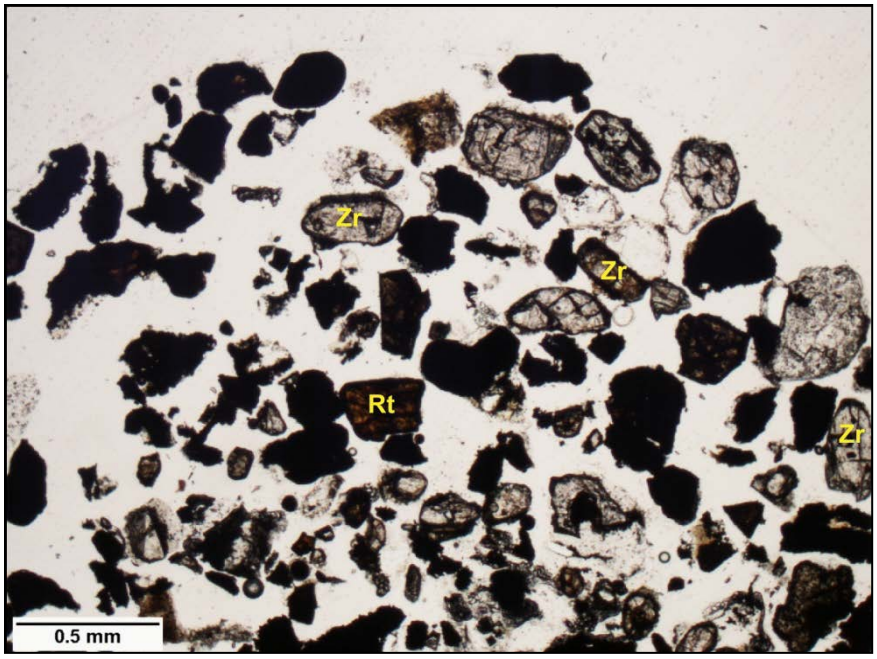

Figure 5.5 Representative photomicrograph of heavy mineral assemblage in a sandstone from Barapukuria (sample IB 4-03), northwestern Bengal Basin (Zr- Zircon, Rt- Rutile).

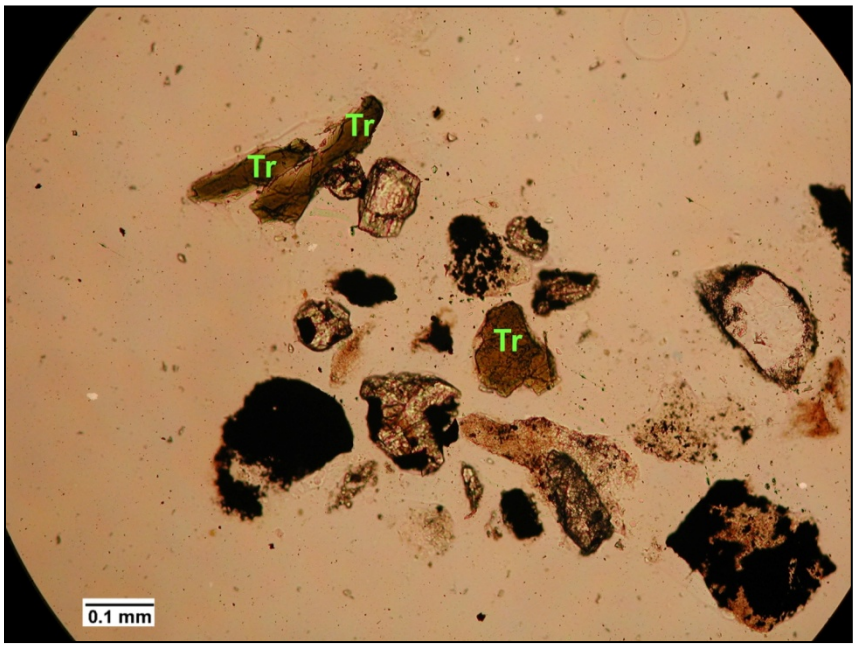

Figure 5.6 Representative photomicrograph of heavy mineral assemblage in a sandstone from Khalashpir (sample IK-02), northwestern Bengal Basin (Tr- Tourmaline).

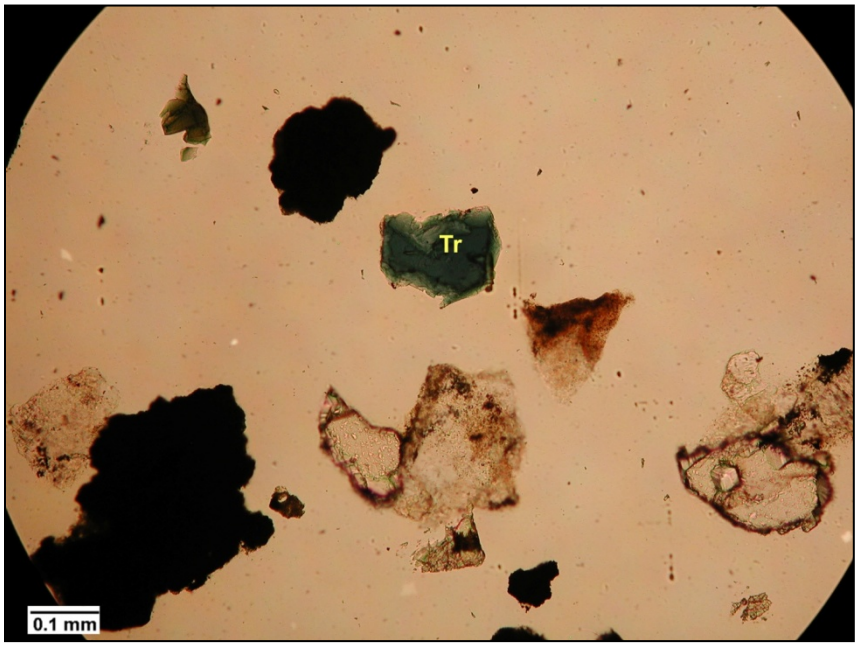

Figure 5.7 Representative photomicrograph of heavy mineral assemblage in a sandstone from Khalashpir (sample IK-08), northwestern Bengal Basin (Tr- Tourmaline).

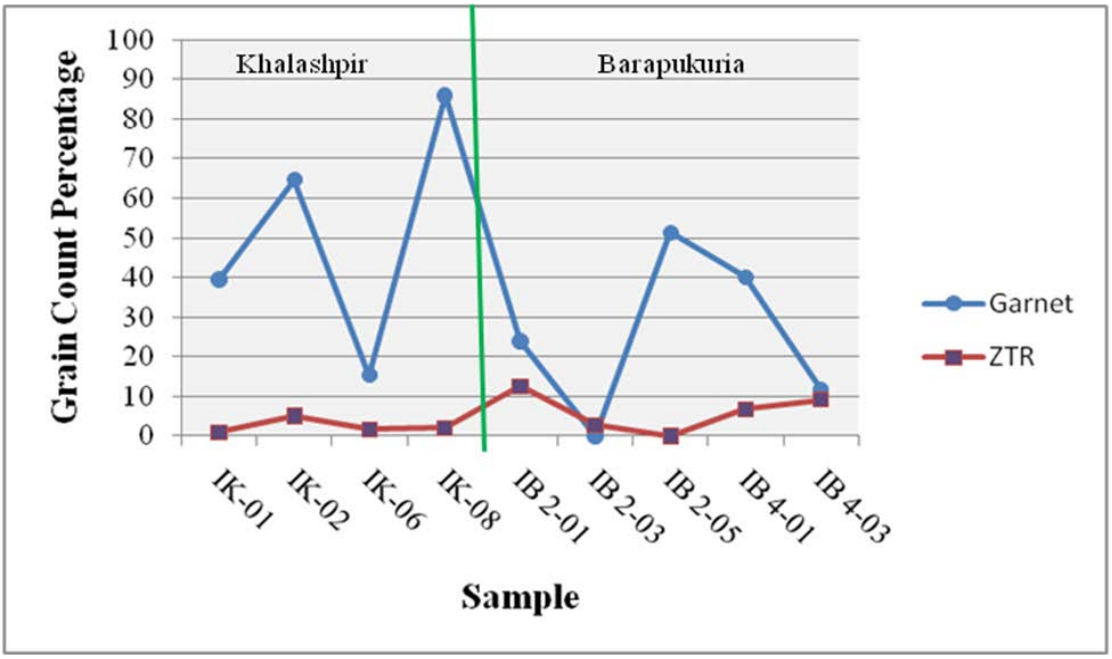

Figure 5.8 Variation in abundance of garnets and ZTR among different Gondwanan sandstone samples.

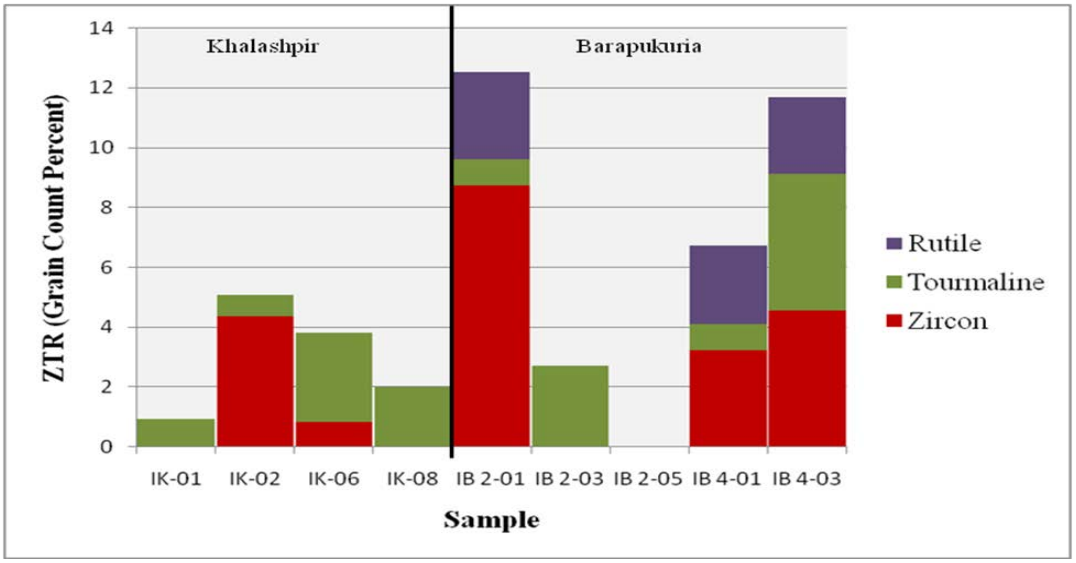

Figure 5.9 Abundance of highly stable heavy minerals (ZTR) among different Gondwanan sandstone samples.

5.4 PROVENANCE

Overall, the weight percent of heavy minerals in Gondwanan sandstones from Khalashpir is higher than those from Barapukuria coal mine (Fig. 5.10 and 5.11). Garnet is the dominant heavy mineral species in almost all the samples after opaque grains (Fig. 5.12). Fluid inclusions are the dominant features of the garnets. Possible sources include the Chotanagpur gneissic complex of Singhum craton and/or the Meghalayan craton, both of which are proximal cratonic areas in India. The east Antarctic shield, which was then nearby, represents another probable source.

The Neo-Proterozoic-Early Cambrian collision between India and Australia, which resulted in the assembly of Gondwanaland (Fitzsimons, 2000b), may have given rise to some metamorphic complexes. The Late Neoproterozoic-Cambrian Pinjarra orogen formed between

Western Australia and eastern India and can be traced all the way to East Antarctica (Fitzsimons, 2000a, 2003). The Leeuwin metamorphic complex of the Pinjarra orogen, which is mostly composed of felsic gneisses (Wilde and Murphy, 1990; Wilde, 1999), could be a possible source of the garnets in the Gondwanan sequences of northwestern Bengal Basin. The Leeuwin complex is dominated by gneisses formed by a single phase of metamorphism of A-type granitoids (Collins, 2003), which record three distinct magmatic pulses (Nelson 1996, 1999, 2002; Collins & Fitzsimons, 2001; Wilde & Nelson, 2001).

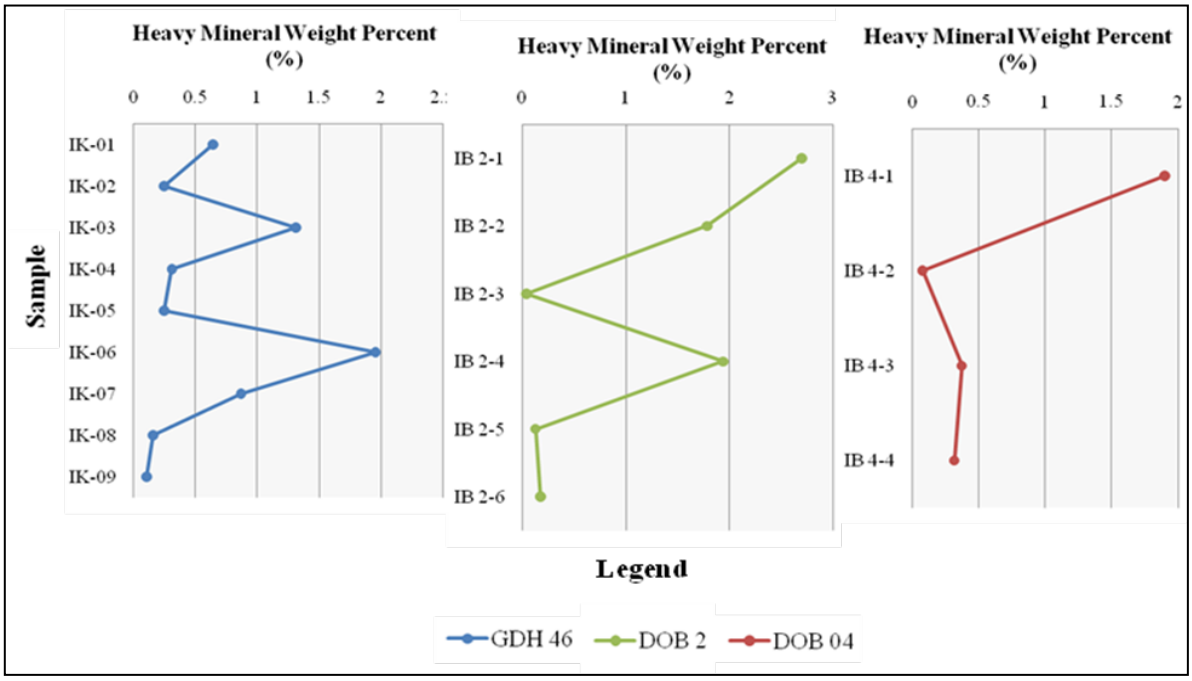

Figure 5.10 Vertical variations in heavy mineral assemblages in Gondwanan sandstones of Bangladesh.

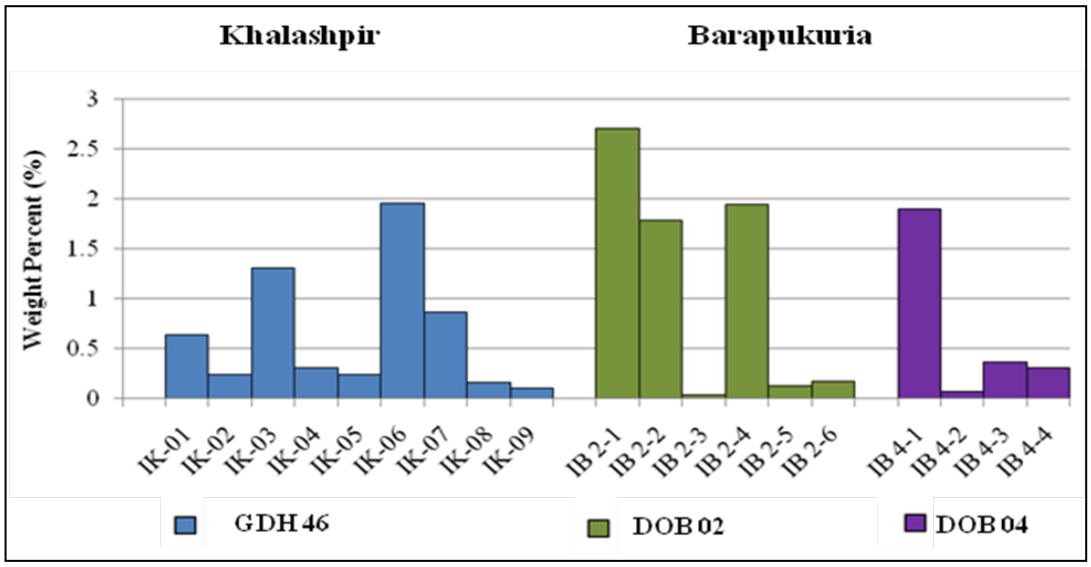

Figure 5.11 Abundance of heavy minerals among different samples of Gondwanan sandstone in Bangladesh.

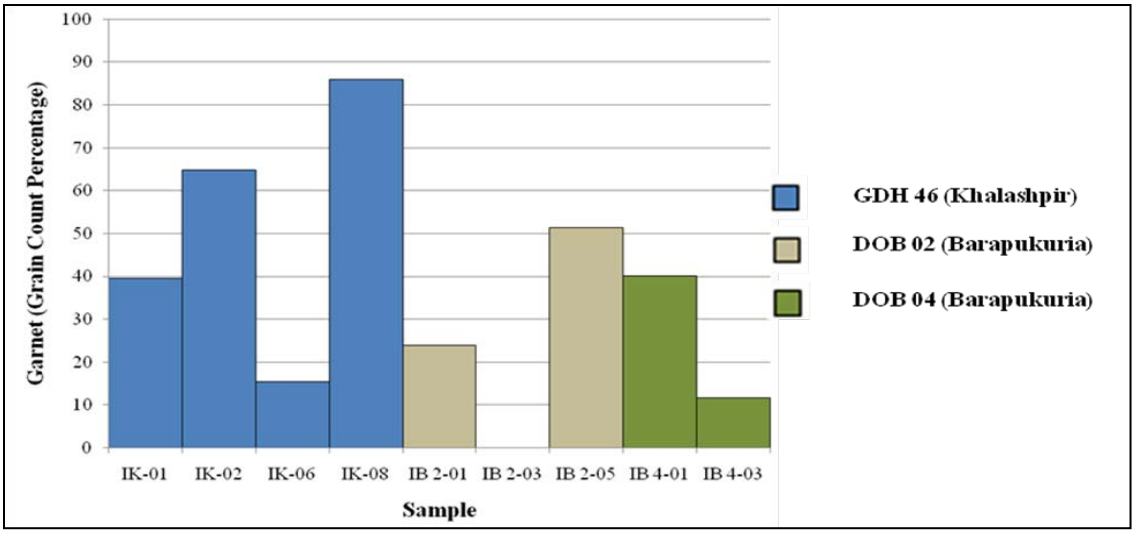

Figure 5.12 Abundance of garnets among different Gondwanan sandstone samples of Bangladesh.

CHAPTER 6: DETRITAL GEOCHRONOLOGY

Studies of detrital geochronology have been helpful in evaluating ages of mountain building processes (Hodges et al., 1994; De Celles et al., 2004). Several dating methods are in practice. U/Pb and $^{40}Ar/^{39}Ar$ are the most widely used techniques to determine the ages of detrital grains.

6.1 $^{40}Ar/^{39}Ar$ DATING OF DETRITAL MUSCOVITE

Single crystal age dating of detrital minerals is very helpful in evaluating the ages of orogens (Hodges et al., 1994, 2005; Najman, 200). This approach provides information on key parameters including timing, magnitude and variations in erosional activities (Burbank et al., 2007). Detrital mineral grains in stratigraphic successions record cooling ages that may aid in understanding orogenic events through time. An interplay between erosion rates and lithology within a tributary catchment was demonstrated based on modern detrital ages, and this provides a basis for refining orogenic histories (Burbank et al., 2007). This conceptual model of detrital ages helps to reconstruct changes in deformation and erosion and to validate proposed models for orogenic evolution.

Tectonic denudation associated with extensional faulting (Davis, 1988) and erosional activities caused by geomorphic processes affect the cooling histories of orogens. Erosion causes unroofing, which moves deeper rocks upward and exposes them at the surface. Detrital minerals having high closure temperatures do not affect the cooling ages as much as it does to the minerals having lower cooling temperatures (Yamada et al., 1995; McDougall and Harrison,

1999). Cooling of minerals through higher temperatures (300-600˚ C) normally occurs at depth of greater than 10 km.

Accuracy of cooling-age determinations of individual mineral grains increased with the development of single crystal dating in 1980's (Cerveny et al., 1988). Cooling ages can be optimized by applying different dating methods for the same sample, such as combining fission-track with U-Pb ages (Carter and Moss, 1999; Reiners et al., 2004). Among other dating methods, $^{39}Ar/^{40}Ar$ and U-Pb are the two most widely used techniques (Gehrels and Kapp, 1998; Brewer et al., 2003; Wobus et al., 2003; Ruhl and Hodges, 2005).

Reconstruction of cooling/unroofing histories of orogens through single crystal dating is based on two specific applications. First, samples collected sequentially within a stratigraphic section can be analyzed to yield a step-by-step reconstruction of changes in the suite of mineral cooling ages emerging from an orogen (Carter and Moss, 1999; White et al., 2002; Reiners et al., 2004). Second, analysis of detrital sediments in modern streams yields a broad sampling of the realm of cooling ages presently exposed within a tributary catchment (Bernet et al. 2004).

6.2 TECHNICAL ASPECTS OF $^{40}Ar/^{39}Ar$ DATING

Argon is a naturally occurring inert gas occupying about 0.94% of the total volume of earth's atmosphere. Common isotopes of argon are ^{40}Ar (99.6%), ^{36}Ar (0.34%), and ^{38}Ar (0.06%). Stable ^{40}Ar (11.2%) is derived from the decay of naturally occurring ^{40}K (half life=1.25×10^{9} yrs) through electron capture and positron emission. The $^{40}Ar/^{36}Ar$ in a rock is determined and compared with the $^{40}Ar/^{39}Ar$ in the atmosphere, which is 295.5 (McDougall and Harrison, 1999). ^{38}Ar forms by the radioactive decay of ^{38}Cl, while ^{37}Ar and ^{36}Ar form by the radioactive decay of ^{40}Ca (Dickin, 1995).

The $^{40}K/^{40}Ar$ dating method was first used in 1930s, based on the decay of ^{40}K to ^{40}Ar with a half life of 1.25 Ga (McDougall and Harrison, 1999). However, the $^{40}Ar/^{39}Ar$ method is different from the $^{40}K/^{40}Ar$ method. In the $^{40}K/^{40}Ar$ technique, K is determined by independent analysis, whereas in the $^{40}Ar/^{39}Ar$ method, ^{39}Ar is produced by neutron irradiation of the sample, and ^{40}Ar with ^{39}Ar are measured simultaneously. However, ^{39}Ar measures the K content in the irradiated sample. The nuclear reaction that takes place during irradiation is:

$$^{39}_{19}K\ (n,p)\ ^{39}_{18}Ar$$

Where, n denotes neutron capture and p indicates proton emission (Faure, 1986).

In order for both K-Ar and $^{40}Ar/^{39}Ar$ methods to be most effective, different mineral phases must be separated, especially in the case of rocks that have slowly cooled or have been thermally disturbed subsequent to crystallization. Also, samples must be pure in order to insure unequivocal interpretation. Moreover, K-Ar ages derived from a sample are used for flux monitoring purposes in $^{40}Ar/^{39}Ar$ dating method.

A significant number of unwanted isotopes usually are produced by irradiation in the nuclear reactor (Fig. 6.1). These effects are neutralized by using laboratory salt and glasses (Scherer, 2007).

The age equation for $^{40}Ar/^{39}Ar$ dating (e.g., McDougall and Harrison, 1999) is as follows:

$$t = (1/\lambda)\ln(^{40}Ar^*/^{39}Ar_K(J)+1)$$

λ is the decay constant for $^{40}K \rightarrow ^{40}Ar$, (=5.543 X 10^{-10}/year). $^{40}Ar^*$ is the ^{40}Ar formed due to radioactive decay in the phase of interest. $^{39}Ar_K$ is the ^{39}Ar formed artificially by bombardment with fast, high-energy neutrons in a nuclear reactor during the irradiation process (Merrihue and Turner, 1966; McDougall and Harrison, 1999) and is used as a proxy for measurement of the

parent potassium. J is the neutron flux (fluence) in the reactor determined from a standard sample (monitor) with a known age that is irradiated at the same time as the sample of interest (Scherer, 2007).

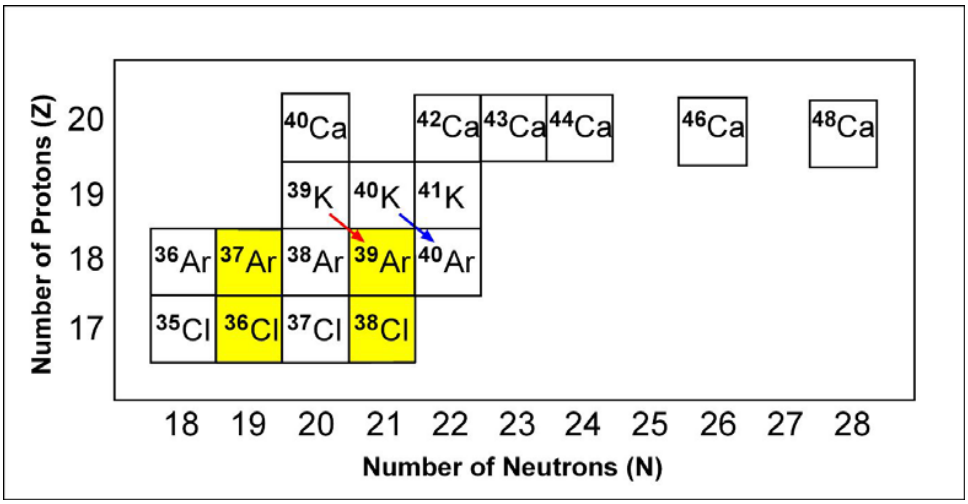

Figure 6.1 Some stable and radioactive isotopes related to $^{40}Ar/^{39}Ar$ dating method. The isotopes in yellow boxes are unstable isotopes. The blue arrow shows the natural decay reaction of $^{40}K \rightarrow ^{40}Ar$. The red arrow shows the ^{39}K (n,p)^{39}ArK reaction during irradiation (From Faure, 1986).

In studies of sediments, the $^{40}Ar/^{39}Ar$ dating method is most commonly applied on muscovites. The $^{40}Ar/^{39}Ar$ dates of muscovite grains provide the time of cooling of source rocks through a closure temperature interval of 300-400˚ C (Hames and Bowring, 1994), assuming that no additional ^{40}Ar is added or lost during transportation and deposition (Hodges et al., 2005).

Age-dating techniques using detrital mineral grains show a range of ages based on different source contributions. The maximum age population in a probability plot suggests greater contribution of detritus from source rocks having that age. Shorter time gaps are related to high relief that results in rapid transport of sediments (Hodges et al., 2005).

6.3 METHODOLOGY

Three sandstone samples for $^{40}Ar/^{39}Ar$ analyses were selected from different levels of the GDH 46 well from the Khalashpir area. The samples used for this method -- IK 02, IK 06, and IK 14 (Fig. 6.2) – were selected in order to identify possible variations in cooling ages of source rocks through time.

Samples were prepared in the Himalayan Research Laboratory at Auburn University. Sandstone samples were crushed in a manner so that the individual muscovite grains were not broken. Crushed samples were sieved to obtain the 0-4 phi grain size fraction. Afterwards, heavy mineral separation was performed using a heavy liquid (tetrabromoethane). Lighter fractions were collected and washed with acetone. A total of more than 100 muscovite grains were collected from each sample under a binocular microscope. Vermeesch (2004) showed that approximately 100 detrital mineral age determinations are needed to detect all age groups that individually constitute more than 5% of the entire population (with 95% certainty). The samples were then sent to the McMaster University Research Reactor in Hamilton, Ontario, Canada for irradiation

.

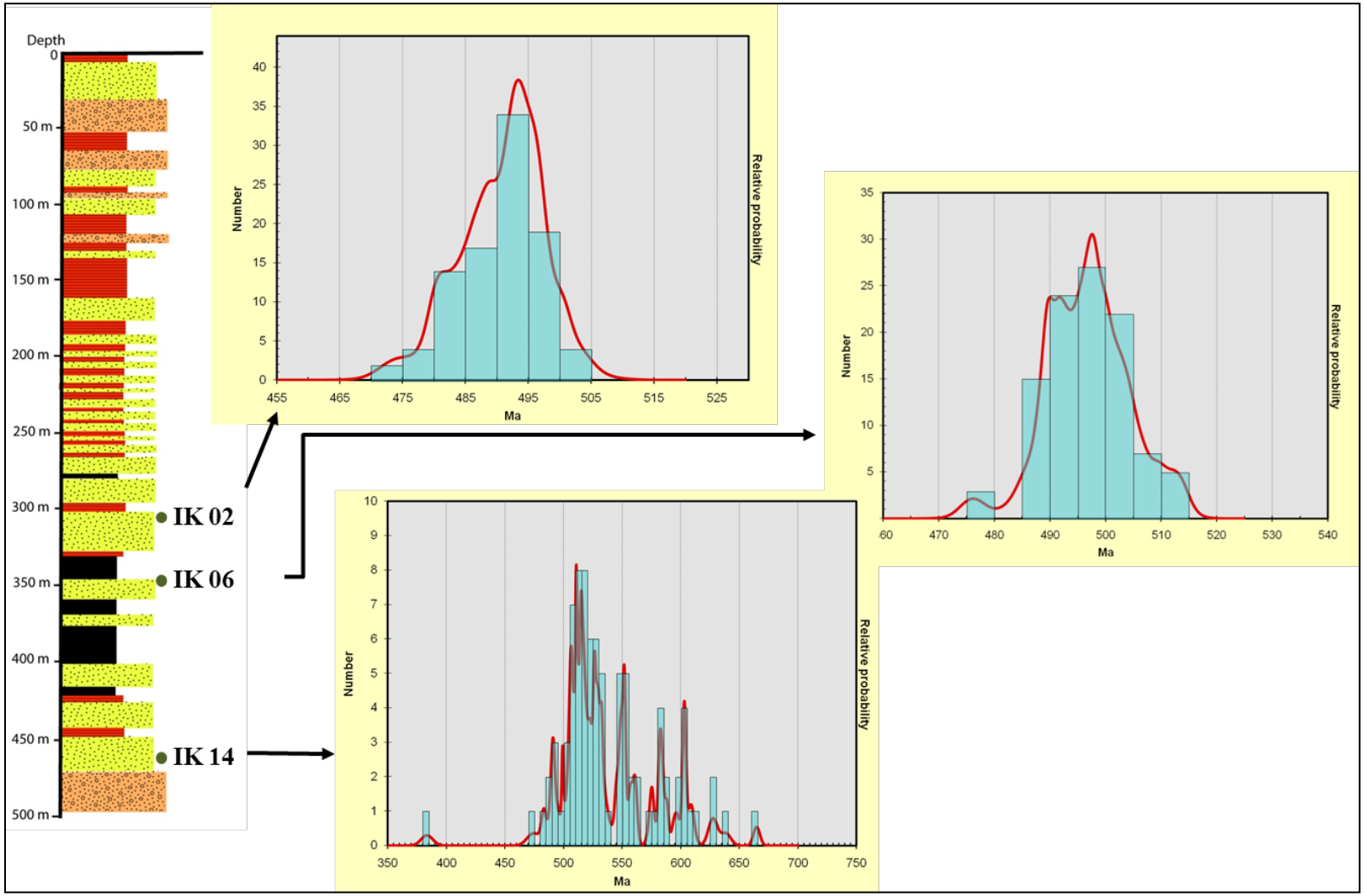

Figure 6.2 Stratigraphic positions of samples used for $^{40}Ar/^{39}Ar$ analyses of single muscovite crystals from samples IK 02, IK 06, and IK 14 from well GDH 46, Khalashpir area, and their corresponding probability plots

After the samples were irradiated, each was analyzed one grain at a time in the Auburn Isotope Mass Analysis Laboratory (ANIMAL) at Auburn University. ANIMAL is equipped with a low-volume, high-sensitivity, 10-cm radius sector mass spectrometer and automated sample extraction system (based on CO_2 laser) for analysis of single crystals (Uddin et al., 2010). Analyses are typically made using a filament current of 2.240 Amp, and potentials for the source and multiplier of 2000 V and –1300 V, respectively. The high sensitivity and low blank of the instrument permits measurement of 10^{-14} mole samples within 0.2% precision.

One hundred and twelve (112) muscovite crystals were loaded for analysis from each sample. The grains were placed in a copper disc with one-hundred twelve holes and analyzed by fusing single muscovite crystals with a CO_2 laser. Samples IK 06 and IK 14 were both analyzed within a time span of 48 hours. Two muscovite grains from the IK 06 sample were selected for incremental heating analysis. Data reduction was carried out using Isoplot (Ludwig, 2003). Analyses yielding 40Ar less than five times the blank were excluded from consideration.

6.4 $^{40}Ar/^{39}Ar$ RESULTS

Relative probability plots for the age populations obtained from $^{40}Ar/^{39}Ar$ method for each sample are shown in figures 6.3, 6.4 and 6.5, and all the data used to generate plots are in Apendices 4, 5, and 6. Distributions of age population in probability plots for each of the samples are not very uniform. Sample IK 02 shows a unimodal distribution of ages, whereas samples IK 06 and IK 14 have bimodal and polymodal age distributions respectively.

The probability plot for IK 02 shows a unimodal distribution of ages. This is shallowest sample used for this study. The age cluster varies from 480 to 500 Ma (Figure 6.3), with the highest peak at 494 Ma.

Sample IK 06 was collected at intermediate depth in the core. Three different clusters of ages are observed in the probability plot (Figure 6.4). However, most ages range from 485 to 515 Ma with peaks at 490 Ma and 498 Ma. A few muscovite grains from this sample were subjected to incremental heating analysis (Fig. 6.6) to compare with the ages derived by single crystal muscovites. The ages derived are ~ 500 Ma.

Sample IK 14, the deepest sample about 40 m above the basal contact, which shows the broadest age populations among the three samples (Fig 6.5). The sample shows four different age clusters. In the dominant cluster, ages range from 475 to 600 Ma. Five discrete peaks were found in that cluster. The highest peak in the relative probability plot is at 510 Ma represented by 48 grains. Other minor peaks are observed at 550 Ma, 605 Ma, 590 Ma and 495 Ma (Fig. 6.5).

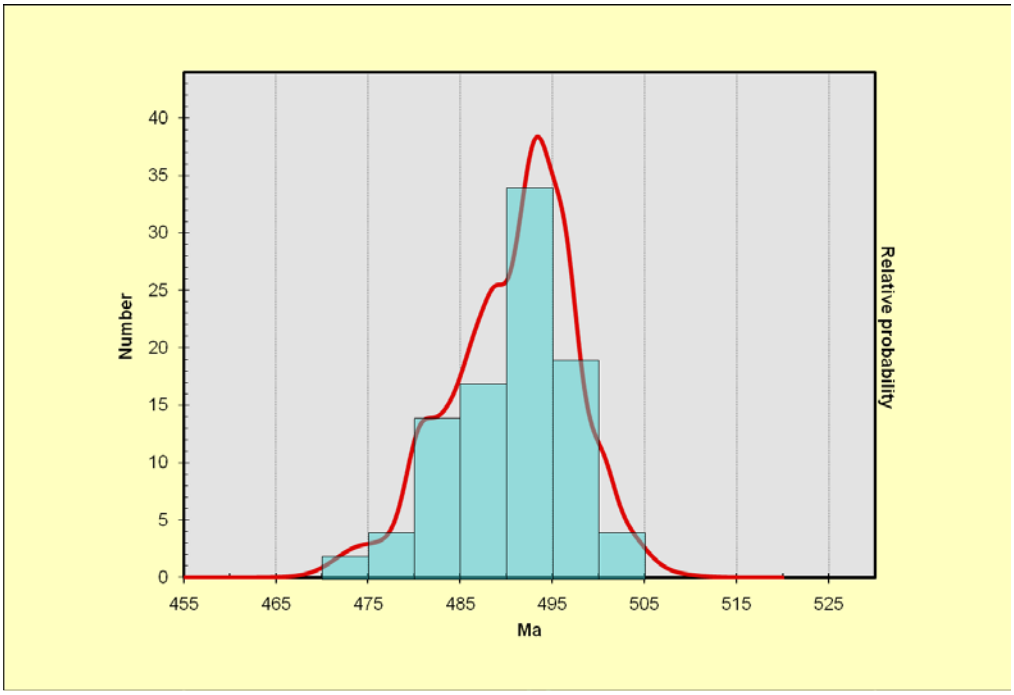

Figure 6.3 Probability plot for $^{40}Ar/^{39}Ar$ of single muscovite crystals from sample IK 02 of well GDH 46, Khalashpir.

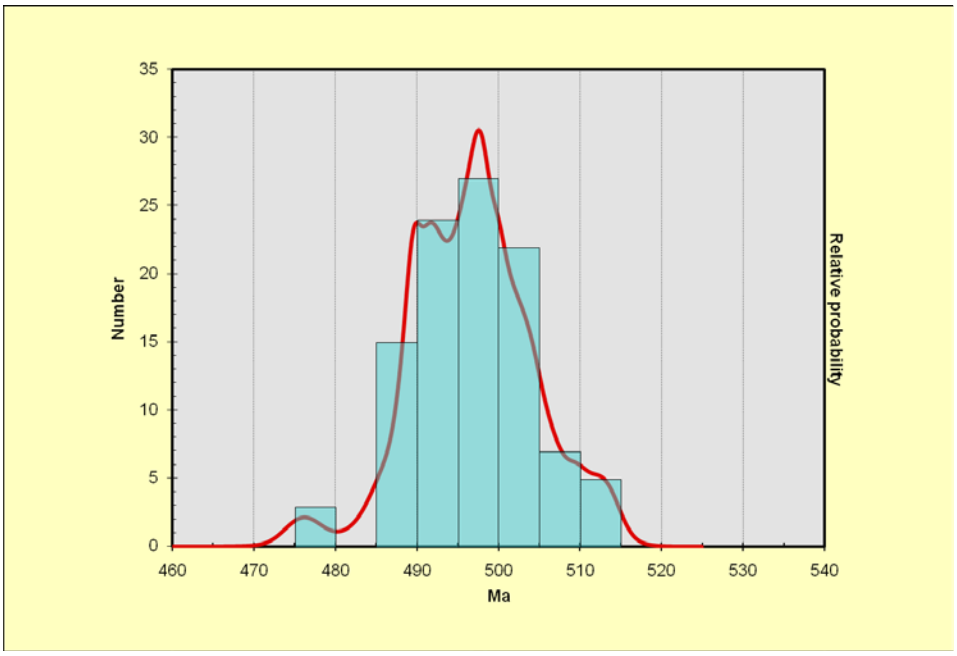

Figure 6.4 Probability plot for $^{40}Ar/^{39}Ar$ of single muscovite crystals from sample IK 06 of well GDH 46, Khalashpir.

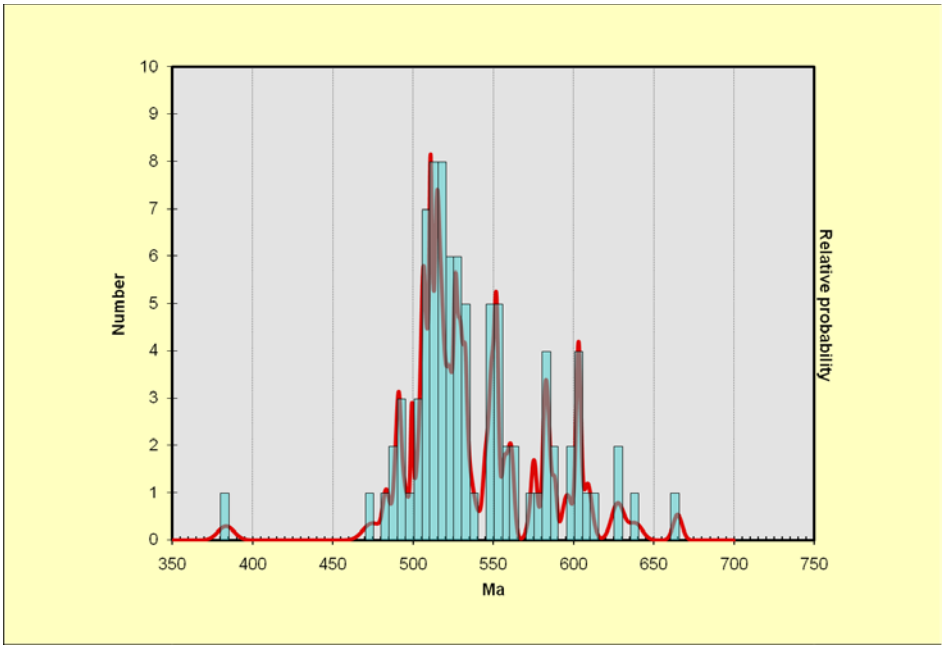

Figure 6.5 Probability plot for $^{40}Ar/^{39}Ar$ of single muscovite crystals from sample IK 14 of well GDH 46, Khalashpir.

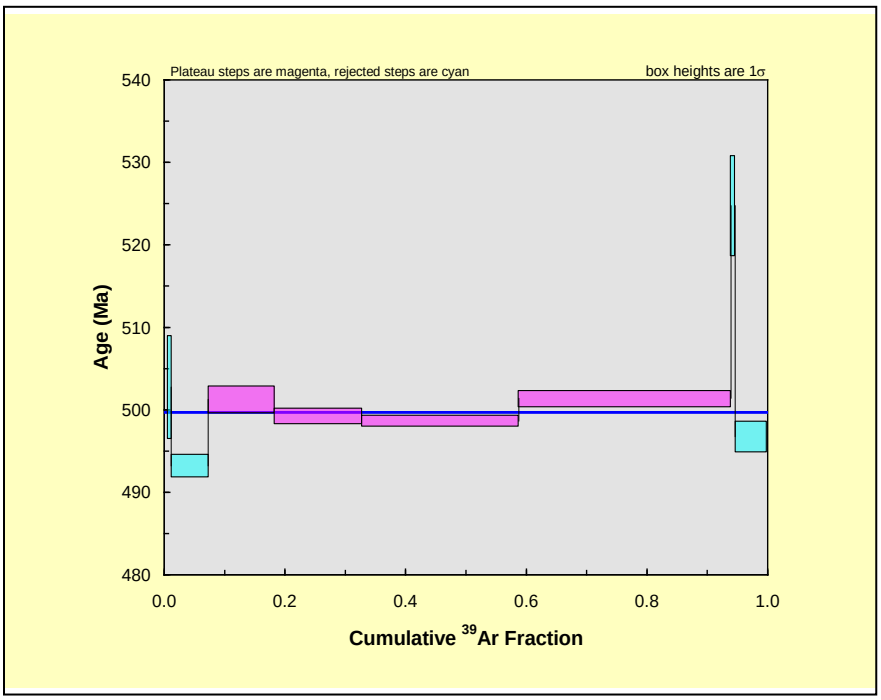

Figure 6.6 Plot for $^{40}Ar/^{39}Ar$ of single muscovite crystal subjected to incremental heating (grain from sample IK 06, well GDH 46, Khalashpir).

6.5 PROVENANCE INTERPRETATION

Comparing the cooling ages of all the muscovite grains from three samples, there is an overlap in ages between the upper two samples from about 485 Ma to 505 Ma. However, the deepest sample shows much older cooling ages (generally 480 – 630 Ma) with very little age overlap with the younger samples. The first two samples were close to one another stratigraphically, and this may explain the common age ranges of these samples.

The dominant ages derived using the $^{40}Ar/^{39}Ar$ method on muscovite crystals are 486 Ma, and 493 Ma (Fig. 6.3), 490, and 495 Ma (Fig. 6.4), and 510, 550, and 600 Ma (Fig. 6.5). The probability plot for the sample IK-14 shows the greatest diversity of ages. This is may indicate derivation from multiple sources. Muscovite grains representing Late Proterozoic to Early Cambrian (600 – 550 Ma) may have been derived from nearby Indian shield areas or the East

Antarctic shield. Specifically, these may be derived from the Millie granite or gneissic complex of the Meghalayan craton where similar age ranges were found (Chatterjee et al., 2007). The Chottanagpur Gneissic Complex and Singhbhum craton also could be the possible source. However, sediment input from other orogenic sources is reflected by the Late Cambrian to Ordovician cooling ages (475 to 515 Ma) for the upper two samples. U-Pb zircon dating of the Balugaon Anorthosite Massif of the Chilka lake domain, Eastern Ghats belt to constrain their emplacement age (Chatterjee et al., 2008). U-Th-Pb chemical dating of monazite cores and reams yield ages of 714±11 Ma and 655±12 Ma respectively. Monazite-allanite rims (463±22 Ma) around apatite record low-grade Pan-African thermal activity (Chatterjee et al., 2008). According to these authors the 714-655 Ma dates correlate with collision of Eastern Ghats–Rayner Block and Western Australia in the mid-Neoproterozoic.

The Terra Australis Orogens that formed during the Neoproterozoic to late Paleozoic are possible sources of sediments in Gondwanan sequences of northwestern Bengal Basin. An orogenic event took place due to subduction of the paleo-Pacific plate beneath eastern Gondwana (Cawood, 2005). This eventually led to the formation of the Ross (Antarctica), Delamerian (SE Australia) and Tyennan (Tasmania) orogenic belts (Frederico et al., 2006). Several studies have been carried out on Ross orogeny in Northern Victoria Land (NVL). The Ross orogen consists of three different metamorphic terranes known as the Wilson (WT), Bowers (BT), and Robertson Bay (RBT) terranes. Detrital zircons from Robertson Bay turbidites have ages as young as 481 Ma (Fioretti et al., 2003) with a major peak at 495 Ma to 500 Ma. The $^{40}Ar/^{39}Ar$ ages from the Robertson Bay terrane shows models at 475.1 Ma and 507 Ma, 519 Ma and 531 Ma, and 585 to 590 Ma (Wright and Dallmeyer, 1991). Whole-rock slate samples from the Bowers terrane also show ages around 500 Ma (Wright and Dallmeyer, 1991). Although these ages match the ages

obtained from this study, India and the Ross orogen (pacific margin of Antarctica) were too far away to supply sediments without any strong drainage system.

Gehrels et al. (2003) studied the Himalayan orogen using U/Pb ages of single crystal zircons from the crystalline rocks of the Lesser Himalayas. Their work yielded an age range of about 508-475 Ma, suggesting proto-Himalayan orogenesis during the Early Paleozoic. These ages are analogous to the ages of samples IK 02 and IK 06 analyzed for the current study. Hence, rocks of the lesser Himalayas are possible sources for detritus in the Gondwanan sequences of the Bengal Basin.

The Neoproterozoic-Early Paleozoic Pinjarra orogen is another possible source of sediments in the Gondwanan sequences of northwestern Bengal basin. The Pinjarra orogen was caused by the collision between India and Western Australia, and bisects eastern Gondwanaland (Collins, 2003). Recent age dates ($^{40}Ar/^{39}Ar$) of gneisses from the Leewin Complex define three different age groups associated with three volcanic pulses. These are at 1200-1050 Ma, 800-650 Ma, and 580-500 Ma (Nelson 1996, 1999, 2002; Collins & Fitzsimons 2001; Wilde & Nelson 2001). The ages of latest magmatic event manifested in the Leewin complex overlap the ages obtained from the current study. Notably, the Pinjarra orogen was closest to the study area and could more readily supply sediments to eastern India. However, there may be still some younger rocks which have not been dated yet.

CHAPTER 7: MICROPROBE ANALYSIS

7.1 INTRODUCTION

Studies of heavy minerals have been used for a long time to evaluate provenance. Sandstones may contain a variety of heavy minerals but only a few may be diagnostic of a particular source. Mineral chemistry of particular designated heavy minerals is helpful in understanding and differentiating source-rock types. Garnet chemistry can help differentiate the grade of metamorphic source rocks. Tourmaline chemistry can help differentiate sediments derived from plutonic source rocks. Chrome-spinel chemistry is useful in differentiating mafic igneous source rocks.

Analyses of mineral chemistry were carried out on selected heavy mineral groups in order to help constrain the provenance of Gondwanan sequences in northwestern Bengal Basin.

7.2 MINERAL CHEMISTRY

In order to determine provenance of sediments, several workers have used garnet, tourmaline, and chrome-spinel minerals (e.g., Kumar, 2004; Zahid; 2005; Rahman, 2008; Henry and Guidotti, 1985; Morton, 1985; Henry and Dutrow, 1990; Morton and Taylor, 1991; Nanayama, 1997, Zhu et. al, 2005).

In the current study, only garnets and tourmalines were studied. Garnet [$X_3Y_2(Si0_4)_3$] commonly is present in metamorphic rocks as well as in some igneous rocks. Garnets are good indicators of the pressure-temperature conditions that existed when the source rock was formed. Increase in metamorphic grade is proportionally related to the ratio of ($Fe^{2+} + Mg^{2+}$)/ ($Ca^{2+} + Mn^{2+}$), which is

represented by X component of the generalized garnet formula (Sturt, 1962; Nandi, 1967). Mg and Fe^{2+} increase proportionally in pelitic schists as metamorphic grade increases (Spear, 1993). Y is occupied by trivalent cations like Fe^{3+} and Cr^{3+}.

Tourmaline has a very complex chemical structure, which is- $XY_3Z_6(BO_3)Si_6O_{18}(OH)_4$. X, Y and Z represent Na^{+}, Ca^{2+}; Mn^{2+}, Fe^{2+}, Al^{3+}, Li^{2+}, Mg^{2+}; and Al^{3+}, Cr^{3+}, Mn^{2+}or Mg^{2+} respectively (Deer et. al, 1992). The cation substitutions in tourmaline reflect a wide variety of igneous and metamorphic conditions. Al-Fe(tot)-Mg and Ca-Fe(tot)-Mg are commonly used tourmaline plots for provenance analysis (e.g., Henry and Guidotti, 1985; Henry and Dutrow, 1992).

7.3 SAMPLE PREPARATION

Heavy minerals were separated for microprobe analysis using a heavy liquid. The procedure of heavy mineral separation is described in Chapter 5. Polished thin sections used for heavy mineral studies were also used for microprobe studies. Polished thin sections were washed carefully with detergent to remove fingerprints that could cause Na contamination.

7.4 ELECTRON MICROPROBE

The electron microprobe (EMP) is used to perform micron-scale quantitative chemical analysis on small volumes of mineral grains (Fig. 7.1). Mcroprobe analysis is a non-destructive method, carried out by producing x-rays through an electron beam incident on a flat surface of the sample. The electron beam produces two different responses as it hits the surface of the sample. A certain fraction of incident beam electrons is scattered backward, which carries information on chemical composition of the sample. Once the electron beam hits the sample, the beam loses energy, which is absorbed by the electrons in the sample. Then these electrons collide with the other ones, and transfer energy.

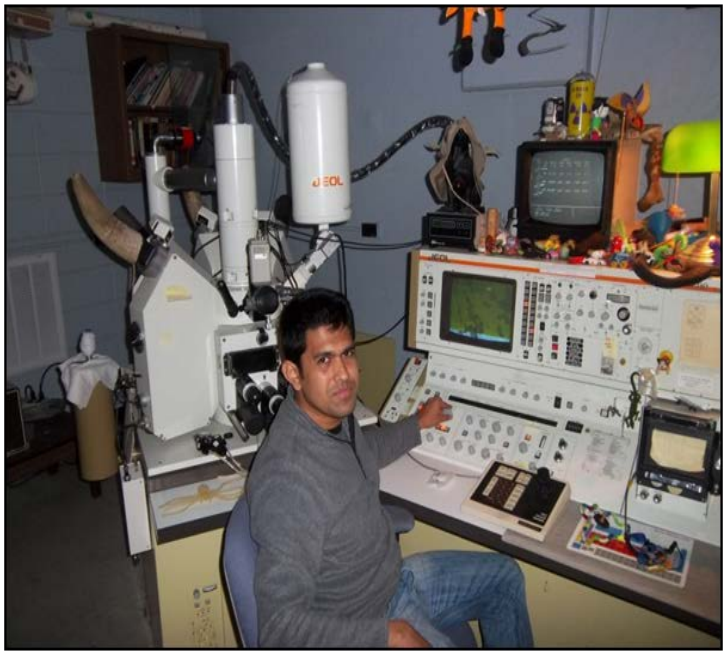

Figure 7.1 Electron microprobe analyzer at the microprobe facility at University of Georgia.

The main purposes of EMP are:

i. To achieve a thorough idea of chemical composition of a small sample both qualitative and quantitative by using x-ray emission spectral analysis without having the sample destroyed.

ii. High-resolution scanning electron and concentration maps (scanning x-ray) are desired through this analysis. Among the scanning electron images, backscattered electron (BSE) show compositional contrast, while secondary electron (SE) will enhance surface and topographic features.

Electron microprobe analysis for this research was carried out at the Department of Geology, University of Georgia, with a JEOL JXA 8600 Superprobe. This is an automated probe with a Geller Micro analytical laboratory dQANT32 stage. An accelerating voltage of 15 KV, a beam current of 15 nA, and a 1-µm beam diameter was used. Analyses were performed with

wavelength dispersive (WDS) spectrometers using 10-second counting times. Calibration of data was carried out using both natural and synthetic standards.

Standard Intensity Calibration:

Measurement of standard x-ray intensities of an element is required before running the microprobe on actual mineral samples. This is done to provide an appropriate standard for the respective minerals. Each type of mineral was run with a different routine based on their composition. Secondary standards were analyzed as unknowns to verify. Throughout the lab session, the analytical environment (e.g., accelerating voltage, beam current, etc.) was kept consistent.

Table 7.1 represents the list of the standards used during this analysis. Most of them came from C.M. Taylor Corporation. The USNM came from the National Museum of Natural History, a branch of the Smithsonian Institution. Two synthetic standards were obtained from the University of Oregon Microprobe Laboratory, and an alamandine standard was obtained from the Harvard Mineral Museum. Calibration for each analysis session was checked using the Kakanui Hornblende (USNM) and Pyrope # 39 (C.M. Taylor) standards.

Table 7.1 Electron microprobe standards used for this study.

Electron Microprobe Standards			
Element	Standard	Source	Comment
Cr	Chromite#5	C M Taylor Corp	
Mn	Spessartine#4b	C M Taylor Corp	
TiO2	Rutile	C M Taylor Corp	
Ca	Sohene# 1A	C M Taylor Corp	
Fe	Hematite# 2	C M Taylor Corp	Used for oxide (spinel) analysis
Fe	Syn. Fayalite Ol-11	Univ. of Oregon	Used for silicate analysis
Ni	Ni metal	C M Taylor Corp	
Si	Diopside 5A	C M Taylor Corp	Si standard for all phases except garnet
Mg	Olivine #1	C M Taylor Corp	
Al	Syn. Spinel	C M Taylor Corp	
K	Orthoclase MAD-10	C M Taylor Corp	
Na	Ameila Albite	USNM	This is a ubiquitous Na Standard
Si	Almandine	Harvard Mineral Museum oxygen standard # 112140	Si standard for garnet analyses
F	Syn. Fluoro-Phologopite	University of Oregon M-6	
Cl	Scapolite	USNM R 6600-1	

7.5 RESULTS

Under the supervision of Mr. Chris Fleisher, a total of 37 grains were analyzed. These include garnets and tourmalines. Although a good search has made, no chrome-spinel grains were found.

7.5.1 Garnet

Garnets are the most abundant minerals in all the samples from both Barapukuria and Khalashpir. Khalashpir samples have more garnets than those from Barapukuria. A total of 29 garnet grains were analyzed (Fig. 7.2) and calculated end members were plotted in figures 7.3 through 7.6. The four end-members calculated are almandine, pyrope, grossular and spessartine, of which almandine is dominant. The average almandine content in garnet grains is 71.21% with a maximum of 91%. Pyrope is intermediate inabundance (average 20.9%), where grossular (avg. 4.24%; max. 14.52%), and spessartine (avg. 3.65; max. 20.43%) contents are low. However, in a few grains, pyrope is dominant.

According to the (Sp+Gro)-Py-Alm plot (Fig. 7.3), almost all the garnets are rich in almandine except one grain from Khalashpir. The (Py+Alm)-Gro-Sp plot (Fig. 7.4) shows that most of the grains are high in (Py+Alm), especially DOB 02 samples from Barapukuria. The (Alm+Sp)-Py-Gro plot (Fig. 7.5) shows that most of the garnets fall in field II, towards the Alm+Sp-end member with almandine and pyrope, and grossular <10%. The Sp-Alm-Py plot indicates that most of the garnets from Barapukuria are distributed between the amphibolite facies and granulite facies (Fig. 7.6). However, almost all the samples from Khalashpir fall within the amphibolite facies zone. The grossular (mol%) distribution of garnets from each well (Fig. 7.7) indicates that all the grains fall within low pressure (lp type) metamorphic regimes, assuming a low calcium protoliths.

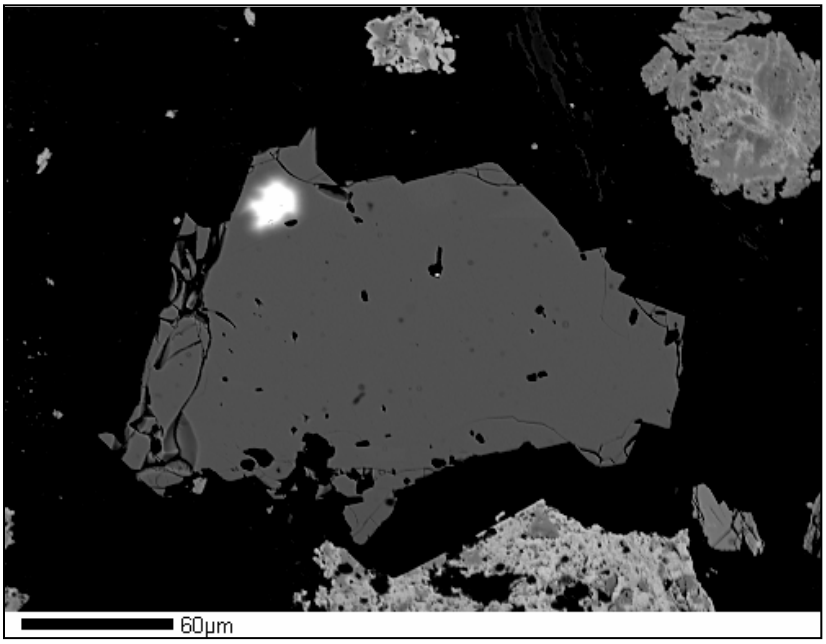

(A)

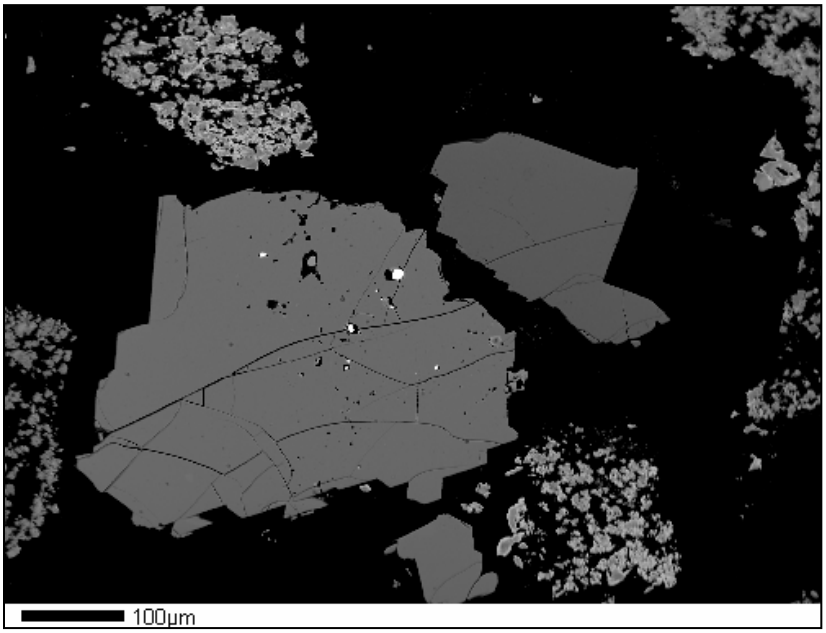

(B)

Figure 7.2 (A-B) Representative BSE photomicrographs of garnet grains in polished section.

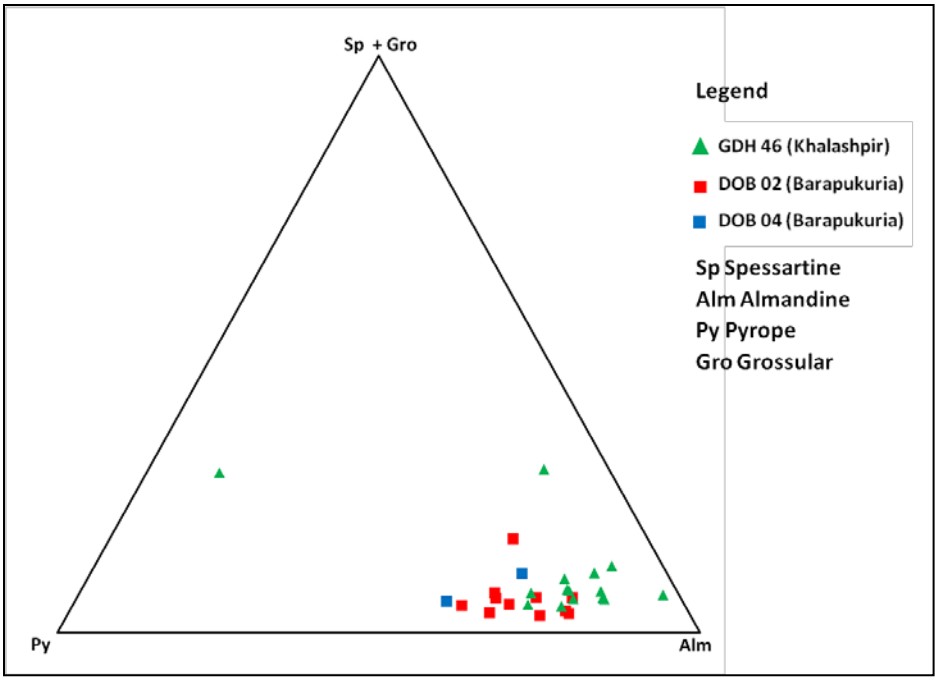

Figure 7.3 Chemical compositions from garnets of Gondwanan sequences plotted on (Sp+Gro)-Py-Alm (adapted from Nanayama, 1997).

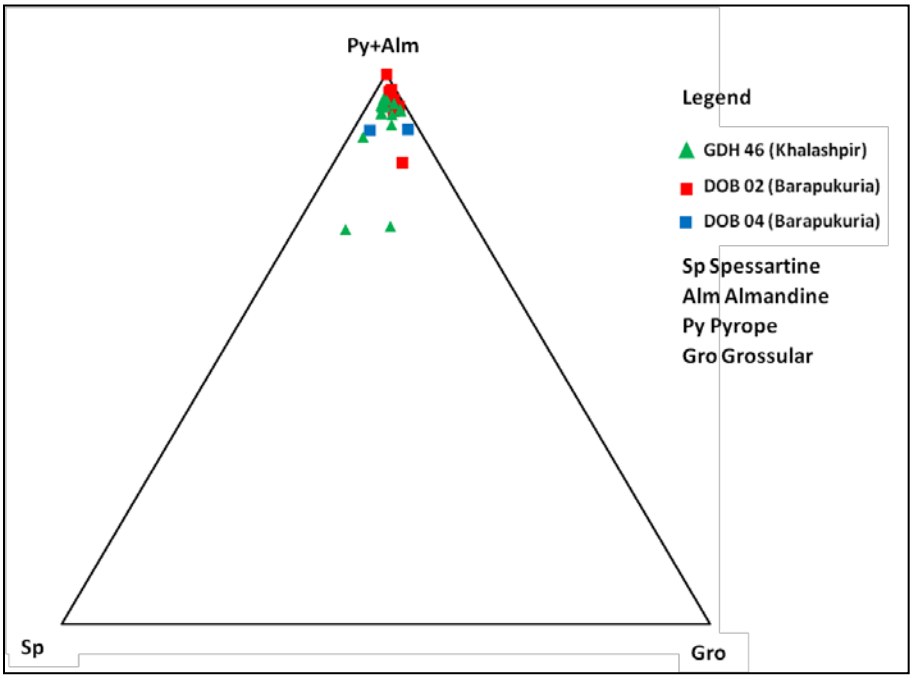

Figure 7.4 Chemical compositions from garnets of Gondwanan sequences plotted on (Py+Alm)-Gro-Sp (adapted from Nanayama, 1997).

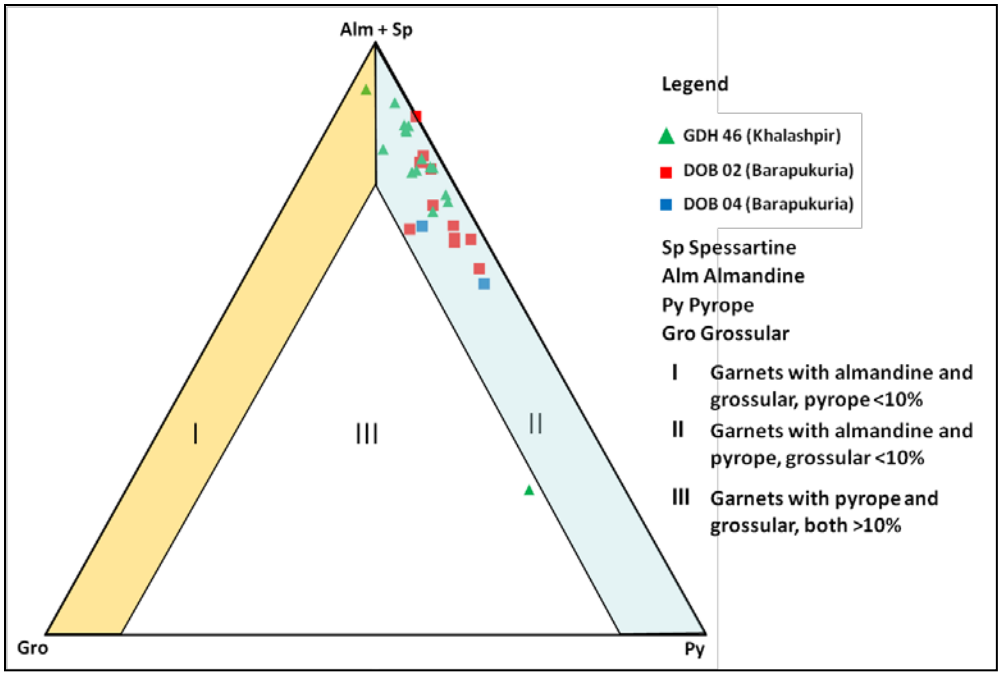

Figure 7.5 Chemical compositions of garnets from Gondwanan sequences of on (Alm+Sp)-Py-Gro (adapter from Nanayama, 1997).

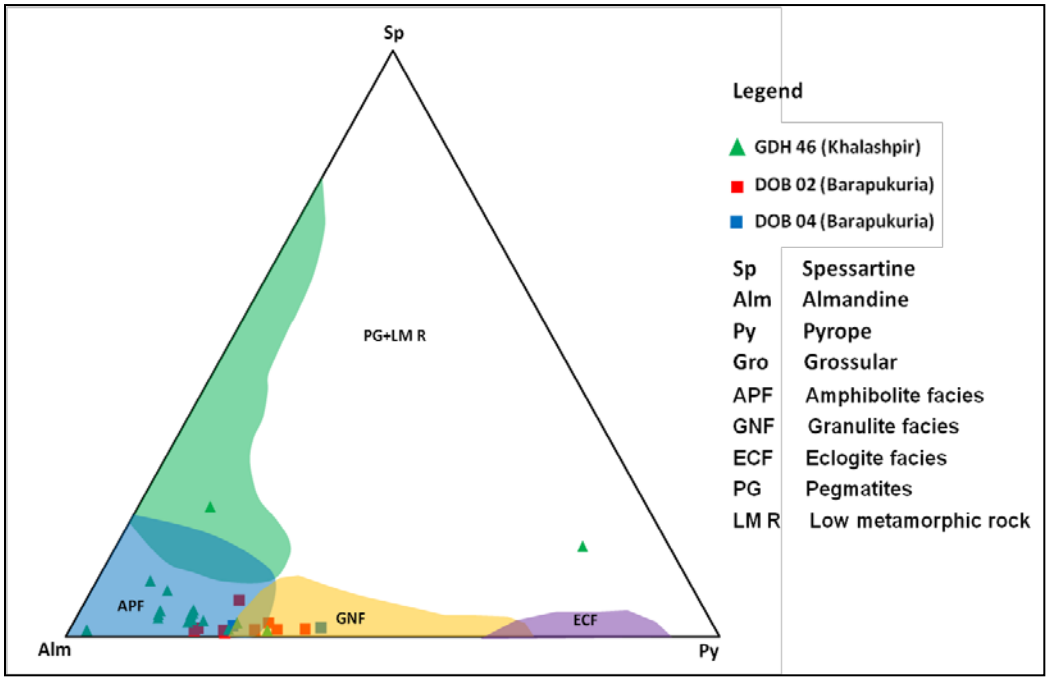

Figure 7.6 Chemical composition of garnets from Gondwanan sequences plotted on Alm-Py-Sp (adapted from Nanayama, 1997).

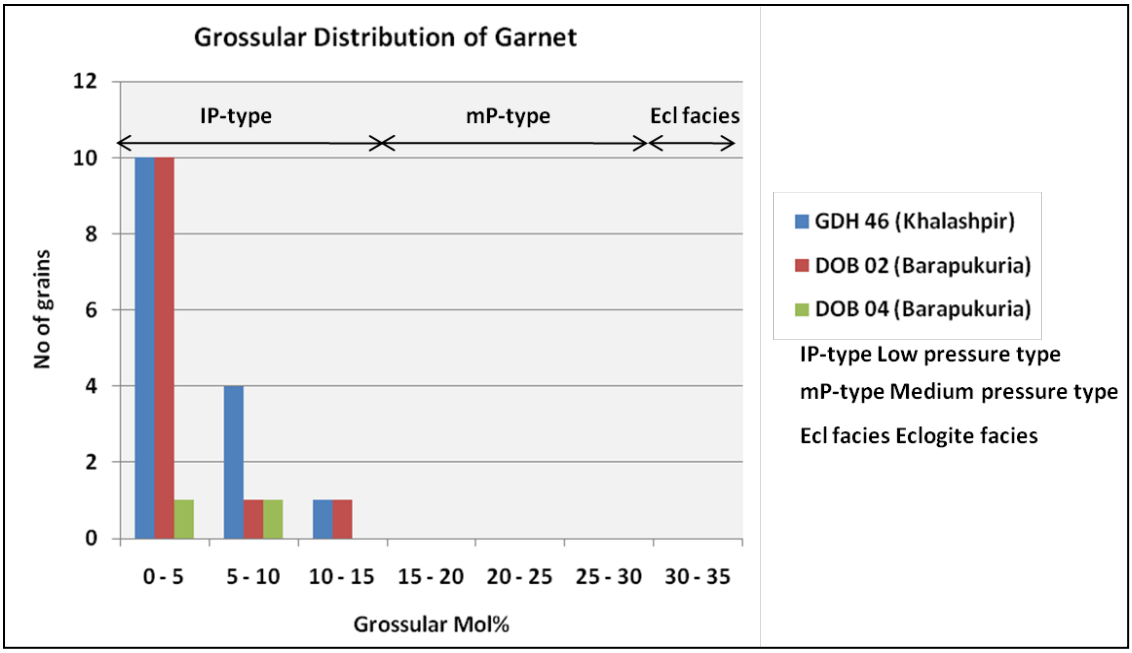

Figure 7.7 Grossular contents of garnets from Gondwanan sequences (adapted from Nanayama, 1997).

7.5.2 Tourmaline

Tourmaline (Fig. 7.8) is very complex in terms of its chemical structure and is usually considered in terms of end-members. A complete solid solution exists between the two end-member series schorl-elbaite and schorl-dravite, although there is a large miscibility gap between elbaite and dravite. Hence, tourmalines are usually described depending on their position in the schorl-elbaite series or in the schorl-dravite series. Garnets were plotted using Al-$Al_{50}Fe_{50(tot)}$-$Al_{50}Mg_{50}$ (Fig. 7.9) and Ca-Fe(tot)-Mg (Fig. 7.10). The Al-$Al_{50}Fe_{50(tot)}$-$Al_{50}Mg_{50}$ plot shows that all the tourmalines fall within the aluminous metapelite and metapsammite fields. However, one grain from Barapukuria falls within the Al-poor metapelite and metapsammite field.

According to the Ca-Fe(tot)-Mg plot (Fig. 7.10), all but one of the tourmaline grains fall within the Ca-poor metapelite, metapsammite, and quartz tourmaline field. The remaining grain, from DOB 04 (Barapukuria), falls in the Li-poor granitoid, pegmatite, and aplite fields.

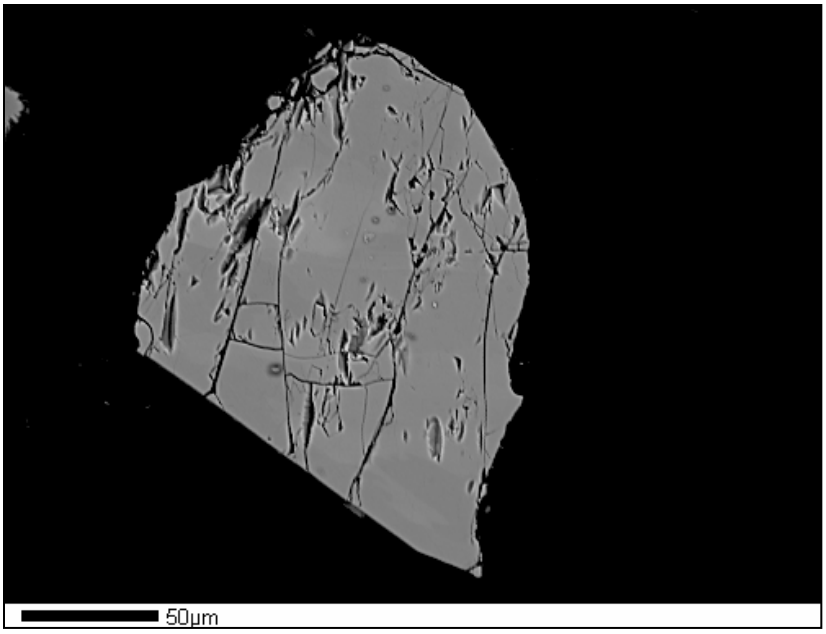

Figure 7.8 Representative photomicrograph of a tourmaline grain used for microprobe study.

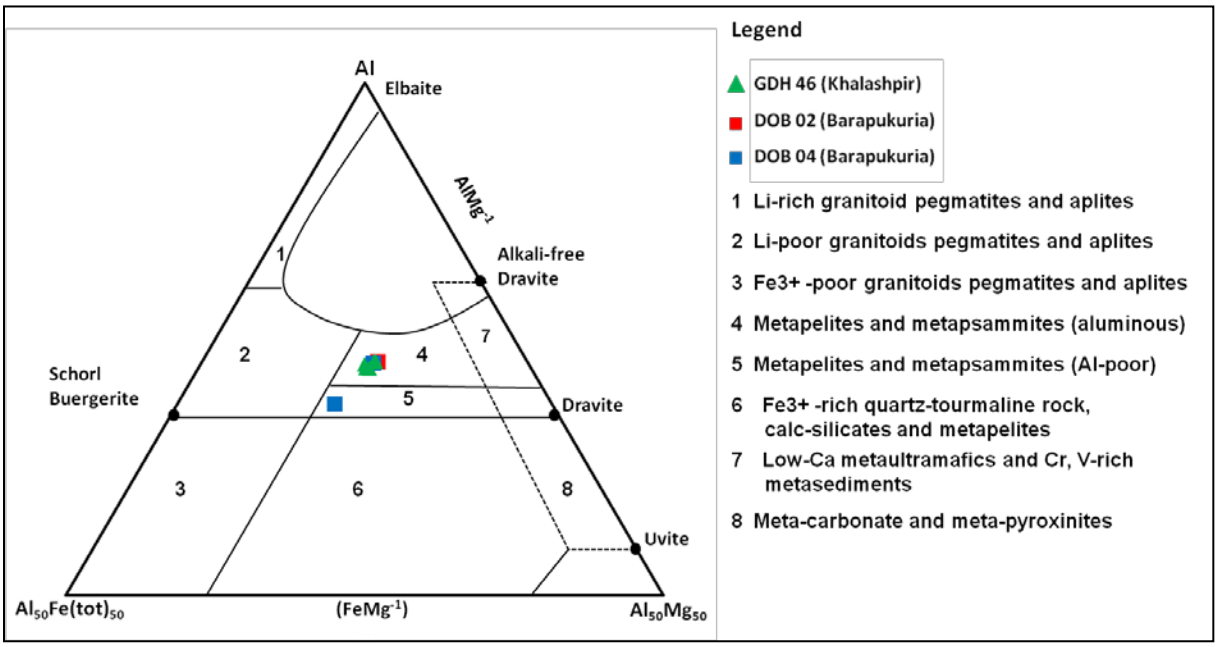

Figure 7.9 Al-Fe (tot)-Mg plot (in molecular proportion) for tourmalines plotted on Al-$Al_{50}Fe_{(tot)50}$-$Al_{50}Mg_{50}$ (adapted from Henry and Guidotti, 1985).

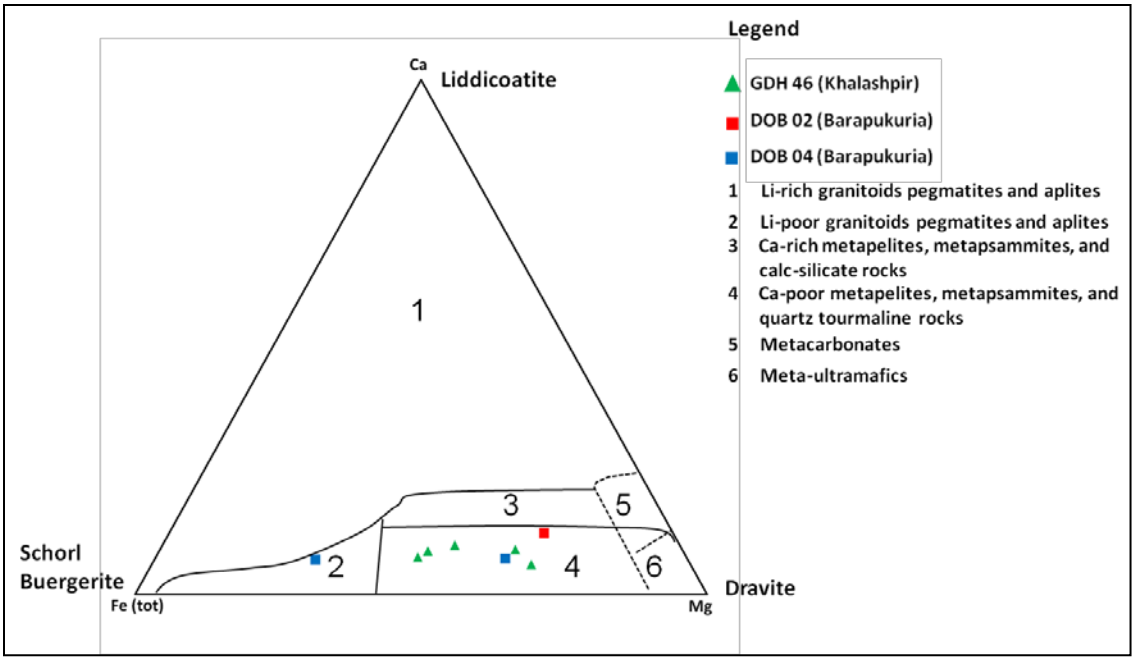

Figure 7.10 Ca-Fe(tot)-Mg plot (in molecular proportion) for tourmalines plotted on Ca-Fe$_{(tot)}$-Mg (adapted from Henry and Guidotti, 1985).

7.6 Discussion

7.6.1 Garnets

Garnets from Khalshpir fall mostly within amphibolite facies fields (Fig. 7.6), being high in alamandine and pyrope and low in grossular content. However, garnets from Barapukuria show derivation from amphibolite and granulite facies source rocks (Fig. 7.6). Garnets from the Gondwanan sequences of northwestern Bengal Basin may have been derived from porphyritic granite (500+/- 14 Ma) of the Meghalayan gneissic complex or Millie granite (607 Ma; Chimote et al., 1988; Crawford, 1969). The adjacent Indian craton or East Antarctic shield also could have been sources.

7.6.2 Tourmaline

Tourmaline grains are indicative of aluminous metapelite and metapsammite sources (Fig. 7.9). The tourmalines from Barapukuria show a provenance from Al-poor metapelites (Fig.

7.9). Tourmalines from Barapukuria also show a source from Li-poor granitoid rocks whereas all the other grains fall within Ca-poor metapelites, metapsammites and quartz tourmaline rocks (Fig. 7.10). These compositional characteristics suggest that sediments may have been derived form Meghalayan gneissic complex or Millie granite. Adjacent cratons of India or Antarctica could also be the source.

CHAPTER 8: SUMMARY AND DISCUSSION

8.1 SANDSTONE PETROGRAPHY

Petrographic studies of Gondwanan sequences recovered in cores from Khalashpir and Barapukuria, Bengal Basin indicated that sandstones are mostly arkosic with some varieties of quartzarenite and litharenite. Quartz is the dominant framework grain, followed by feldspar, mica, organic matter, and lithic grains, in descending order. Abundance of feldspar indicates that the sandstones are immature and likely were transported from nearby cratons. However, dominance of lithic fragments in some of the samples indicates that there may have been a sediment influx from proximal Neoproterozoic to Late Cambrian orogens.

The adjacent Indian shield or the east Antarctic shield could be the possible source. However, the Millie Granite of the northeast Meghalayan Craton also may have supported sediments. Several orogens developed during the Neoproterozoic to Late Cambrian as part of the final assemblage of Rodinia. The most likely sources of orogenic sediments is Pinjarra orogen, which developed due to the collision between India and Australia during the Neoproterozoic to Ordovician (Fig. 8.1). Sediments also may have come from proto-Himalayan orogenic sources, particularly the Lesser Himalayan rocks, which are composed of Neoproterozoic to Lower Paleozoic metamorphic rocks and granite bodies (Fig. 8.2; Gehrels et al., 2003).

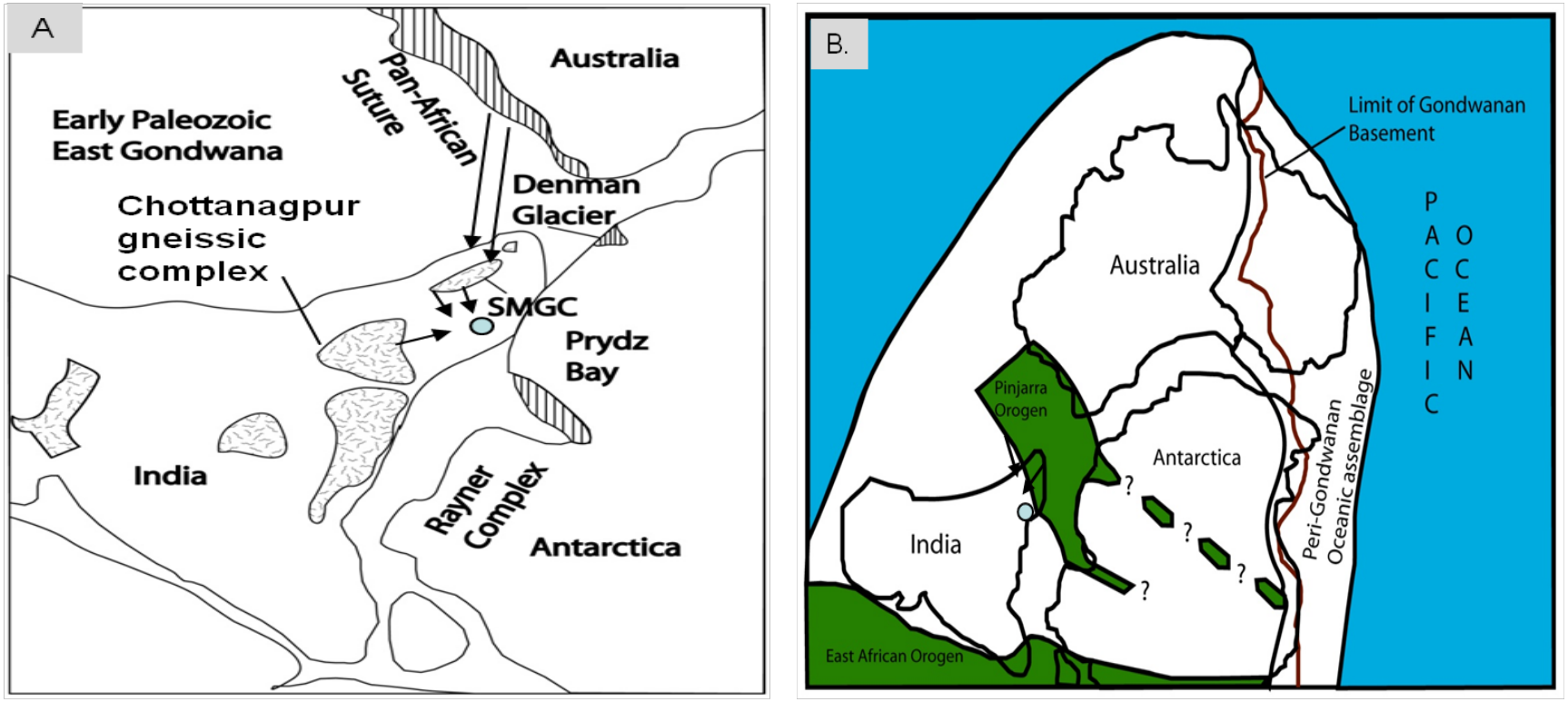

Figure 8.1 (A-B) Possible sediment sources for Gondwanan sequences of Bangladesh. (A) shows nearby cratonic areas, and (B) shows paleogeography at 500-600 Ma. SMGC=Shillong Meghalayan Gneissic Complex (after Fitzsimons 2003; Cawood 2005; Torvisk et al., 2009), blue dots in A and B represent the study area, and green color in B represents orogens.

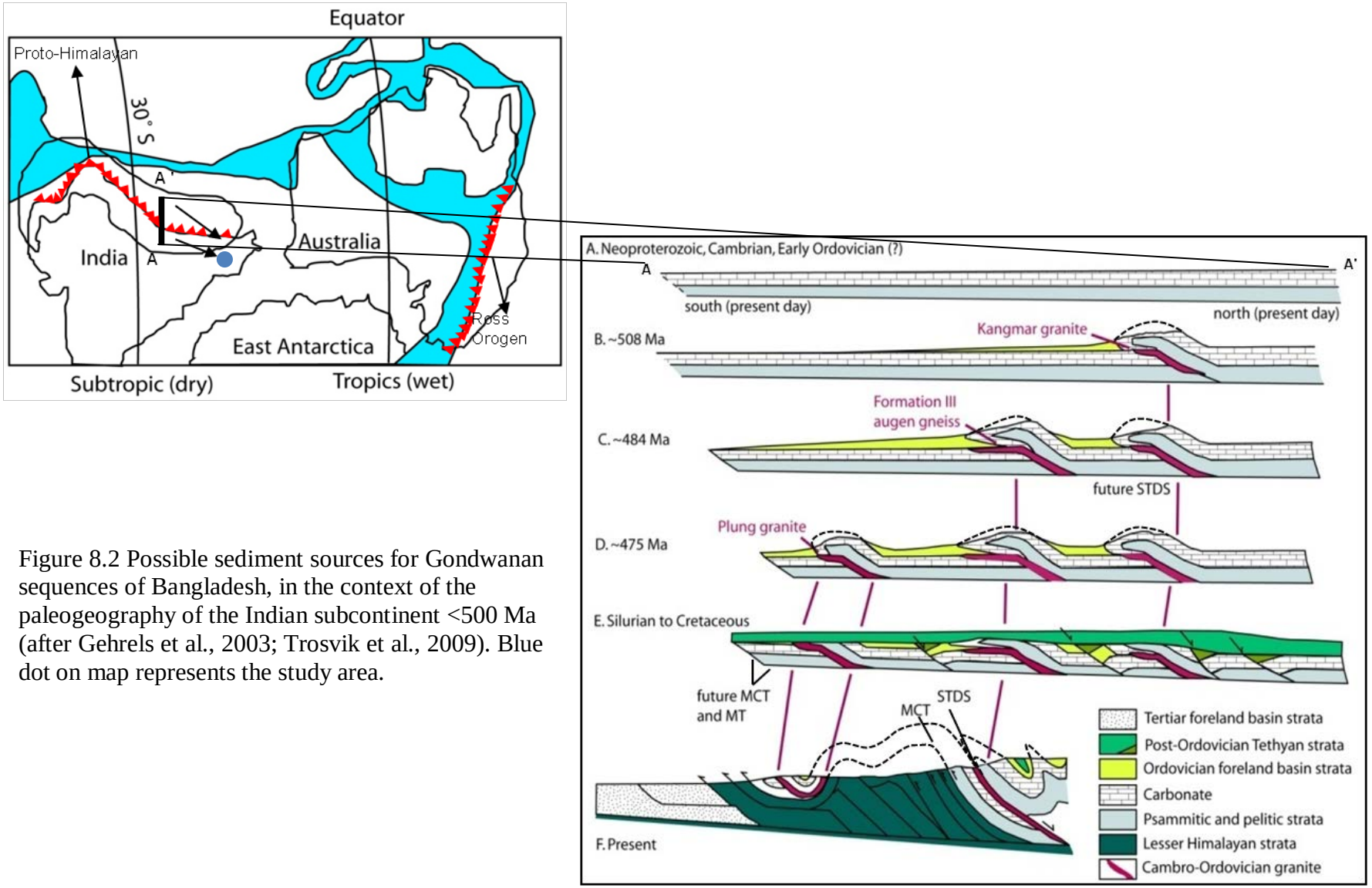

Figure 8.2 Possible sediment sources for Gondwanan sequences of Bangladesh, in the context of the paleogeography of the Indian subcontinent <500 Ma (after Gehrels et al., 2003; Trosvik et al., 2009). Blue dot on map represents the study area.

8.2 HEAVY MINERAL ANALYSIS

Heavy minerals are rare in Gondwanan sequences of Bangladesh. Assemblages of heavy minerals are dominated by three to four species. Garnet is the dominant type along with the opaque grains. Small amounts of tourmaline and zircon are also observed. Rutile is only observed in Barapukuria cores.

Studies of heavy minerals suggest that these may have been derived from the proximal Chottanagpur gneissic complex of Singhum craton and/or Meghalayn cratons of India. The felsic gneisses of Leeuwin metamorphic complex of Neoproterozoic-Early Cambrian Pinjarra orogen also could have contributed sediments to the study area.

8.3 DETRITAL GEOCHRONOLOGY

The ages of muscovites show different age clusters. The oldest age distribution represents cooling ages of about 500 to 650 Ma. The younger age clusters reflect age distributions from 480 to 515 Ma. These age distributions indicate that sediments may have been derived from multiple sources. The older age distribution suggests that the sediments of Gondwanan sequences may have been derived from igneous intrusions and metamorphic complexes of the Indian craton, the East Antarctic craton, or the Millie Granite and/or gneissic complexes of the Meghalyan craton (Fig. 8.3; Crawford et al., 1969; Chimote et al., 1988; Chatterjee et al., 2007). Eastern Ghats–Rayner Block and Western Australia in the mid-Neoproterozoic may have also contributed. Overlaps of the cooling ages between samples may be related to changes in the relative contributions of muscovites from different sources through time. Earlier, older source terranes such as Leewin complex of the Pinjarra orogen (580-500 Ma; Nelson 1996, 1999, 2002; Collins

& Fitzsimons 2001; Wilde & Nelson 2001) were more imported. Later, rocks in the proto-Himalayan orogen (Lesser Himalayan rocks; ~475 Ma to 508 Ma; Gehrels et al., 2003) may have become dominant sources.

Studies of Cenozoic sediments of the Bengal basin (Rahman, 2008; Hossain, 2009; Uddin et al., 2010) and Bengal Fan (Copeland and Harrision, 1990) reveal that cooling and depositional ages are almost identical or vary within 1 to 2 million years. This reflects the rapid uplift and exhumation rates of the Himalayas. In contrast, the large difference (>100 Ma) between muscovite cooling ages and depositional ages observed in the current study indicates that the Permo-Carboniferous Gondwanan sediments of the Bengal Basin did not originate from Himalayan or Taiwan type active and rapidly unroofed orogenic belts.

8.4 MICROPROBE ANALYSIS

Garnet is the most abundant heavy mineral in the sandstones of northwestern Bengal Basin. Garnets from both Khalashpir and Barapukuria are rich in alamandine. Grossular content suggests that all the garnets analyzed for this study represent low-pressure types indicating derivation of garnets from low-grade metamorphic source terrains.

According to Ca-Fe(tot)-Mg plots, tourmalines from Khalashpir were sourced from Ca-poor metapelites, metapsammites, and quartz tourmaline rocks. Tourmalines from Barapukuria also show similar sources but also indicate influences from Li-poor granitoids, pegmatites, and aplites.

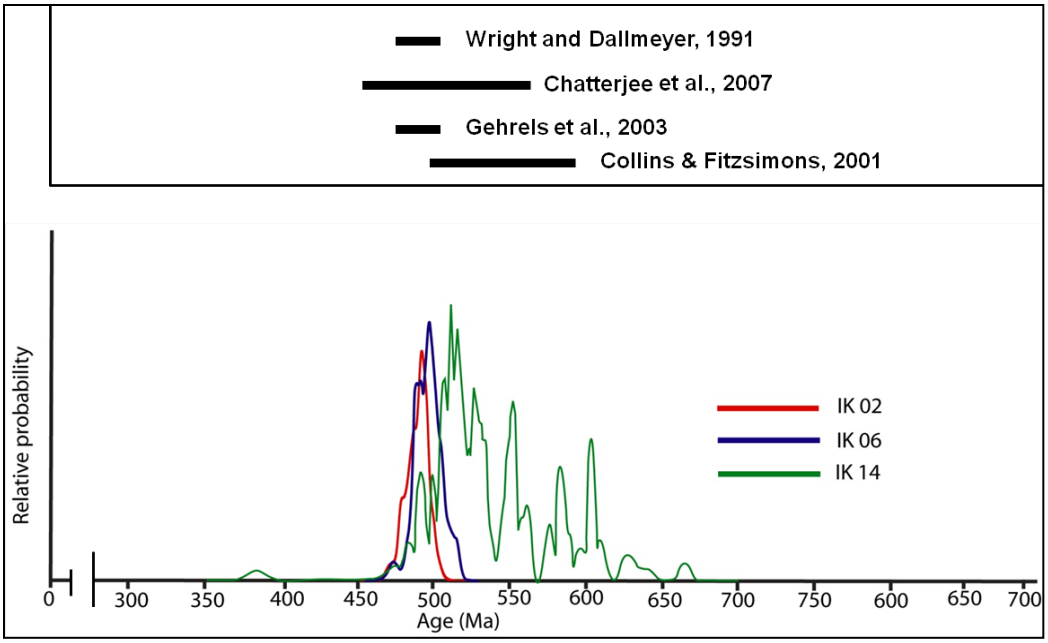

Figure 8.3 $^{40}Ar/^{39}Ar$ cooling ages of single grain muscovite from the Gondwanan sandstone of Bangladesh. The upper panel represents age ranges of various geochronologic dates in different areas which could be source areas for sediments of this study. The age dates from top to bottom (upper panel) were obtained from Robertson Bay terrane, Ross orogen; Millie granite and gneissic complex of Meghalayan craton; proto-Himalayan orogen, and Leewin complex, Pinjarra orogen, respectively.

8.5 PETROGRAPHIC COMPARISONS WITH OTHER INDIAN BASIN

Sandstone compositions recognized in the current study are compared with those in other Gondwana basins in Figure 8.4. Petrographic studies of Gondwanan sequences of Damodar basin, India (Hota et al., 2011) suggests that sandstones are quartz arenite, lithic arenite, and lithic arkose for the Karharbari Formation, Barakar Formation, and Barren Measures, respectively. This indicates that the souces may have changed through time. Gondwanan sandstones from Nepal are quartz arenitic and arkosic (Fig. 8.4). Petrographic studies by Huque et al. (2003) suggest that the sandstones analyzed from GDH 40 of Barapukuria are arkosic and lithic arkose. The differences in composition between the present study and study by Huque et al.

(2003) may have altered to differences in point-counting protocol, although local changes in sediment sources cannot be ruled out. Differences in sandstone compositions among various Gondwanan basins may be attributed to differences in (1) source terranes, (2) routing systems or drainage patterns; and (iii) geomorphic and structural positions of the basins.

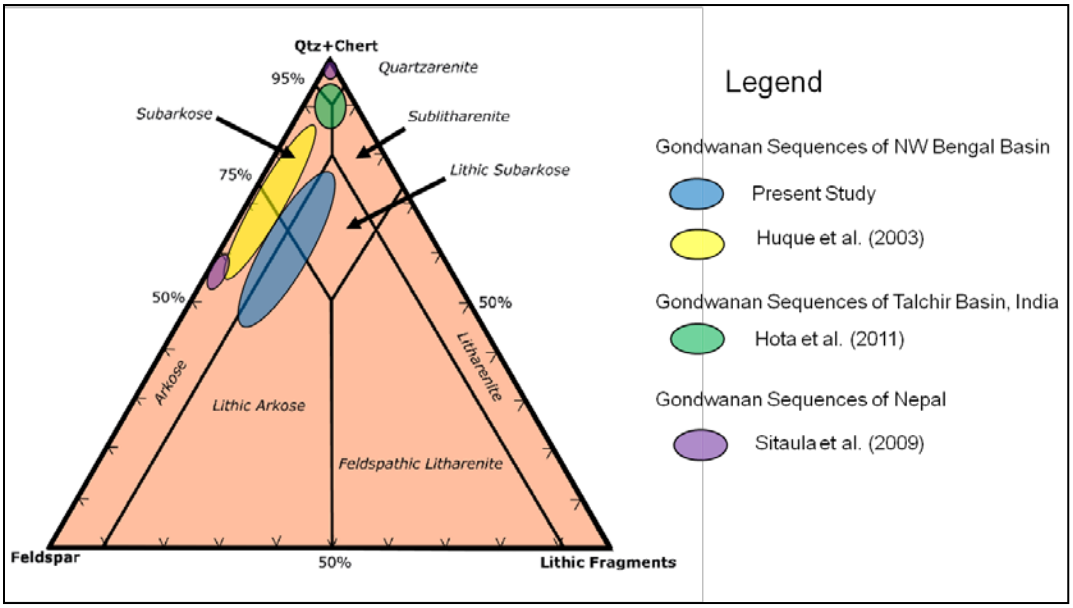

Figure 8.4 Comparison of average sandstone modes of Gondwanan sequences from different areas of the Indian subcontinent.

CHAPTER 9: CONCLUSIONS

The following conclusions can be drawn based on the results obtained in the current study:

i. Gondwanan sediments of northwestern Bengal Basin may have been derived from multiple source terranes.

ii. Sandstone composition reveals differences among from coeval sediments from India, Nepal, and other nearby wells of the Bengal Basin.

iii. Based on $^{40}Ar/^{39}Ar$ geochronology, sediments may have been derived from three distinct sources. The oldest sediments were derived from adjacent cratonic areas of India. Subsequently, sediments were derived from the orogens associated with the India-Australia collision and the Proto-Himalayan orogen.

iv. Garnet is the dominant heavy mineral content of the Gondwanan sequences of Bengal Basin. Absence of rutile in Khalashpir core may be caused by change of sources locally. Although existence of orogenic sources is evident, the absence of chrome-spinel suggests that the sediments may not have been related to obducted ophiolites.

v. Unlike Cenozoic sediments of the Bengal Basin and Bengal Fan sediments derived from unroofing of active Himalayan belts, Gondwanan sediments of these basins did not derive from active orogenic belts as depositional ages (~ 250 to 360 Ma) are more than 100 Ma younger than cooling ages (>450 Ma). Further studies

using core samples from several other locations in Bangladesh are needed to have more definitive by establish the provenance (s) of Gondwanan sediments in the Bengal Basin of Bangladesh.

REFERENCES

Acharyya, S.K., 2000, Break up of Australia-India-Madagascar block, opening of the Indian ocean and continental accretion in southeast Asia with special reference to the characteristics of the peri-Indian collicion zones: Gondwana Research, v. 3, p. 425-443.

Ahmad, F., 1957, Observations on the Umaira marine bed: Records of the Geological Survey of India, v. 84, p. 469-475.

Ahmad, F., and Khan, Z.A., 1993, Marine incursions in Lower Gondwana Group in central India, Gondwana Geological magazine special volume, Birbal Sahni Center Nat. Symposium Gondwana, India, p. 1-7.

Akhtar, A., and Kosanke, R.M., 2000, Palynomorphs of Permian Gondwana coal from borehole GDH-38, Barapukuria Coal Basin, Bangladesh: Journal of Asian Earth Sciences, v. 31, p. 107-117.

Akhtar, A., 2001, Gondwana sediment of Bangladesh and its correlation with those of other regions of the world on the basis of spore-pollen: Gondwana Research, v. 4, p. 135-136.

Alam, M., Alam, M.M., Curray, J.R., Chowdhury, M.L.R., and Gani, M.R., 2003, An overview of the sedimentary geology of the Bengal Basin in relation to the regional tectonic framework and basin-fill history: Sedimentary Geology, v. 155, p. 179-208.

Amano, K., and Taira, A., 1992, Two-phase uplift of Higher Himalayas since 17 Ma: Geology, v. 20, p. 391-394.

Archbold, N.W., Cisterna, G.A., and Simanauskas, T., 2004, The Gondwanan Carboniferous-Permian boundary revisited: New data from Australia and Argentina: International Association for Gondwana Research, Japan, v. 7, p. 125-133.

Aslam, M., Arora, M., and Tewari, R.C., 1991, Heavy mineral suite in the Barakar sandstone of Moher sub-basin, Singrauli coalfield, central India: Journal of the Geological Society of India, v. 29, p. 66-75.

Bakr, M.A., Rahman, Q.M.A. and Islam, M.M., 1986, Barapukuria coal deposit, Parbatipur Upazila, District; Geological Survey Report (unpublished), 57 p.

Bakr, M.A., Rahman, Q.M.A., Islam, M.M., Islam, M.K., Uddin, M.N., Resan, S.A., Haider, M.J., Sultan-Ul-Islam, M., Ali, M.W., Chowdhury, M., Mannan, K.H. and Anam, A.N.M.H., 1996, Geology of coal deposit of Barapukuria basin, Dinajpur District, Bangladesh: Records of The Geological Survey of Bangladesh, v. 8, 16 p.

Baksi, A. K., Barman, T. R., Paul, D. K. and Farrar, E., 1987, Wide spread early Cretaceous flood basalt volcanism in Eastern India: geochemical data from the Rajmahal-Bengal-Sylhet traps: Chemical Geology, v. 63, p. 133-141.

Banerjee, I., 1966. Turbidites in a glacial sequence: a study from the Talchir Formation, Ranigunj coalfield: India Journal of Geology, v. 74, p. 593–606.

Basu, A., 1975, Petrology of Holocene alluvial sand derived from plutonic source rocks: Implication to paleoclimate interpretation: Journal of Sedimentary Petrology, v. 4, p. 694-709.

Bateman, R.M., and Catt, J.A., 1985, Modification of heavy mineral assemblages in English coversands by acid pedochemical weathering: Catena, v. 12, p. 1-21.

Bernet, M., Brandon, M.T., Garver, J.I. and Molitor, B.R., 2004, Fundamentals of detrital zircon fission-track analysis for provenance and exhumation studies with examples from the European Alps. In: Detrital Thermochronology-Provenance Analysis, Exhumation, and Landscape Evolution of Mountain Belts (Eds M. Bernet and C. Spiegel): Geological Society of America Special Paper, v. 378, p. 25-36.

Biswas, S.K., 2003, Regional tectonic framework of the Pranhita-Godavari basin, India: Journal of Asian Earth Science, v. 21, p. 1-9.

Blakey, R.C., 2008, Gondwana paleogeography from assembly to breakup-A 500 m.y. odyssey: Geological Society of America, Special Paper 441, 28 p.

Bostick, N.H., Betterton, W.J., Gluskoter, H.J., and Islam, M.N., 1991, Petrography of Permian “Gondwana” coals from boreholes in northwestern Bangladesh, based on semiautomated reflectance scanning: Organic Geochemistry, v. 17, p. 399-413.

Brewer, I.D., Burbank, D.W., and Hodges, K.V., 2003, Modeling detrital cooling-age populations: Insights from two Himalayan catchments: Basin Research, v. 15, p. 305-320.

Brookfield, M.E., 1993, The Himalayan passive margin from Precambrian to Cretaceous times: Sedimentary Geology, v. 84, p. 1-35.

Burbank, D.W., Brewer, I.D., Sobel, E.R., and Bullen, M.E., 2007, Single-crystal dating and the detrital record of orogenesis, in sedimentary processes, environments and basins: A tribute to Peter Friend, G. Nichols, E. Williams and C. Paola, John Wiley and Sons (Eds.), p. 253-281.

Carer, A., and Moss, S.J., 1999, Combined detrital zircon fission-track and U-Pb dating: a new approach to understanding hinterland evolution: Geology, v. 27, p. 235-238.

Casshyap, S.M. and Tewari, R.C., 1991, Depositional model and tectonic evolution of Gondwana basins, In: Venkatachala, B.S., Maheswari, H.K. (Eds.), Indian Gondwana Memoir of Geological Society of India, v. 21, p. 95-206.

Catuneanu, O., Wopfner, H., Eriksson, P.G., Carincross, B., Rubidge, B.S., Smith, R.M.H., and Hancox, P.J., 2005, The Karoo basins of south-central Africa: Journal of African Earth Sciences, v. 43, p. 211-253.

Cawood, P.A., 2005, Terra Australis Orogen: Rodinia breakup and development of the Pacific and Iapetus margins of Gondwana during the Neoproterozoic and Paleozoic: Earth Science Reviews, v. 69, p. 249-279.

Cerveny, P.F., Naeser, N.D., Zeitler, P.K., Naeser, C.W., and Johnson, N.M., 1988, History of uplift and relief of the Himalaya during the past 18 millionyears; evidence from sandstone of the Siwalik Group. In: New Perspective in Basin Analysis, K.L. Kleinspehn and C. Paola (Eds.), p. 43-61. Springer-Verlag, New York.

Chakraborty, C., Mandal, N., and Ghosh, S.K., 2003, Kinematics of the Gondwana basins of peninsular India: Tectonophysics, v. 377, p. 299-324.

Chtterjee, N., Mazumdar, A.C., Bhattacharaya, A., and Saikia, R.R., 2007, Mesoproterozoic granulites of the Shillong-Meghalaya Plateau: Evidence of western continuation of the Prydz Bay Pan-African suture into Northeastern India: Precambrian Research, v. 152, p. 1-26.

Chatterjee, N., Crowley, J.L., and Ghose, N.C., 2008, Geochronology of the 1.55 Ga Bengal anorthosite and Grenvillian metamorphism in the Chottanagpur gneissic complex, eastern India: Precambrian Research, v. 161, p. 303-316.

Chaudhuri, S., 1985, Marine influence in Hutar coalfield: Palaeobotanist, v. 36, p. 30-36.

Chimote, J.S., Pandey, B.K, Bagchi, A.K., Basu, A.N., Gupta, J.N. and Saraswat, A.C., 1988, Rb-Sr whole-rock isochron age for the Mylliem Granite, E.K. Hills, Meghalya: Proceedings of 4th National Symposium on Mass Spectometry, IISC, Bangalore.

Collins, A.S., 2003, Structure and age of the northern Leeuwin Complex, Western Australia: constraints from field mapping and U-Pb isotopic analysis: Australian Journal of Earth Sciences, v. 50, p. 585-599.

Collins, A.S., and Fitzsimons, I. C. W., 2001, Structural, isotopic and geochemical constraints on the evolution of the Leeuwin Complex, SW Australia, In: Sircombe K. N. & Li Z. X. eds. From Basins to Mountains: Rodinia at the Turn of the Century, pp. 16–19. Geological Society of Australia Abstracts 65.

Collins, A.S., and Pisarevsky, S.A., 2005, Amalgamation eastern Gondwana: The evolution of the Circum-Indian Orogens: Earth-Science Reviews, v. 79, p. 229-270.

Condie, K.C., 1982, Plate tectonics and crustal evolution: (New York: Pergamon Press) 2nd ed., p. 310.

Copeland, P., and Harrison, M., 1990, Episodic rapid uplift in the Himalaya revealed by $^{40}Ar/^{39}Ar$ analysis of detrital K-feldspar and muscovite, Bengal fan: Geological Society of America, v. 18, no. 4, p. 354-357.

Courtillot, V.E., and Renne, P.R., 2003, On the ages of flood basalt events: Comptes Rendus Geosciences, v. 335, p. 113-140.

Crawford, A.R., 1969, Reconnaissance Rb-Sr dating of Precambrian rocks of southern peninsular India, Geological Society of India, v. 10, p. 117-166.

Crook, K.A.W., 1974, Lithogenesis and geotectonics: the significance of compositional variations in flysch arenites (graywackes), In: Dott, R.H., and Shaver, R.H. (Eds.), Modern and ancient geosynclinal sedimentation: SEPM Special Publication, v. 19, p. 304-310.

Dasgupta, P., 2002, Architecture and facies pattern of a sublacustrine fan, Jharia basin, India, Sedimentary Geology, v. 148, p. 373– 387.

Davis, G.A., 1988, Rapid upward transport of mid-crustal mylonitic gnesses in the footwall of a Miocene detachment fault, Whipple Mountains, southeastern California: International Journal of Earth Sciences, v. 77, p. 191-209.

Deer, W.A., Howie, R.A., and Zussman, J., 1992, An introduction to the rock-forming minerals: Longman Scientific Technical, Harlow, United Kingdom, 696 p.

Dickin, A.P., 1995, Radiogenic Isotope Geology: New York, Cambridge Press, 452 p.

Dickerson, P.W., 2004, Pampean orogen: An intraplate component of early Paleozoic deformation?: Gondwana Research, v. 7, no. 1, p. 115–124, doi: 10.1016/S1342-937X(05)70310-5.

Dickinson, W.R., 1970, Interpreting detrital modes of greywacke and arkose: Journal of Sedimentary Petrology, v. 40, p. 695-707.

Dickinson, W.R.,1982, Composition of sandstones in circum-Pacific subduction complexes and fore-arc basins: American Association of Petroleum Geologists Bulletin, v. 66, p. 121-137.

Dickinson, W.R., 1985, Interpreting provenance relations from detrital modes of sandstones, in Zuffa, G.G., ed., Reading Provenance from Arenites: Dordecht, The Netherlands, Riedel, p. 333-361.

Dickinson, W.R., and Suczek, C., 1979, Plate tectonics and sandstone compositions: American Association of Petroleum Geologists Bulletin, v. 63, p. 2164-2182.

Dorsey, R. J., 1988, Provenance evolution and unroofing history of a modern arc continent collision: Evidence from petrography of Plio-Pleistocene sandstones, eastern Taiwan: Journal of Sedimentary Petrology, v. 58, p. 208-218.

Dryden, A.L., and Dryden, C., 1946, Comparative rates of weathering of some common heavy minerals: Journal of Sedimentary Petrology, v. 16, p 91-96.

Dutta, A.B., 1965, *Fenestella* sp. From the Talchir of Daltongunj coalfield: Quaternary Journal of Geological Minerals Metallurgical Society India, v. 37, p. 133-134.

Dutta, P., 2002, Gondwana lithostratigraphy of Peninsular India: Gondwana Research (Gondwana Newsletter Sec), v. 5, p. 540-553.

Ethridge, F.G., 1977, Petrology, transport, and environment in isochronous Upper Devonian sandstone and siltstone units, New York: Journal of Sedimentary Petrology, v. 47, p. 53-65.

Faure, G., 1986, Principles of Isotope Geology, second edition: New York, John Wiley and Sons, 589 p.

Feistmantel, O., 1876. Note on the age of some fossil floras of India: Rec. Geol. Surv. India 9 (3), 68– 79.

Fioretti, A.M., Black, P., Henjes-Kunst, F. and Visona`, D., 2003, Detrital zircon age patterns from a large gneissic xenolith from Cape Phillips granite and from Robertson Bay Group metasediments, northern Victoria Land, Antarctica. 9th International Symposium on Antarctic earth Science, 8–12 September, Potsdam, Terra Nostra, 2003/4, pp 94–95.

Fitzsimons, I.C.W., 2000a, Grenville-age basement provinces in East Antarctica: Evidence for three separate collisional orogens: Geology v. 28, p. 879–882.

Fitzsimons, I.C.W., 2000b, A review of tectonic elements in the East Antarctic Shield, and their implications for Gondwana and earlier supercontinents: Journal of African Earth Sciences v. 31, p. 3–23.

Fitzsimons, I.C.W., 2003, Proterozoic basement provinces of southern and southwestern Australia, and their correlation with Antarctica. In: Yoshida M., Windley B. F. & Dasgupta S. eds. Proterozoic East Gondwana: Supercontinent Assembly and Breakup: Geological Society of London Special Publication 206, p. 93–130.

Fleet, W.F., 1926, Petrological notes on the Old Red Sandstones of the West Midlands: Geological Magazine, v. 63, p. 505-516.

Flores, R.M., 1972, Delta front-delta plain facies of the Pennsylvanian Haymond Formation, northeast marathon Basin, Texas: Geological Society of America Bulletin, v. 83, p. 3415-3424.

Fluteau, F., Besse, J., Broutin, J., and Ramstein, G, 2001, The Late Permian climate. What can be inferred from climate modeling concerning Pangea scenarios and Hercynian range altitude? Palaeogeography, Palaeoclimatology, Palaeoecology, v. 167, p. 39-71.

Frederico, L., Capponi, G., and Crispini, L., 2006, The Ross orogeny of the transarctic mountains: a northern Victoria Land perspective: International Journal of Earth Sciences, v. 95, p. 759-770.

Frielingsdorf, J., Islam, Sk. A., Block, M., Rahman, Md. M., and Rabbani, Md. G., 2008, Tectonic subsidence modeling and Gondwana source rock hydrocarbon potential, northwest Bangladesh modeling of Kuchma, Singra and Hazipur wells: Marine and Petroleum Geology, v. 25, p. 553-564.

Freise, F.W., 1931, Untersuchung von Mineralen auf Ab-nutzbarkeit bei Verfrachtung im Wasser: Tschermaks Mineralogy of Petrology, v. 41, p. 1-7

Fox, C. S., 1931, The Gondwana System and related formations: Mem. Geological Survey of India 58 (iv), p. 241.

Garzanti, E., Vezzoli, G., Ando, S., Lave, J., Attal, M., France-Lanord, C., and DeCelles, P., 2007, Quantifying sand provenance and erosion (Marsyandi River, Nepal Himalaya): Earth and Planetary Science Letters, v. 258, p. 500-515.

Gehrels, G.E., and Kapp, P.A., 1998, Detrital zircon geochronology and regional correlation of metasedimentary rocks in the Coast Mountains, southeastern Alaska: Canadian Journal of Earth Sciences, v. 35, p. 269-279.

Gehrels, G.E., DeCelles, P.G., Martin, A., Ojha, T.P., and Pinhassi, G., 2003, Initiation of the Himalayan orogen as an early Paleozoic thin-skinned thrust belt: GSA Today, v. 13, p. 4-9.

Ghosh, P.K., and Mitra, N.D., 1975, History of Talchir sedimentation in Damodar Valley Basin, Memoir Geological Survey of India, v. 105, 117 p.

Ghosh, S.K., 1954, Discovery of a new locality of marine Gondwana formation near Manendragarh in Madhya Pradesh, Science and Culture, v. 19, p. 620.

Ghosh, S.C., 2002, The Raniganj Coal Basin: an example of an Indian Gondwana rift: Sedimentary Geology, v. 147, p. 155-176.

Ghosh, S.K., 2001, First record of marine bivalves from the Talchir Formation of the Satpura Gondwana basin, India: Palaeobiogeographic implications: Gondwana Research (Gondwana Newsletter Section) 6/2, p. 312-320.

Graham, S. A., Dickinson, W. R., and Ingersoll, R. V., 1975, Himalayan - Bengal model for flysh dispersal in the Appalachian - Ouachita system: Geological Society of America Bulletin, v. 86, p. 273-286.

Graham, S.A., Ingersoll, R.V., and Dickinson, W.R., 1976, Common provenance for lithic grains in Carboniferous sandstones from Ouachita Mountains and Black Warrior Basin: Journal of Sedimentary Petrology, v. 46, p. 620-632.

Gray, D.R., Foster, D.A., Meert, J.G., Goscombe, B.D., Armstrong, R., Truow, R.A.J. and Passchier, C.W., A., 2008, A Damara perspective on the assembly of southwestern Gondwana: Geological Society of London, Special Publication, no. 294, p. 257-278.

Grimm, W.D., 1973, Stepwise heavy mineral weathering in the residual quartz gravel, Bavarian Molasse (Germany): Contribution to Sedimentology, v. 1, p 103-125

Hames, W.E., and Bowring, S.A., 1994, An empirical evaluation of the argon diffusion geometry in muscovite: Earth and Planetary Science Letters, v. 124, p. 161-167.

Henry, D.J., and Dutrow, B.L., 1990, Tourmaline as a low grade clastic metasedimentary rock: an example of the petrogenetic potential of tourmaline: Contributions to Mineralogy and Petrology, v. 112, p. 203-218.

Henry, D.J., and Guidotti, C.V., 1985, Tourmaline as a petrogenetic indicator mineral: an example from the staurolite grade metapelites of NW Maine: American Mineralogists, v. 70, p. 1-15.

Hess, H.H., 1966, Notes on operation of Frantz isodynamic magnetic separator, Princeton University: User manual guide, 6 p.

Hodges, K. V., Hames, W. E., Olszewski, W., Burchfiel, B. C., Royden, L. H., and Chen, Z., 1994, Thermobarometric and $^{40}Ar/^{39}Ar$ geochronologic constraints on Eohimalayan metamorphism in the Dinggye area, Southern Tibet: Contributions to Mineralogy and Petrology, v. 117, p. 151-163.

Hodges, K.V., Rhul, K.W., Wobus, C.W., and Pringle, M.S., 2005, $^{40}Ar/^{39}Ar$ thermochronology of the detrital minerals, *in* Thermochronology, Reviews inMineralogy and Geochemistry, Reiners, P.W., and Ehlers, T.A., eds., Mineralogical Society of America, Washington, D.C., v. 58, p. 235-257.

Hossain, M.S., 2009, Overpressure in the eastern Bengal Basin, Bangladesh, and its relation to compressional tectonics [unpublished M.S. Thesis], Auburn University, Auburn, AL, 119 p.

Hossain, H.M.Z., Islam, M.S.U., Ahmed, S.S., and Hossain, I., 2002, Analysis of sedimentary facies and depositional environments of the Permian Gondwana sequence in borehole GDH-45, Khalaspir Basin, Bangladesh: Geosciences Journal, v. 6, p. 227-236.

Hota, R.N., Das, B.K., Sahoo, M., and Maejima, W., 2011, Provenance variability during Damuda sedimentation in the Talchir Gondwana Basin, India – A statistical assessment: International Journal of Geosciences, v. 2, p. 120-137.

Huque, M.A., Rahman, M.Z., Akhter, S.H., and Bhuiyan, A.H., 2003, Thin-section petrography of the Permian Gondwana coal bearing sandstones of the Barapukuria Basin, Dinajpur, Bangladesh: Bangladesh Journal of Geology, v. 22, p. 71-82.

Imam, M. B., and Hussain, M., 2002, A review of hydrocarbon habitats in Bangladesh: Journal of Petroleum Geology, v. 25, p. 31–52.

Ingersoll, R.V., Bullard, T.F., Ford, R.L., Grimm, J.P., Pickle, J.D., and Sares, S.W., 1984, The effect of grain size on detrital modes: A test of the Gazzi-Dickinson point-counting method: Journal of Sedimentary Petrology, v. 54, p. 103-116.

Ingersoll, R.V., and Suczek, C.A., 1979, Petrology and provenance of Neogene sand from Nicobar and Bengal Fans, DSDP sites 211 and 218: Journal of Sedimentary Research, v. 49, p. 1217-1228.

Ingersoll, R.V., Graham, S.A., and Dickinson, W.R., 1995, Remnant ocean basins, in Busby, C.J., and Ingersoll, R.V., eds., Tectonics of sedimentary basins: Blackwell Science, Cambridge, p. 363-391.

Islam, M.M., Resan, S.A., Haider, M.J., Islam, M.S., Ali, M.W., and Chwodhury, M-E-A., 1987, Subsurface geology and coal deposit of Barapukuria area, Parbatipur Upazila, Dinajpur District, Bangladesh: Geological Survey Report (Unpublished).

Islam, M.N., Uddin, M.N., Resan, S.A., Sultan-ul-Islam, M. and Ali, M.W., 1992, Geology of the Khalashpir coal basin, Pirganj, Rangpur, Bangladesh: Combined report of Government of the People's Republic of Bangladesh, Ministry of Energy and Mineral Resources and Geological Survey of Bangladesh, 59 p.

Islam, M.S., 1990, Palynology of the Permian strata in the borehole GDH – 38 in Barapukuria basin, Dinajpur, Bangladesh: Bangladesh Journal of Geology, v. 9, p. 29-39.

Islam, M.R., and Hayashi, D., 2008, Geology and coal bed methane resource potential of the Gondwana Barapukuria Coal Basin, Dinajpur, Bangladesh: International Journal of Coal Geology 75, p. 127-143.

Johnsson, M.J., 1993, The system controlling the composition of clastic sediments, *in* Johnsson, M.J. and Basu, A., eds., Processes controlling the composition of clastic sediments: Geological Society of America Special Paper 284, p. 1-19.

Khan, A. A., 1991, Tectonics of the Bengal Basin: Journal of Himalayan Geology, v. 2, p. 91–101.

Khan, M.R., and Muminullah, M., 1980, Stratigraphy of Bangladesh. Proc. Seminar and Exhibition organized by Ministry of Petroleum and Mineral Resources, Government of Bangladesh, Dhaka, 1980, p. 35-40.

Khan, A.A., Sattar, and G.S., Rahman, T., 1994, Tectogenesis of the Gondwana rifted basins of Bangladesh in the so-called Garo-Rajmahal gap and their pre-drift regional tectonic correlation: Ninth International Gondwana Symposium, p 647-655.

Kuehl, S. A., Harju, T. M., and Moore, W. S., 1989, Shelf sedimentation of the Ganges-Brahmaputra river system: Evidence for sediment bypassing to the Bengal fan: Geology v. 17, p. 1132-1135.

Kumar, P., 2004, Provenance history of Cenozoic sediments near Digboi-Margherita area, eastern syntaxis of the Himalayas, Assam, northeast India [M.S. Thesis]: Auburn University, Auburn, Alabama, 131 p.

Li, Z.X., and Powell, C.McA., 2001, An outline of the palaeogeographic evolution of the Australasian region since the beginning of the Neoproterozoic: Earth-Science Reviews, v. 53, p. 237–277, doi: 10.1016/S0012-8252(00)00021-0.

Ludwig, K.R., 2003, User's manual for Isoplot, v. 3.0, a geochronological toolkit for Microsoft Excel: Berkeley Geochronological Center, Special Publication no. 4.

Mack, G.H., 1984, Exceptions to the relationship between plate tectonics and sandstone composition, Journal of Sedimentary Petrology, v. 54, p. 212-220.

Mange, M. A., and Maurer, H. F. W., 1992, Heavy Minerals in Color: London, Chapman & Hall, London, 147 p.

Mann, W.R., and Cavarock, V.V., 1973, Composition of sand released from three source areas under humid, low relief weathering in the North Carolina piedmont: Journal of Sedimentary Petrology, v. 43, p. 870-881.

McBride E.F., 1963, A classification of common sandstones: Journal of Sedimentary Research, v. 33, p. 664-669.

McDougall, I., and Harrison, M.T., 1999, Geochronology and Thermochronology by the $^{40}Ar/^{39}Ar$ Method: New York, Oxford University Press, 269 p.

McDougall, I., and McElhinny, M.W., 1970, The Rajmahal Traps of India- K/Ar ages and paleomagnetism: Earth Planetary Science Letters, v. 9, 371-378.

Medlicott, H.B., 1873, Notes on the Satpura Coal Basin. Mem. Geol. Surv. India 10, p. 133-188.

Milkov, A.V., 2000, World wide distribution of submarine mud volcanoes and associated gas hydrate: Marine Geology, v. 167, p. 29 -42.

Mishra, S., Deomurari, M.P., Wiedenbeck, M., Goswami, J.N., Ray, S., and Saha, A.K., 1999, $^{207}Pb/^{206}Pb$ zircon ages and the evolution of the Singhbhum Craton, eastern India: an ion microprobe study: Precambrian Research, v. 93, p. 139-151.

Morton, A.C., 1984, Stability of detrital heavy minerals in Tertiary sandstones of the North Sea Basin: Clay Mineralogy, v. 19, p 287-308.

Morton, A.C., 1985, Heavy minerals in provenance studies, in Zuffa, G.G., eds., Provenance of Arenites: Boston, D. Reidel Publishing Company, p. 249-277.

Morton, A.C., 1986, Dissolution of apatite in North Sea Jurassic sandstone: Implications for the generation of secondary porosity: Clay Mineralogy, v. 21, p 711-733.

Morton, A. C., and Hallsworth, C., 1994, Identifying provenance-specific features of detrital heavy mineral assemblages in sandstones: Sedimentary Geology, v. 90, p. 241-256.

Morton, A.C., and Hallsworth, C.R., 1999, Processes controlling the composition of heavy mineral assemblages in sandstones: Sedimentary Geology, v. 124, p. 3-30.

Morton, A.C., and Taylor, P.N., 1991, Geochemical and isotopic constraints on the nature and age of basement rocks from Rockall Bank, NE Atlantic: Journal of the Geological Society, London, v. 148, p. 630-634.

Mukhopadhyay, G., Mukhopadhyay, S.K., Roychowdhury, M., and Parui, P.K., 2010, Stratigraphic correlation between different Gondwana basins of India: Journal Geological Society of India, v. 76, p. 251-266.

Nanayama, F., 1997, An electron microprobe study of the Amazon Fan: Proceedings of the Ocean Drilling Program, Scientific Results, v. 155, p. 147-168.

Najman, Y., and Garzanti, E., 2000, Reconstructing early Himalayan tectonic evolution and paleogeography from Tertiary foreland basin sedimentary rocks, northern India: Geological Society of America Bulletin, v. 112, p. 435-449.

Narain, H., 1994, Gondwanan palaeomagnetism and crustal structures, Proc. IX International Gondwana Symposium, Oxford and IBH Pub., New Delhi, p. 951-952.

Nelson, D.R., 1996, Compilation of SHRIMP U–Pb zircon geochronology data, 1995: Geological Survey of Western Australia Record 1996/5.

Nelson, D. R., 1999, Compilation of SHRIMP U–Pb zircon geochronology data, 1998: Geological Survey of Western Australia Record 1999/2.

Nelson, D.R., 2002, Compilation of Geochronological Data, 2001: Geological Survey of Western Australia Record 2002/2.

Pascoe, E.H., 1959, A Manual of the Geology of India and Burma, 3rd Edition, Government Press, Delhi, 1343 p.

Peavy, T., 2008, Provenance of lower Pennsylvanian Pottsville Formation, Cahaba synclinorium, Alabama [Unpublished M.S. Thesis]: Auburn University, Auburn, AL, 106 p.

Potter, P.E., 1978, Petrology and chemistry of modern big river sands: Journal of Geology, v. 86, p. 423-449.

Pettijohn, F.J., 1941, Persistence of heavy minerals and geologic age: Journal of Geology, v. 49, p 610-625.

Rahman, M.W., 2008, Sedimentation and tectonic evolution of Cenozoic sequence from Bengal and Assam foreland basin, Eastern Himalayas [Unpublished M.S. Thesis]: Auburn, Auburn University, 180 p.

Rao, C.S.R, 1982. Coalfields of India. Vol-II, Coal resources of Tamil Nadu, Andhra Pradesh, Orissa and Maharashtra. Geological Survey of India Bulletin Series A, 45 p.

Rao, C.S.R, 1983, Coal resources of Madhya Pradesh, Jammu & Kashmir, Bull. Geological Survey India, Ser. A no. 45 Coalfields of India III: 1-204.

Rao, C.S.R., 1987, Coalfields of India. Vol-IV, Part I. Coal resources of Bihar. Geological Survey of India Bulletin Series A, 45.

Ray, S., and Chakraborty, T., 2002, Lower Gondwana fluvial succession of the Pench-Kanhan valley, India: Stratigraphic architecture and depositional controls: Sedimentary Geology, v. 151, p. 243-271.

Reed, F.R.C., 1927, The Permo-Carboniferous marine fauna from Umaria coalfield, Record of Geological Survey of India, 60.

Reimann, K.U., 1993, Geology of Bangladesh; Gebruder Borntraeger, Berlin-Stuttgat, 160 p.

Reiners, P.W., Spell, T.L., Nicolescu, S., and Zanetti, K.A., 2004, Zircon (U-Th)/He thermochronometry: Geochemical Cosmochemial Acta, v. 68, p. 1857-1887.

Robinson, P. L., 1967, The Indian Gondwanan formations – a review: First Symposium on Gondwana Stratigraphy, Mar Del Plata, Argentina, UNESCO, Paris, p. 201–268.

Ruhl, K.W., and Hodges, K.V., 2005, The use of detrital mineral cooling ages to evaluate steady-state assumptions in active orogens: an example from the central Nepalese Himalayan: Tectonics, v. 24, TC4015, 10.1029/2004TC001712.

Salt, C.A., Alam, M. M., and Hossain, M. M., 1986, Bengal Basin: Current exploration of the hinge zone of southwestern Bangladesh, In: Proc. 6th Offshore Southeast Asia Conference: Singapore p. 55-67.

Scherer, A., 2007, $^{40}Ar/^{39}Ar$ dating and errors, www.geoberg.de, (June, 2009).

Scholle, P.A., 1979, A color illustrated guide to constituents, textures, cements, and porosities of sandstones and associated rocks: AAPG Memoir 28, 201 p.

Scotese, C.R., 1998, Quicktime Computer Animations: PALEOMAP Project Department of Geology: Arlington, Texas, University of Texas at Arlington, CD-ROM.

Sengupta, S., 1970, Gondwana sedimentation around Bhimaram, Pranhita-Godavari valley: Journal of Sedimentary Research, v. 40, p. 140-170.

Segev, A., 2002, Flood basalts, continental breakup and the dispersal of Gondwana: Evidence for periodic migration of upwelling mantle flows (plumes): EGU Stephen Mueller Special Publication Series, v. 2, p. 171-191.

Sitaula, R.P., 2009, Petrofacies and paleotectonic evolution of Gondwanan and post-Gondwanan sequences of Nepal [unpublished M.S. Thesis]: Auburn University, Auburn, AL, 186 p.

Smith, A.J., 1963. Evidence for a Talchir (Lower Gondwana) glaciation: Striated pavement and boulder bed at Irai, central India: Journal of Sedimentary Petrology, v. 33, p. 739– 750.

Spear, F.S., 1993, Metamorphic Phase Equilibria And Pressure-Temperature-Time Paths: Mineralogical Society of America, Washington, DC, 799 p.

Stampfli, G.M., and Borel, G.D., 2002, A plate tectonic model for the Paleozoic and Mesozoic constrained by dynamic plate boundaries and restored synthetic ocean isochrons: Earth and Planetary Science Letters, v. 196, p. 17–33, doi: 10.1016/S0012-821X(01)00588-X.

Stover, L.E., 1964, Palynology of coals from the EDH-5 bore, East Pakistan Jersy Production Research Company.

Suess, E., 1885, Das Satilitz der Ende, Band l., Wien, Leipzig.

Suttner, L.J., 1974, Sedimentary petrologic provinces: An evaluation, *in* Ross, C.A., ed., Paleogeographic Provinces and Provinciality, Society of Economic Paleontologists and Mineralogists, Special Publication, no. 21, p. 75-84.

Suttner, L.J., Basu, A., and Mack, G.H., 1981, Climate and the origin of quartz arenite: Journal of Sedimentary Petrology, v. 51, p. 1235-1246.

Sweet, K., Klein, G.D.V., and Smit, D.E., 1971, A Cambrian tidal sandbody--The Eriboll sandstone of northwest Scotland: an ancient-recent analog: Journal of Geology, v. 79, p. 400-415.

Trosvik, T.H., Paulsen, T.S., Hughes, N.C., Myrow, P.M., and Ganerod, M., 2009, The Tethyan Himalaya: palaeogeography and tectonic constraints from Ordovician palaeomagnetic data: Journal of the Geological Society, London, v. 166, p. 679-687.

Tucker, M., 1988, Techniques in Sedimentology: Blackwell Scientific Publications, London, 395 p.

Uddin, A., Kumar, P., Sarma, J.N., and Akhter, S.H., 2007, Heavy-mineral constraints on provenance of Cenozoic sediments from the foreland basins of Assam, India and

Bangladesh: Erosional history of the eastern Himalayas and the Indo-Burman ranges, in Mange, M.A., and Wright, D.T., (Eds.), Heavy Minerals in Use, Development in Sedimentology, Elsevier, Amsterdam, v. 58, p. 823-847.

Uddin, A., and Lundberg, N., 2004, Miocene sedimentation and subsidence during continent–continent collision, Bengal basin, Bangladesh: Sedimentary Geology, v. 164, p. 131-146.

Uddin, A., and Lundberg, N., 1998a, Cenozoic history of the Himalayan-Bengal system: sand composition in the Bengal Basin, Bangladesh: Geological Society of America Bulletin, v. 110, p. 497-511.

Uddin, A., and Lundberg, N., 1998b, Unroofing history of the Eastern Himalaya and the Indo-Burman ranges: Heavy-mineral study of Cenozoic sediments from the Bengal basin, Bangladesh: Journal of Sedimentary Research, v. 68, p. 465-472.

Uddin, A., Hames, W.E., and Zahid, K.M., 2010, Laser $^{40}Ar/^{39}Ar$ age constraints on Miocene sequences from the Bengal basin: Implications for middle Miocene denudation of the eastern Himalayas: Journal of Geophysical Research, v. 115, B07416, doi:10.1029/2009JB006401.

Uddin, M.N., and Islam, M.S.U., 1992. Depositional environments of the Gondwana rocks in the Khalashpir basin, Rangpur District, Bangladesh: Bangladesh Journal of Geology, v. 11, p. 31–40.

Valdiya, K.S., 1997, Himalaya, the Northern Frontier of East Gondwanaland: Gondwana Research, v. 1, p. 3-9.

Veevers, J.J., 2004, Gondwanaland from 650-500 Ma assembly through 320 Ma merger in Pangea to 185-100 Ma breakup: Supercontinental tectonics via stratigraphy and radiometric dating, Earth-Science Reviews, v. 68, p. 1-132.

Veevers, J.J., 2006, Updated Gondwana (Permian-Cretaceous) earth history of Australia: Gondwana Research, v. 9, p. 231-260.

Veevers, J.J., and Tiwari, R.C., 1995, Gondwana master basin of peninsular India between Tethys and the interior of the Gondwanaland province of Pangea: Geological Society of America, Memoir 187, 71 p.

Velbel, M.A., 1985, Mineralogically mature sandstone in accretional prisms: Journal of Sedimentary Petrology, v. 55, p. 685-690.

Venkatachala, B.S., and Tiwari, R.C., 1995, Lower Gondwana marine incursions: Periods and pathways: Palaeobotanist, v. 36, p. 24-29.

Vermeesch, P., 2004, How many grains needed for a provenance study?: Earth and Planetary Science Letters, v. 224, p. 441-451.

Wadia, D.N., 1919, Geology of India, 3rd edition, Macmillan and Co Ltd., London, 536 p.

Wanke, H., and Konig, H., 1959, Eine neue Methode zur Kalium-Argon-Altersbestimmung und ihre Anwendung auf Steinmeteorite: Z. Naturforschung, v. 14a, p. 860-866.

Wardell, A., 1991, Techno-Economic Feasibility Study of Barapukuria Coal Project (unpubl.), Dinajpur, Bangladesh.

White, N.M., Pringle, M., and Garzanti, E., 2002, Constraints on the exhumation and erosion of the High Himalayan Slab, NW India, from foreland basin deposits: Earth and Planetary Science Letters, v. 195, p. 29-44.

Wilde, S.A., 1999, Evolution of the western margin of Australia during the Rodinian and Gondwanan supercontinent cycles: Gondwana Research, v. 2, p. 481–499.

Wilde, S.A., and Murphy, D.M.K., 1990, The nature and origin of the Late Proterozoic high-grade gneisses of the Leeuwin Block, Western Australia: Precambrian Research, v. 47, p. 251–270.

Wilde, S.A., and Nelson, D.R., 2001, Geology of the western Yilgarn Craton and Leeuwin Complex, Western Australia—a field guide: Geological Survey of Western Australia Record 2001/15.

Wright, T.O., and Dallmeyer, R.D., 1991, The age of cleavage development in the Ross orogen, northern Victoria Land, Antarctica: Evidence from $^{40}Ar/^{39}Ar$ whole-rock slate ages: Journal of Structural Geology, v. 13, p. 677-690.

Yamada, R., Tagami., Nishimura, S., and Ito, H., 1995, Annealing kinetics of fission tracks in zircon: an experimental study: Chemical Geology, v. 122, p. 249-258.

Yoshida, M., Kampunzu, A.B., Li, Z.X., and Watanabe, T., 2003, Assembly and break-up of Rodinia and Gondwana: Evidence from Eurasia and Gondwana: Introduction, International Association for Gondwana Research, Japan, v. 6, no. 2, p. 139-142.

Young, S.W., 1976, Petrographic textures of detrital polycrystalline quartz as an aid to interpreting crystalline source rocks: Journal of Sedimentary Research, v. 46, p. 595-603.

Zaher, M.A., and Rahman, A., 1980, Prospects and investigations for minerals in the northern part of Bangladesh in Petroleum and Mineral Resources of Bangladesh, Seminar and Exhibition: Dhaka, Government of People's Republic of Bangladesh, p. 9-18.

Zahid, K.M., 2005, Provenance and basin tectonics of Oligocene-Miocene sequences of the Bengal Basin, Bangladesh [M.S. Thesis]: Auburn University, Auburn, Alabama, 142 p.

Zhu, B., Delano, J.W., and Kidd, S.F.W., 2005, Magmatic compositions and source terranes estimated from melt inclusions in detrital Cr-rich spinels: An example from mid-Cretaceous sandstones in the eastern Tethys Himalaya: Earth and Planetary Science Letters, v. 233, p. 295-309.

APPENDIX 1: Micropobe Analysis Data of Garnet from the Gonwanan sequences of the northwestern Bangladesh

Sample No.	SiO2	TiO2	Al2O3	MgO	FeO	CaO	MnO	Cr2O3	Total
IK-1 G1	36.46	0.0182	21.37	2.8123	34.77	0.9169	3.35	0.055	99.75
IK-1 G2	36.35	0.0036	20.69	0.6323	40.94	1.9003	0.4782	0.0543	101.05
IK-1 G3	35.24	0	20.77	2.4819	26.87	2.6861	8.81	0.1011	96.96
IK-1 G4	36.81	0.0722	21.83	4.34	34.45	1.6372	1.2686	0.0443	100.46
IK-2 G1	36.96	0.0439	21.77	4.22	34.49	0.8234	1.6347	0.0331	99.98
IK-2 G2	36.58	0	21.48	3.07	36.88	1.0025	1.3865	0	100.38
IK-2 G3	37.37	0.0209	21.54	5.94	32.49	2.026	0.5355	0.0112	99.93
IK-2 G4	36.73	0.017	21.15	3.01	36.7	0.7189	1.6303	0	99.96
IK-6 G1	36.91	0	21.91	4.23	34.14	1.0013	1.9582	0.0774	100.23
IK-6 G2	37.08	0.0318	21.61	4.95	33.29	1.6417	1.8912	0	100.49
IK-6 G3	37	0.0037	21.52	4.08	32.83	1.8855	1.6733	0	98.98
IK-6 G4	36.28	0.0364	21.48	3.06	37.15	1.0021	1.9445	0.0767	101.03
IK-6 G5	36.22	0.0157	21.36	2.007	36.08	0.762	4.13	0.0109	100.59
IK-8 G1	37.17	0.0366	21.11	4.93	34.66	0.6618	1.1973	0	99.77
IK-8 G2	37.35	0.0074	21.78	6.35	32.86	0.9082	1.0518	0	100.31
IB2-1 G1	37.44	0.0271	22.35	7.65	30.92	1.8155	0.4815	0.1147	100.8
IB2-1 G2	2.1408	0	1.2922	2.8977	36.48	0.06	0	0.0373	42.91
IB2-1 G3	34.19	0.0499	21.64	4.71	33.96	0.7969	0.6169	0	95.96
IB2-1 G4	36.22	0.0194	22.11	4.97	36.81	0.828	0.4688	0	101.43
IB2-1 G5	36.04	0.0219	21.64	4.26	34.91	1.2055	1.0681	0.0787	99.23
IB2-1 G6	37.07	0.0734	22.25	6.01	34.09	1.8884	0.4704	0.0907	101.95
IB2-3 G1	36.71	0.0209	21.82	5.61	29.98	3.95	2.6193	0.0575	100.76
IB2-3 G2	36.59	0.0691	22.46	9.25	28.73	1.2706	0.5872	0.1382	99.08
IB2-3 G3	36.65	0.0074	22.57	7.67	31.03	1.7126	1.0664	0	100.7
IB2-5 G1	37.41	0.0565	22.28	7.2	31.95	1.3488	0.533	0	100.77
IB2-5 G2	37.07	0.0467	22.6	8.37	31.48	0.8307	0.5683	0	100.97
IB2-5 G3	35.52	0.0243	22.05	6.25	34.97	0.829	0.303	0	99.94
IB4-01 G1	38.15	0.0235	22.5	9.94	27.87	1.4715	0.702	0.0347	100.7
IB4-01 G2	37.16	0.0394	21.9	5.93	31.49	3.09	0.7953	0.0344	100.45

APPENDIX 2: Four end members of Garnet from the Gonwanan sequences of the northwestern Bangladesh

End Members (Four Members)					
Sample No.	Pyrope	Almandine	Grossular	Spessartine	Total
IK-1 G1	11.30	78.40	2.65	7.65	100.00
IK-1 G2	2.51	91.01	5.41	1.08	100.00
IK-1 G3	10.13	61.55	7.88	20.44	100.00
IK-1 G4	16.98	75.60	4.60	2.82	100.00
IK-2 G1	16.82	77.12	2.36	3.70	100.00
IK-2 G2	12.15	81.88	2.85	3.12	100.00
IK-2 G3	22.91	70.30	5.62	1.17	100.00
IK-2 G4	12.02	82.22	2.06	3.70	100.00
IK-6 G1	16.78	75.96	2.85	4.41	100.00
IK-6 G2	60.92	11.33	14.52	13.22	100.00
IK-6 G3	16.45	74.25	5.46	3.83	100.00
IK-6 G4	11.89	81.01	2.80	4.29	100.00
IK-6 G5	7.98	80.51	2.18	9.33	100.00
IK-8 G1	19.31	76.16	1.86	2.66	100.00
IK-8 G2	24.39	70.81	2.51	2.30	100.00
IB2-1 G1	28.79	65.27	4.91	1.03	100.00
IB2-1 G2	12.38	87.44	0.18	0.00	100.00
IB2-1 G3	19.08	77.18	2.32	1.42	100.00
IB2-1 G4	18.77	77.98	2.25	1.01	100.00
IB2-1 G5	16.83	77.35	3.42	2.40	100.00
IB2-1 G6	22.46	71.47	5.07	1.00	100.00
IB2-3 G1	20.97	62.86	10.61	5.56	100.00
IB2-3 G2	34.76	60.56	3.43	1.25	100.00
IB2-3 G3	28.50	64.68	4.57	2.25	100.00
IB2-5 G1	27.28	67.90	3.67	1.15	100.00
IB2-5 G2	31.06	65.53	2.22	1.20	100.00
IB2-5 G3	23.46	73.65	2.24	0.65	100.00
IB4-01 G1	36.77	57.84	3.91	1.48	100.00
IB4-01 G2	22.58	67.25	8.45	1.72	100.00

APPENDIX 3: Micropobe Analysis Data of Tourmaline from the Gonwanan sequences of the northwestern Bangladesh

Sample No.	SiO2	TiO2	Al2O3	MgO	FeO	CaO	MnO	K20	Na2O	Cr2O3	Total
IK1-T1	35.47	0.89	33.39	7.21	5.39	0.88	0.02	0.03	1.64	0.05	84.98
IK1-T2	34.73	1.34	33.63	6.88	5.76	1.35	0.00	0.07	1.48	0.02	85.26
IK6-T1	34.92	0.53	32.31	5.54	10.12	1.22	0.05	0.03	1.51	0.00	86.26
IK6- T2	35.12	1.08	30.27	6.23	10.54	1.56	0.00	0.05	1.56	0.02	86.45
IK8-T1	34.54	1.47	33.28	7.69	4.96	2.01	0.00	0.15	1.22	0.10	85.45
IB2-1 T1	35.05	1.32	33.80	7.80	4.78	1.98	0.00	0.11	1.03	0.00	85.91
IB4- 3 T1	35.54	0.08	33.65	7.36	6.82	1.16	0.00	0.09	1.49	0.00	86.26
IB4- 3 T2	38.03	0.02	22.06	7.17	29.55	2.40	0.42	0.00	0.03	0.02	99.71
Standard 1	39.73	4.90	14.64	12.90	10.99	10.63	0.04	2.32	2.30	0.00	98.55

End Member Calculation

Ca	Mg	Fe (tot)	Total	Al	Al50Fe(tot)50	Al50Mg50	Total
0.16	1.86	0.78	2.80	6.81	3.79	4.33	14.93
0.25	1.77	0.83	2.85	6.84	3.84	4.30	14.98
0.23	1.43	1.47	3.13	6.60	4.03	4.02	14.65
0.29	1.61	1.53	3.43	6.19	3.86	3.90	13.94
0.35	1.88	1.45	3.69	6.45	3.95	4.17	14.56
0.36	1.97	0.68	3.01	6.76	3.72	4.37	14.86
0.21	1.87	0.97	3.06	6.76	3.87	4.32	14.95
0.41	1.69	3.90	5.99	4.10	4.00	2.89	10.99

APPENDIX 4(i): $^{40}Ar/^{39}Ar$ Age data of detrital muscovite from the northwestern Bengal Basin (IK-02)

Blank			2.04753		0.09150		0.00190		0.00031		0.000038							
Sample	P	t	40 V		39 V		38 V		37 V		36 V		Moles 40Ar*	%Rad	R	Age (Ma)		%-sd
au16.3f.mus.2a.txt	1.5	10	7.24270 ±	0.00580	0.33789 ±	0.00061	0.00427 ±	0.00005	-0.00005 ±	0.00016	0.000039 ±	0.000038	3.93E-14	99.84%	21.40064	496.83 ±	1.25	0.25%
au16.3f.mus.3a.txt	1.5	10	8.15265 ±	0.00970	0.39436 ±	0.00075	0.00503 ±	0.00005	0.00025 ±	0.00020	0.000148 ±	0.000030	4.42E-14	99.46%	20.56253	479.74 ±	1.20	0.25%
au16.3f.mus.4a.txt	1.5	10	4.98046 ±	0.00835	0.23963 ±	0.00060	0.00298 ±	0.00005	0.00131 ±	0.00036	0.000125 ±	0.000029	2.70E-14	99.26%	20.63091	481.14 ±	1.69	0.35%
au16.3f.mus.45a.txt	2	7	1.28333 ±	0.00179	0.05854 ±	0.00029	0.00080 ±	0.00003	-0.00020 ±	0.00020	0.000285 ±	0.000031	6.97E-15	93.44%	20.48316	478.12 ±	4.46	0.93%
au16.3f.mus.44a.txt	2	7	1.64633 ±	0.00119	0.07826 ±	0.00029	0.00094 ±	0.00003	0.00039 ±	0.00017	0.000064 ±	0.000017	8.94E-15	98.86%	20.79649	484.53 ±	2.39	0.49%
au16.3f.mus.43a.txt	2	7	1.70512 ±	0.00167	0.08114 ±	0.00033	0.00100 ±	0.00004	0.00005 ±	0.00016	0.000010 ±	0.000017	9.25E-15	99.83%	20.97845	488.25 ±	2.50	0.51%
au16.3f.mus.42a.txt	2	7	0.81793 ±	0.00090	0.03898 ±	0.00029	0.00049 ±	0.00004	-0.00010 ±	0.00018	-0.000014 ±	0.000015	4.44E-15	100.52%	20.98406	488.36 ±	4.57	0.94%
au16.3f.mus.41a.txt	2	7	2.57243 ±	0.00297	0.12148 ±	0.00054	0.00144 ±	0.00004	0.00004 ±	0.00021	-0.000012 ±	0.000014	1.40E-14	100.14%	21.17505	492.25 ±	2.38	0.48%
au16.3f.mus.40a.txt	2	7	2.20782 ±	0.00168	0.10279 ±	0.00039	0.00132 ±	0.00004	0.00030 ±	0.00016	0.000001 ±	0.000014	1.20E-14	99.98%	21.47441	498.33 ±	2.14	0.43%
au16.3f.mus.39a.txt	2	7	2.04753 ±	0.00149	0.09677 ±	0.00028	0.00124 ±	0.00005	0.00041 ±	0.00012	0.000015 ±	0.000016	1.11E-14	99.78%	21.11267	490.98 ±	1.86	0.38%
au16.3f.mus.38a.txt	2	7	2.75543 ±	0.00329	0.13105 ±	0.00040	0.00156 ±	0.00004	0.00058 ±	0.00013	0.000057 ±	0.000017	1.50E-14	99.39%	20.89828	486.61 ±	1.86	0.38%
au16.3f.mus.37a.txt	2	7	2.09943 ±	0.00198	0.09820 ±	0.00028	0.00122 ±	0.00003	0.00045 ±	0.00029	-0.000003 ±	0.000021	1.14E-14	100.04%	21.37871	496.39 ±	2.09	0.42%
au16.3f.mus.36a.txt	2	7	3.18742 ±	0.00156	0.14962 ±	0.00052	0.00190 ±	0.00004	0.00071 ±	0.00010	0.000004 ±	0.000028	1.73E-14	99.97%	21.29560	494.70 ±	2.16	0.44%
au16.3f.mus.35a.txt	2	7	2.65652 ±	0.00221	0.12652 ±	0.00035	0.00158 ±	0.00005	0.00016 ±	0.00021	-0.000023 ±	0.000025	1.44E-14	100.25%	20.99768	488.64 ±	1.97	0.40%
au16.3f.mus.34a.txt	2	7	1.95313 ±	0.00197	0.09150 ±	0.00041	0.00111 ±	0.00005	-0.00041 ±	0.00022	0.000038 ±	0.000017	1.06E-14	99.43%	21.22198	493.20 ±	2.60	0.53%
au16.3f.mus.33a.txt	2	7	2.14848 ±	0.00153	0.10036 ±	0.00025	0.00124 ±	0.00003	-0.00011 ±	0.00018	0.000057 ±	0.000016	1.17E-14	99.21%	21.23986	493.57 ±	1.71	0.35%
au16.3f.mus.32a.txt	2	7	1.90228 ±	0.00224	0.08934 ±	0.00041	0.00116 ±	0.00003	0.00041 ±	0.00013	-0.000002 ±	0.000032	1.03E-14	100.03%	21.29331	494.65 ±	3.39	0.69%
au16.3f.mus.31a.txt	2	7	1.63535 ±	0.00171	0.07585 ±	0.00029	0.00090 ±	0.00004	-0.00013 ±	0.00021	0.000073 ±	0.000017	8.88E-15	98.68%	21.27400	494.26 ±	2.53	0.51%
au16.3f.mus.30a.txt	2	7	1.73303 ±	0.00171	0.08150 ±	0.00043	0.00102 ±	0.00004	0.00019 ±	0.00017	0.000038 ±	0.000016	9.41E-15	99.35%	21.12671	491.27 ±	2.95	0.60%
au16.3f.mus.29a.txt	2	7	4.55566 ±	0.00351	0.22041 ±	0.00077	0.00280 ±	0.00004	0.00020 ±	0.00024	0.000012 ±	0.000017	2.47E-14	99.92%	20.65350	481.61 ±	1.81	0.38%
au16.3f.mus.28a.txt	2	7	2.12789 ±	0.00266	0.10153 ±	0.00042	0.00129 ±	0.00004	0.00066 ±	0.00023	0.000015 ±	0.000014	1.15E-14	99.80%	20.91681	486.99 ±	2.32	0.48%
au16.3f.mus.27a.txt	2	7	3.64382 ±	0.00241	0.17338 ±	0.00044	0.00214 ±	0.00004	0.00046 ±	0.00018	0.000003 ±	0.000018	1.98E-14	99.98%	21.01240	488.94 ±	1.46	0.30%
au16.3f.mus.26a.txt	2	7	3.07068 ±	0.00271	0.14272 ±	0.00048	0.00177 ±	0.00004	0.00088 ±	0.00026	-0.000028 ±	0.000031	1.67E-14	100.27%	21.51627	499.18 ±	2.30	0.46%
au16.3f.mus.25a.txt	2	7	4.24244 ±	0.00274	0.20020 ±	0.00039	0.00254 ±	0.00004	0.00042 ±	0.00021	0.000027 ±	0.000017	2.30E-14	99.81%	21.15083	491.76 ±	1.18	0.24%
au16.3f.mus.24a.txt	2	7	1.13759 ±	0.00178	0.05303 ±	0.00026	0.00054 ±	0.00005	0.00031 ±	0.00019	0.000040 ±	0.000017	6.17E-15	98.96%	21.22916	493.35 ±	3.43	0.70%
au16.3f.mus.23a.txt	2	7	1.68719 ±	0.00131	0.08158 ±	0.00028	0.00102 ±	0.00004	0.00033 ±	0.00015	0.000120 ±	0.000021	9.16E-15	97.91%	20.24957	473.32 ±	2.45	0.52%
au16.3f.mus.22a.txt	2	7	0.06431 ±	0.00038	0.00438 ±	0.00006	-0.00002 ±	0.00004	0.00020 ±	0.00018	0.000016 ±	0.000018	3.49E-16	92.81%	13.64278	332.10 ±	30.08	9.06%
au16.3f.mus.21a.txt	2	7	6.54155 ±	0.00331	0.31188 ±	0.00086	0.00375 ±	0.00006	0.00095 ±	0.00030	0.000059 ±	0.000033	3.55E-14	99.74%	20.91970	487.05 ±	1.55	0.32%
au16.3f.mus.20a.txt	2	7	0.01231 ±	0.00019	0.00085 ±	0.00004	-0.00002 ±	0.00004	0.00002 ±	0.00024	-0.000050 ±	0.000024	6.68E-17	219.44%	14.53963	351.93 ±	205.64	58.43%
au16.3f.mus.19a.txt	2	7	0.31323 ±	0.00058	0.01515 ±	0.00008	0.00020 ±	0.00003	0.00042 ±	0.00020	-0.000002 ±	0.000016	1.70E-15	100.20%	20.68379	482.23 ±	7.63	1.58%
au16.3f.mus.18a.txt	2	7	7.88891 ±	0.00334	0.37192 ±	0.00060	0.00444 ±	0.00006	0.00039 ±	0.00024	-0.000062 ±	0.000028	4.28E-14	100.23%	21.21121	492.99 ±	0.97	0.20%
au16.3f.mus.17a.txt	2	7	0.07780 ±	0.00025	0.00429 ±	0.00005	0.00007 ±	0.00003	0.00020 ±	0.00021	-0.000033 ±	0.000017	4.22E-16	112.57%	18.14594	429.55 ±	29.06	6.76%
au16.3f.mus.16a.txt	2	7	3.02400 ±	0.00197	0.14222 ±	0.00044	0.00179 ±	0.00005	0.00037 ±	0.00027	0.000006 ±	0.000016	1.64E-14	99.94%	21.24977	493.77 ±	1.72	0.35%
au16.3f.mus.15a.txt	2	7	3.84469 ±	0.00290	0.18024 ±	0.00076	0.00229 ±	0.00004	0.00069 ±	0.00019	-0.000060 ±	0.000022	2.09E-14	100.47%	21.33112	495.42 ±	2.28	0.46%
au16.3f.mus.14a.txt	2	7	8.98415 ±	0.00839	0.42293 ±	0.00069	0.00542 ±	0.00009	0.00120 ±	0.00015	0.000337 ±	0.000017	4.88E-14	98.89%	21.00775	488.84 ±	0.97	0.20%
au16.3f.mus.13a.txt	2	7	13.11620 ±	0.01346	0.61545 ±	0.00178	0.00760 ±	0.00010	0.00198 ±	0.00033	0.000098 ±	0.000023	7.12E-14	99.78%	21.26456	494.07 ±	1.54	0.31%
au16.3f.mus.12a.txt	2	7	6.05132 ±	0.00446	0.28499 ±	0.00084	0.00356 ±	0.00006	0.00057 ±	0.00013	0.000006 ±	0.000013	3.28E-14	99.97%	21.22821	493.33 ±	1.53	0.31%
au16.3f.mus.11a.txt	2	7	5.88473 ±	0.00540	0.27554 ±	0.00048	0.00345 ±	0.00005	0.00003 ±	0.00019	0.000081 ±	0.000013	3.19E-14	99.59%	21.26968	494.17 ±	1.02	0.21%
au16.3f.mus.9a.txt	2	7	3.04431 ±	0.00254	0.14535 ±	0.00064	0.00178 ±	0.00004	-0.00003 ±	0.00008	-0.000005 ±	0.000019	1.65E-14	100.05%	20.94408	487.54 ±	2.36	0.48%
au16.3f.mus.8a.txt	2	7	5.70897 ±	0.00261	0.27205 ±	0.00081	0.00338 ±	0.00006	0.00045 ±	0.00025	0.000155 ±	0.000020	3.10E-14	99.20%	20.81686	484.95 ±	1.56	0.32%
au16.3f.mus.7a.txt	2	7	7.03437 ±	0.00377	0.32820 ±	0.00065	0.00408 ±	0.00005	0.00036 ±	0.00021	0.000054 ±	0.000019	3.82E-14	99.77%	21.38433	496.50 ±	1.09	0.22%
au16.3f.mus.6a.txt	2	7	6.22869 ±	0.00230	0.29003 ±	0.00054	0.00366 ±	0.00005	0.00001 ±	0.00026	0.000128 ±	0.000018	3.38E-14	99.39%	21.34520	495.71 ±	1.04	0.21%
au16.3f.mus.5a.txt	2	7	3.90257 ±	0.00327	0.18825 ±	0.00068	0.00233 ±	0.00004	0.00046 ±	0.00023	0.000110 ±	0.000019	2.12E-14	99.17%	20.55848	479.66 ±	1.92	0.40%
au16.3f.mus.46a.txt	2	7	0.81092 ±	0.00092	0.03784 ±	0.00011	0.00044 ±	0.00004	-0.00009 ±	0.00024	0.000061 ±	0.000024	4.40E-15	97.77%	20.95083	487.68 ±	4.54	0.93%
au16.3f.mus.47a.txt	2	7	1.82778 ±	0.00221	0.08565 ±	0.00042	0.00103 ±	0.00003	0.00015 ±	0.00011	0.000072 ±	0.000023	9.92E-15	98.83%	21.08914	490.50 ±	3.12	0.64%
au16.3f.mus.48a.txt	2	7	1.70822 ±	0.00255	0.08109 ±	0.00034	0.00098 ±	0.00004	-0.00042 ±	0.00018	-0.000006 ±	0.000027	9.27E-15	100.11%	21.06501	490.01 ±	3.17	0.65%
au16.3f.mus.49a.txt	2	7	1.89125 ±	0.00260	0.08929 ±	0.00064	0.00107 ±	0.00003	-0.00058 ±	0.00021	0.000089 ±	0.000023	1.03E-14	98.61%	20.88712	486.38 ±	3.99	0.82%

APPENDIX 4(ii): $^{40}Ar/^{39}Ar$ Age data of detrital muscovite from the northwestern Bengal Basin (IK-02)

Blank			2.21234			0.06547			0.00099			0.00057			0.000043								
Sample	P	t	40 V			39 V			38 V			37 V			36 V			Moles 40Ar*	%Rad	R		Age (Ma)		%-sd
au16.3f.mus.50a.txt	2	7	2.74704	±	0.00235	0.12975	±	0.00046	0.00151	±	0.00004	-0.00069	±	0.00026	0.000125	±	0.000023	1.49E-14	98.66%	20.88649	486.37	±	2.17	0.45%
au16.3f.mus.51a.txt	2	7	6.20891	±	0.00327	0.29663	±	0.00068	0.00400	±	0.00010	0.00005	±	0.00026	-0.000007	±	0.000028	3.37E-14	100.03%	20.93154	487.29	±	1.32	0.27%
au16.3f.mus.52a.txt	2	7	1.26186	±	0.00200	0.05931	±	0.00034	0.00071	±	0.00003	-0.00027	±	0.00019	-0.000012	±	0.000017	6.85E-15	100.27%	21.27366	494.25	±	3.58	0.72%
au16.3f.mus.53a.txt	2	7	2.21234	±	0.00288	0.10324	±	0.00033	0.00131	±	0.00003	0.00069	±	0.00018	0.000031	±	0.000018	1.20E-14	99.58%	21.34014	495.61	±	2.09	0.42%
au16.3f.mus.54a.txt	2	7	3.94761	±	0.00214	0.18245	±	0.00031	0.00221	±	0.00005	-0.00011	±	0.00029	0.000028	±	0.000018	2.14E-14	99.79%	21.59160	500.70	±	1.13	0.22%
au16.3f.mus.55a.txt	2	7	2.14025	±	0.00138	0.10230	±	0.00055	0.00125	±	0.00004	0.00019	±	0.00029	-0.000015	±	0.000025	1.16E-14	100.21%	20.92134	487.08	±	3.13	0.64%
au16.3f.mus.56a.txt	2	7	2.74752	±	0.00308	0.12848	±	0.00046	0.00167	±	0.00003	0.00021	±	0.00025	0.000071	±	0.000018	1.49E-14	99.23%	21.22034	493.17	±	2.09	0.42%
au16.3f.mus.57a.txt	2	7	3.59212	±	0.00165	0.16767	±	0.00050	0.00221	±	0.00006	0.00021	±	0.00018	0.000042	±	0.000018	1.95E-14	99.65%	21.34981	495.80	±	1.68	0.34%
au16.3f.mus.58a.txt	2	7	2.06374	±	0.00120	0.09664	±	0.00042	0.00123	±	0.00003	0.00036	±	0.00029	0.000042	±	0.000018	1.12E-14	99.40%	21.22757	493.32	±	2.53	0.51%
au16.3f.mus.59a.txt	2	7	1.63883	±	0.00169	0.07562	±	0.00018	0.00092	±	0.00003	0.00010	±	0.00017	0.000119	±	0.000018	8.89E-15	97.86%	21.20909	492.94	±	2.10	0.43%
au16.3f.mus.60a.txt	2	7	1.40048	±	0.00169	0.06547	±	0.00018	0.00080	±	0.00003	0.00006	±	0.00025	0.000017	±	0.000019	7.60E-15	99.64%	21.31435	495.08	±	2.43	0.49%
au16.3f.mus.61a.txt	2	7	3.26687	±	0.00265	0.15532	±	0.00054	0.00196	±	0.00004	-0.00005	±	0.00019	0.000059	±	0.000017	1.77E-14	99.47%	20.92198	487.09	±	1.88	0.39%
au16.3f.mus.62a.txt	2	7	1.40137	±	0.00183	0.06708	±	0.00021	0.00086	±	0.00004	0.00098	±	0.00029	0.000028	±	0.000017	7.61E-15	99.41%	20.76950	483.98	±	2.40	0.50%
au16.3f.mus.63a.txt	2	7	1.40596	±	0.00084	0.06554	±	0.00040	0.00079	±	0.00003	0.00000	±	0.00022	0.000012	±	0.000015	7.63E-15	99.75%	21.39876	496.80	±	3.40	0.69%
au16.3f.mus.64a.txt	2	7	1.76126	±	0.00150	0.08161	±	0.00032	0.00106	±	0.00004	0.00038	±	0.00013	0.000013	±	0.000017	9.56E-15	99.78%	21.53287	499.51	±	2.48	0.50%
au16.3f.mus.65a.txt	2	7	1.74770	±	0.00213	0.08254	±	0.00023	0.00099	±	0.00003	0.00001	±	0.00017	0.000019	±	0.000017	9.49E-15	99.69%	21.10713	490.87	±	2.05	0.42%
au16.3f.mus.66a.txt	2	7	2.28919	±	0.00155	0.10937	±	0.00040	0.00146	±	0.00004	0.00006	±	0.00015	0.000045	±	0.000014	1.24E-14	99.41%	20.80715	484.75	±	2.00	0.41%
au16.3f.mus.67a.txt	2	7	3.84012	±	0.00340	0.18076	±	0.00046	0.00226	±	0.00005	0.00013	±	0.00026	0.000038	±	0.000013	2.08E-14	99.71%	21.18169	492.38	±	1.42	0.29%
au16.3f.mus.68a.txt	2	7	2.14927	±	0.00164	0.09847	±	0.00033	0.00126	±	0.00004	0.00014	±	0.00026	0.000027	±	0.000013	1.17E-14	99.62%	21.74459	503.80	±	1.96	0.39%
au16.3f.mus.69a.txt	2	7	1.57134	±	0.00092	0.07231	±	0.00024	0.00092	±	0.00003	-0.00037	±	0.00018	0.000059	±	0.000013	8.53E-15	98.90%	21.49193	498.69	±	2.10	0.42%
au16.3f.mus.70a.txt	2	7	3.10112	±	0.00203	0.14556	±	0.00064	0.00180	±	0.00004	-0.00001	±	0.00020	0.000013	±	0.000016	1.68E-14	99.88%	21.27969	494.38	±	2.31	0.47%
au16.3f.mus.71a.txt	2	7	3.47698	±	0.00213	0.16361	±	0.00038	0.00197	±	0.00004	-0.00014	±	0.00025	-0.000023	±	0.000028	1.89E-14	100.19%	21.25170	493.81	±	1.68	0.34%
au16.3f.mus.72a.txt	2	7	1.68982	±	0.00225	0.07922	±	0.00024	0.00094	±	0.00003	0.00057	±	0.00020	0.000008	±	0.000016	9.17E-15	99.86%	21.30252	494.84	±	2.12	0.43%
au16.3f.mus.73a.txt	2	7	3.92073	±	0.00171	0.18469	±	0.00047	0.00222	±	0.00004	-0.00028	±	0.00021	0.000035	±	0.000016	2.13E-14	99.74%	21.17250	492.20	±	1.39	0.28%
au16.3f.mus.74a.txt	2	7	3.43334	±	0.00382	0.15915	±	0.00068	0.00199	±	0.00006	0.00000	±	0.00025	0.000013	±	0.000015	1.86E-14	99.89%	21.54933	499.85	±	2.29	0.46%
au16.3f.mus.75a.txt	2	7	2.10968	±	0.00262	0.09921	±	0.00044	0.00115	±	0.00003	-0.00010	±	0.00024	0.000004	±	0.000015	1.15E-14	99.94%	21.25267	493.83	±	2.51	0.51%
au16.3f.mus.76a.txt	2	7	3.91310	±	0.00180	0.18474	±	0.00050	0.00227	±	0.00004	0.00082	±	0.00014	0.000069	±	0.000014	2.12E-14	99.48%	21.07179	490.15	±	1.46	0.30%
au16.3f.mus.77a.txt	2	7	1.02476	±	0.00133	0.04721	±	0.00034	0.00061	±	0.00004	0.00045	±	0.00024	0.000043	±	0.000016	5.56E-15	98.76%	21.43692	497.57	±	4.40	0.88%
au16.3f.mus.78a.txt	2	7	1.07592	±	0.00135	0.05179	±	0.00032	0.00066	±	0.00004	0.00026	±	0.00020	0.000023	±	0.000014	5.84E-15	99.38%	20.64569	481.45	±	3.61	0.75%
au16.3f.mus.79a.txt	2	7	2.53356	±	0.00304	0.12179	±	0.00039	0.00151	±	0.00004	0.00091	±	0.00024	0.000049	±	0.000016	1.38E-14	99.44%	20.68532	482.26	±	1.91	0.40%
au16.3f.mus.80a.txt	2	7	1.14735	±	0.00142	0.05370	±	0.00029	0.00062	±	0.00003	0.00033	±	0.00013	0.000030	±	0.000015	6.23E-15	99.24%	21.20541	492.87	±	3.36	0.68%
au16.3f.mus.82a.txt	2	7	1.10976	±	0.00221	0.05290	±	0.00035	0.00063	±	0.00002	0.00052	±	0.00021	0.000084	±	0.000025	6.02E-15	97.77%	20.51184	478.71	±	4.68	0.98%
au16.3f.mus.84a.txt	2	7	0.46424	±	0.00072	0.02216	±	0.00022	0.00020	±	0.00003	0.00086	±	0.00014	0.000068	±	0.000027	2.52E-15	95.67%	20.04771	469.17	±	9.73	2.07%
au16.3f.mus.85a.txt	2	7	1.30587	±	0.00157	0.06125	±	0.00026	0.00069	±	0.00003	0.00054	±	0.00012	0.000095	±	0.000026	7.09E-15	97.86%	20.86363	485.90	±	3.63	0.75%
au16.3f.mus.86a.txt	2	7	1.56080	±	0.00149	0.07327	±	0.00045	0.00079	±	0.00005	0.00007	±	0.00021	0.000019	±	0.000015	8.47E-15	99.64%	21.22673	493.30	±	3.40	0.69%
au16.3f.mus.87a.txt	2	7	0.02494	±	0.00023	0.00119	±	0.00006	0.00000	±	0.00004	0.00009	±	0.00017	0.000019	±	0.000012	1.35E-16	77.36%	16.15494	387.11	±	74.18	19.16%
au16.3f.mus.88a.txt	2	7	0.98357	±	0.00124	0.04655	±	0.00016	0.00054	±	0.00003	0.00048	±	0.00027	0.000010	±	0.000012	5.34E-15	99.72%	21.07015	490.11	±	2.58	0.53%
au16.3f.mus.89a.txt	2	7	1.79559	±	0.00124	0.08388	±	0.00053	0.00105	±	0.00004	0.00030	±	0.00018	0.000033	±	0.000015	9.75E-15	99.47%	21.29291	494.65	±	3.38	0.68%
au16.3f.mus.90a.txt	2	7	1.04154	±	0.00126	0.04765	±	0.00013	0.00054	±	0.00004	-0.00001	±	0.00019	0.000030	±	0.000013	5.65E-15	99.15%	21.67288	502.35	±	2.38	0.47%
au16.3f.mus.91a.txt	2	7	0.98474	±	0.00134	0.04753	±	0.00018	0.00055	±	0.00003	-0.00024	±	0.00023	0.000066	±	0.000013	5.34E-15	98.03%	20.30893	474.54	±	2.75	0.58%
au16.3f.mus.92a.txt	2	7	1.48452	±	0.00223	0.06976	±	0.00043	0.00079	±	0.00004	0.00012	±	0.00025	0.000015	±	0.000012	8.06E-15	99.71%	21.21913	493.15	±	3.37	0.68%
au16.3f.mus.93a.txt	2	7	1.21913	±	0.00134	0.05554	±	0.00031	0.00067	±	0.00003	0.00143	±	0.00036	0.000175	±	0.000013	6.62E-15	95.77%	21.02250	489.14	±	3.30	0.67%
au16.3f.mus.94a.txt	2	7	0.72757	±	0.00141	0.03416	±	0.00025	0.00041	±	0.00003	0.00006	±	0.00018	0.000057	±	0.000015	3.95E-15	97.69%	20.80897	484.79	±	4.88	1.01%
au16.3f.mus.95a.txt	2	7	1.13322	±	0.00112	0.05297	±	0.00025	0.00072	±	0.00004	-0.00031	±	0.00020	-0.000012	±	0.000025	6.15E-15	100.31%	21.39260	496.67	±	4.02	0.81%
au16.3f.mus.96a.txt	2	7	1.64629	±	0.00156	0.07597	±	0.00047	0.00096	±	0.00003	-0.00050	±	0.00019	0.000084	±	0.000016	8.94E-15	98.49%	21.34303	495.66	±	3.46	0.70%
au16.3f.mus.97a.txt	2	7	2.18011	±	0.00191	0.10170	±	0.00040	0.00130	±	0.00003	-0.00016	±	0.00022	-0.000044	±	0.000028	1.18E-14	100.60%	21.43576	497.55	±	2.74	0.55%
au16.3f.mus.98a.txt	2	7	1.14106	±	0.00081	0.05240	±	0.00035	0.00064	±	0.00005	-0.00020	±	0.00019	-0.000005	±	0.000015	6.19E-15	100.13%	21.77448	504.40	±	3.95	0.78%
au16.3f.mus.99a.txt	2	7	0.05085	±	0.00048	0.00257	±	0.00005	0.00005	±	0.00002	-0.00005	±	0.00017	-0.000014	±	0.000026	2.76E-16	108.14%	19.75339	463.09	±	70.90	15.31%

APPENDIX 5(i): $^{40}Ar/^{39}Ar$ Age data of detrital muscovite from the northwestern Bengal Basin (IK-06)

Blank			3.91217		0.23315		0.00289		0.00390		0.000162							
Sample	P	t	40 V		39 V		38 V		37 V		36 V		Moles 40Ar*	%Rad	R	Age (Ma)		%-sd
au16.3k.mus.03a.txt	1.6	10	0.72921 ±	0.00069	0.03301 ±	0.00012	0.00042 ±	0.00002	0.00250 ±	0.00085	-0.000005 ±	0.000009	5.11E-15	100.23%	22.10092	510.84 ±	2.78	0.54%
au16.3k.mus.04a.txt	1.6	10	0.96533 ±	0.00116	0.04468 ±	0.00019	0.00052 ±	0.00003	0.00054 ±	0.00128	-0.000004 ±	0.000010	6.76E-15	100.13%	21.60698	500.87 ±	2.64	0.53%
au16.3k.mus.05a.txt	1.6	10	0.68631 ±	0.00092	0.03129 ±	0.00013	0.00040 ±	0.00002	0.00099 ±	0.00071	-0.000001 ±	0.000010	4.81E-15	100.04%	21.93663	507.53 ±	3.02	0.60%
au16.3k.mus.06a.txt	1.6	10	1.95849 ±	0.00154	0.08812 ±	0.00051	0.00111 ±	0.00003	0.00386 ±	0.00118	0.000021 ±	0.000010	1.37E-14	99.70%	22.15945	512.02 ±	3.10	0.60%
au16.3k.mus.07a.txt	1.6	10	0.49368 ±	0.00049	0.02242 ±	0.00010	0.00028 ±	0.00002	0.00145 ±	0.00111	0.000001 ±	0.000011	3.46E-15	99.94%	22.00456	508.90 ±	4.12	0.81%
au16.3k.mus.08a.txt	1.6	10	1.54445 ±	0.00107	0.07185 ±	0.00024	0.00089 ±	0.00003	-0.00014 ±	0.00119	-0.000011 ±	0.000010	1.08E-14	100.21%	21.49494	498.60 ±	1.99	0.40%
au16.3k.mus.103a.txt	1.6	10	1.09964 ±	0.00180	0.05132 ±	0.00024	0.00074 ±	0.00014	0.00083 ±	0.00092	0.000080 ±	0.000030	7.70E-15	97.86%	20.97020	487.93 ±	4.77	0.98%
au16.3k.mus.104a.txt	1.6	10	0.42733 ±	0.00069	0.02023 ±	0.00015	0.00029 ±	0.00003	0.00300 ±	0.00125	0.000038 ±	0.000011	2.99E-15	97.43%	20.57987	479.96 ±	5.26	1.10%
au16.3k.mus.105a.txt	1.6	10	0.82183 ±	0.00121	0.03777 ±	0.00016	0.00047 ±	0.00002	0.00166 ±	0.00077	0.000025 ±	0.000011	5.76E-15	99.13%	21.57151	500.15 ±	3.05	0.61%
au16.3k.mus.106a.txt	1.6	10	0.57636 ±	0.00091	0.02722 ±	0.00012	0.00031 ±	0.00002	0.00326 ±	0.00109	0.000023 ±	0.000010	4.04E-15	98.86%	20.93462	487.21 ±	3.36	0.69%
au16.3k.mus.107a.txt	1.6	10	1.41224 ±	0.00158	0.06603 ±	0.00019	0.00085 ±	0.00002	0.00390 ±	0.00082	0.000018 ±	0.000009	9.89E-15	99.65%	21.31314	494.91 ±	1.84	0.37%
au16.3k.mus.108a.txt	1.6	10	0.72788 ±	0.00092	0.03334 ±	0.00013	0.00042 ±	0.00002	0.00005 ±	0.00085	0.000016 ±	0.000010	5.10E-15	99.37%	21.69266	502.60 ±	2.86	0.57%
au16.3k.mus.6a.txt	1.6	10	4.31071 ±	0.00356	0.19808 ±	0.00024	0.00256 ±	0.00004	0.00081 ±	0.00087	0.000214 ±	0.000016	3.02E-14	98.53%	21.44361	497.56 ±	0.91	0.18%
au16.3k.mus.7a.txt	1.6	10	4.97006 ±	0.00401	0.23410 ±	0.00051	0.00289 ±	0.00004	-0.00247 ±	0.00091	0.000128 ±	0.000020	3.48E-14	99.24%	21.06776	489.92 ±	1.29	0.26%
au16.3k.mus.8a.txt	1.6	10	11.33782 ±	0.00319	0.52303 ±	0.00162	0.00643 ±	0.00008	0.01010 ±	0.00096	0.000162 ±	0.000017	7.94E-14	99.58%	21.58737	500.47 ±	1.58	0.31%
au16.3k.mus.9a.txt	1.6	10	5.08633 ±	0.00233	0.23315 ±	0.00044	0.00286 ±	0.00002	-0.00148 ±	0.00099	0.000038 ±	0.000021	3.56E-14	99.78%	21.76692	504.10 ±	1.16	0.23%
au16.3k.mus.10a.txt	1.6	10	0.85746 ±	0.00108	0.03991 ±	0.00027	0.00046 ±	0.00002	-0.00598 ±	0.00112	0.000004 ±	0.000010	6.01E-15	99.87%	21.44315	497.55 ±	3.82	0.77%
au16.3k.mus.11a.txt	1.6	10	3.91217 ±	0.00275	0.18262 ±	0.00042	0.00223 ±	0.00003	-0.00313 ±	0.00093	0.000039 ±	0.000010	2.74E-14	99.71%	21.35774	495.82 ±	1.26	0.25%
au16.3k.mus.12a.txt	1.6	10	3.27955 ±	0.00193	0.15381 ±	0.00043	0.00192 ±	0.00004	-0.00027 ±	0.00151	0.000055 ±	0.000010	2.30E-14	99.51%	21.21640	492.95 ±	1.47	0.30%
au16.3k.mus.13a.txt	1.6	10	6.21723 ±	0.00326	0.29279 ±	0.00077	0.00364 ±	0.00005	-0.00138 ±	0.00070	0.000227 ±	0.000010	4.35E-14	98.92%	21.00459	488.63 ±	1.35	0.28%
au16.3k.mus.14a.txt	1.6	10	0.01414 ±	0.00026	0.00078 ±	0.00003	0.00001 ±	0.00002	0.00478 ±	0.00123	0.000010 ±	0.000010	9.90E-17	81.43%	14.89041	359.52 ±	97.18	27.03%
au16.3k.mus.15a.txt	1.6	10	9.75664 ±	0.00547	0.45022 ±	0.00099	0.00572 ±	0.00007	-0.00153 ±	0.00138	0.000403 ±	0.000021	6.83E-14	98.78%	21.40614	496.80 ±	1.19	0.24%
au16.3k.mus.16a.txt	1.6	10	5.42251 ±	0.00506	0.25389 ±	0.00107	0.00309 ±	0.00003	0.00015 ±	0.00121	0.000094 ±	0.000009	3.80E-14	99.49%	21.24829	493.59 ±	2.16	0.44%
au16.3k.mus.17a.txt	1.6	10	6.01978 ±	0.00462	0.28057 ±	0.00061	0.00350 ±	0.00004	-0.00036 ±	0.00130	0.000074 ±	0.000016	4.22E-14	99.64%	21.37782	496.22 ±	1.22	0.25%
au16.3k.mus.18a.txt	1.6	10	6.65721 ±	0.00382	0.31287 ±	0.00083	0.00385 ±	0.00004	-0.00188 ±	0.00072	0.000150 ±	0.000020	4.66E-14	99.33%	21.13564	491.30 ±	1.41	0.29%
au16.3k.mus.19a.txt	1.6	10	7.69159 ±	0.00660	0.35756 ±	0.00055	0.00442 ±	0.00007	-0.00065 ±	0.00064	0.000069 ±	0.000018	5.39E-14	99.74%	21.45400	497.77 ±	0.94	0.19%
au16.3k.mus.20a.txt	1.6	10	8.52242 ±	0.00545	0.39367 ±	0.00057	0.00480 ±	0.00005	-0.00171 ±	0.00086	0.000111 ±	0.000009	5.97E-14	99.61%	21.56452	500.01 ±	0.81	0.16%
au16.3k.mus.21a.txt	1.6	10	9.75867 ±	0.00537	0.45078 ±	0.00073	0.00567 ±	0.00005	0.00062 ±	0.00111	0.000257 ±	0.000024	6.83E-14	99.22%	21.47974	498.29 ±	0.93	0.19%
au16.3k.mus.22a.txt	1.6	10	2.48489 ±	0.00236	0.11303 ±	0.00024	0.00143 ±	0.00002	0.00031 ±	0.00057	0.000078 ±	0.000011	1.74E-14	99.07%	21.78100	504.39 ±	1.36	0.27%
au16.3k.mus.23a.txt	1.6	10	2.92819 ±	0.00238	0.13764 ±	0.00055	0.00163 ±	0.00002	-0.00080 ±	0.00095	0.000022 ±	0.000019	2.05E-14	99.78%	21.22608	493.14 ±	2.22	0.45%
au16.3k.mus.24a.txt	1.6	10	6.11920 ±	0.00344	0.28726 ±	0.00068	0.00350 ±	0.00003	0.00104 ±	0.00084	0.000124 ±	0.000021	4.29E-14	99.40%	21.17423	492.09 ±	1.31	0.27%
au16.3k.mus.25a.txt	1.6	10	2.26728 ±	0.00179	0.10695 ±	0.00043	0.00132 ±	0.00002	0.00074 ±	0.00076	0.000038 ±	0.000016	1.59E-14	99.51%	21.09467	490.47 ±	2.28	0.46%
au16.3k.mus.26a.txt	1.6	10	0.10962 ±	0.00035	0.00447 ±	0.00005	0.00011 ±	0.00001	-0.00198 ±	0.00087	0.000090 ±	0.000015	7.68E-16	75.86%	18.55324	437.97 ±	24.69	5.64%
au16.3k.mus.27a.txt	1.6	10	3.30126 ±	0.00299	0.14743 ±	0.00035	0.00192 ±	0.00003	-0.00088 ±	0.00107	0.000070 ±	0.000015	2.31E-14	99.37%	22.25133	513.86 ±	1.49	0.29%
au16.3k.mus.28a.txt	1.6	10	1.15749 ±	0.00101	0.05321 ±	0.00016	0.00069 ±	0.00002	-0.00301 ±	0.00062	0.000060 ±	0.000019	8.11E-15	98.46%	21.41397	496.96 ±	2.96	0.59%
au16.3k.mus.29a.txt	1.6	10	11.46939 ±	0.00421	0.52221 ±	0.00128	0.00662 ±	0.00006	0.00530 ±	0.00105	0.000128 ±	0.000027	8.03E-14	99.67%	21.89205	506.63 ±	1.31	0.26%
au16.3k.mus.30a.txt	1.6	10	4.26052 ±	0.00243	0.19666 ±	0.00053	0.00252 ±	0.00004	-0.00357 ±	0.00107	0.000152 ±	0.000022	2.98E-14	98.95%	21.43541	497.39 ±	1.59	0.32%
au16.3k.mus.31a.txt	1.6	10	7.41509 ±	0.00417	0.34766 ±	0.00093	0.00440 ±	0.00005	0.00092 ±	0.00077	0.000041 ±	0.000021	5.19E-14	99.84%	21.29415	494.52 ±	1.41	0.28%
au16.3k.mus.32a.txt	1.6	10	3.24896 ±	0.00207	0.15412 ±	0.00031	0.00194 ±	0.00003	-0.00079 ±	0.00096	0.000009 ±	0.000016	2.28E-14	99.92%	21.06234	489.81 ±	1.28	0.26%
au16.3k.mus.33a.txt	1.6	10	4.42747 ±	0.00301	0.20390 ±	0.00052	0.00252 ±	0.00004	-0.00182 ±	0.00109	0.000024 ±	0.000015	3.10E-14	99.84%	21.67816	502.31 ±	1.42	0.28%
au16.3k.mus.34a.txt	1.6	10	1.52496 ±	0.00137	0.06983 ±	0.00032	0.00090 ±	0.00003	0.00056 ±	0.00105	0.000006 ±	0.000017	1.07E-14	99.89%	21.81214	505.02 ±	2.89	0.57%
au16.3k.mus.35a.txt	1.6	10	3.67062 ±	0.00312	0.16892 ±	0.00031	0.00210 ±	0.00003	0.00031 ±	0.00058	0.000039 ±	0.000018	2.57E-14	99.69%	21.66191	501.98 ±	1.26	0.25%
au16.3k.mus.36a.txt	1.6	10	6.45083 ±	0.00289	0.30339 ±	0.00047	0.00386 ±	0.00004	0.00101 ±	0.00071	0.000282 ±	0.000020	4.52E-14	98.71%	20.98851	488.31 ±	0.92	0.19%
au16.3k.mus.37a.txt	1.6	10	3.23628 ±	0.00272	0.15010 ±	0.00042	0.00185 ±	0.00004	0.00146 ±	0.00138	0.000057 ±	0.000017	2.27E-14	99.48%	21.44876	497.66 ±	1.65	0.33%
au16.3k.mus.38a.txt	1.6	10	3.58545 ±	0.00366	0.16957 ±	0.00054	0.00204 ±	0.00003	-0.00015 ±	0.00096	0.000141 ±	0.000021	2.51E-14	98.84%	20.89932	486.49 ±	1.84	0.38%
au16.3k.mus.39a.txt	1.6	10	3.36236 ±	0.00195	0.15424 ±	0.00058	0.00204 ±	0.00005	-0.00035 ±	0.00072	0.000098 ±	0.000018	2.35E-14	99.14%	21.61224	500.97 ±	2.06	0.41%
au16.3k.mus.40a.txt	1.6	10	3.51735 ±	0.00280	0.16432 ±	0.00054	0.00200 ±	0.00004	-0.00373 ±	0.00133	0.000065 ±	0.000016	2.46E-14	99.45%	21.28632	494.37 ±	1.81	0.37%
au16.3k.mus.41a.txt	1.6	10	2.25537 ±	0.00190	0.10362 ±	0.00036	0.00133 ±	0.00003	-0.00277 ±	0.00087	0.000054 ±	0.000021	1.58E-14	99.30%	21.61082	500.95 ±	2.28	0.46%
au16.3k.mus.42a.txt	1.6	10	1.99368 ±	0.00173	0.09422 ±	0.00050	0.00115 ±	0.00003	-0.00634 ±	0.00132	0.000006 ±	0.000016	1.40E-14	99.92%	21.13617	491.31 ±	2.90	0.59%
au16.3k.mus.43a.txt	1.6	10	1.71383 ±	0.00131	0.07918 ±	0.00025	0.00095 ±	0.00002	0.00136 ±	0.00119	0.000056 ±	0.000010	1.20E-14	99.05%	21.43963	497.48 ±	1.84	0.37%
au16.3k.mus.44a.txt	1.6	10	1.34337 ±	0.00180	0.06281 ±	0.00023	0.00073 ±	0.00003	-0.00098 ±	0.00089	0.000032 ±	0.000008	9.41E-15	99.30%	21.23556	493.33 ±	2.12	0.43%
au16.3k.mus.45a.txt	1.6	10	3.86397 ±	0.00265	0.17642 ±	0.00086	0.00212 ±	0.00004	0.00332 ±	0.00073	0.000066 ±	0.000009	2.71E-14	99.50%	21.79211	504.61 ±	2.53	0.50%
au16.3k.mus.46a.txt	1.6	10	2.40251 ±	0.00230	0.11171 ±	0.00031	0.00143 ±	0.00003	0.00238 ±	0.00125	0.000085 ±	0.000009	1.68E-14	98.96%	21.28448	494.33 ±	1.59	0.32%
au16.3k.mus.47a.txt	1.6	10	2.76488 ±	0.00341	0.13104 ±	0.00025	0.00163 ±	0.00004	0.00256 ±	0.00134	-0.000036 ±	0.000015	1.94E-14	100.39%	21.10083	490.59 ±	1.35	0.28%
au16.3k.mus.48a.txt	1.6	10	3.08162 ±	0.00432	0.14139 ±	0.00034	0.00183 ±	0.00005	0.00080 ±	0.00113	0.000135 ±	0.000010	2.16E-14	98.70%	21.51220	498.95 ±	1.49	0.30%
au16.3k.mus.49a.txt	1.6	10	2.48623 ±	0.00186	0.11716 ±	0.00054	0.00142 ±	0.00002	0.00163 ±	0.00092	0.000012 ±	0.000009	1.74E-14	99.86%	21.19133	492.44 ±	2.35	0.48%
au16.3k.mus.50a.txt	1.6	10	2.36771 ±	0.00225	0.11448 ±	0.00040	0.00134 ±	0.00002	-0.00620 ±	0.00255	0.000093 ±	0.000009	1.66E-14	98.84%	20.43764	477.04 ±	1.82	0.38%

APPENDIX 5(ii): $^{40}Ar/^{39}Ar$ Age data of detrital muscovite from the northwestern Bengal Basin (IK-06)

Blank			2.93485			0.29536			0.00129			0.00046			0.000069									
Sample	P	t	40 V			39 V			38 V			37 V			36 V			Moles 40Ar*	%Rad	R		Age (Ma)		%-sd
au16.3k.mus.51a.txt	1.6	10	2.69103	±	0.00230	0.12869	±	0.00051	0.00151	±	0.00003	-0.00222	±	0.00146	0.000006	±	0.000008	1.88E-14	99.93%	20.89553	486.41	±	2.01	0.41%
au16.3k.mus.52a.txt	1.6	10	2.50764	±	0.00226	0.11657	±	0.00033	0.00146	±	0.00002	-0.00011	±	0.00111	0.000163	±	0.000009	1.76E-14	98.08%	21.09887	490.55	±	1.60	0.33%
au16.3k.mus.53a.txt	1.6	10	1.46909	±	0.00228	0.06674	±	0.00014	0.00082	±	0.00004	-0.00076	±	0.00141	0.000063	±	0.000009	1.03E-14	98.73%	21.72979	503.35	±	1.61	0.32%
au16.3k.mus.54a.txt	1.6	10	2.05713	±	0.00233	0.09504	±	0.00031	0.00120	±	0.00002	-0.00010	±	0.00121	0.000091	±	0.000008	1.44E-14	98.69%	21.36239	495.91	±	1.83	0.37%
au16.3k.mus.55a.txt	1.6	10	2.15851	±	0.00222	0.09990	±	0.00024	0.00122	±	0.00003	0.00171	±	0.00114	0.000025	±	0.000009	1.51E-14	99.66%	21.53355	499.38	±	1.45	0.29%
au16.3k.mus.56a.txt	1.6	10	1.01013	±	0.00169	0.04606	±	0.00021	0.00055	±	0.00002	-0.00020	±	0.00096	0.000020	±	0.000008	7.07E-15	99.41%	21.80270	504.83	±	2.74	0.54%
au16.3k.mus.57a.txt	1.6	10	2.02291	±	0.00159	0.09491	±	0.00016	0.00120	±	0.00002	0.00018	±	0.00101	0.000055	±	0.000010	1.42E-14	99.20%	21.14423	491.48	±	1.15	0.23%
au16.3k.mus.58a.txt	1.6	10	2.13231	±	0.00160	0.09970	±	0.00036	0.00121	±	0.00003	0.00101	±	0.00171	0.000078	±	0.000010	1.49E-14	98.92%	21.15801	491.76	±	1.95	0.40%
au16.3k.mus.59a.txt	1.6	10	6.23890	±	0.00320	0.29536	±	0.00038	0.00363	±	0.00006	0.00021	±	0.00088	0.000066	±	0.000009	4.37E-14	99.69%	21.05729	489.71	±	0.72	0.15%
au16.3k.mus.60a.txt	1.6	10	2.93485	±	0.00277	0.14325	±	0.00051	0.00179	±	0.00004	-0.00037	±	0.00101	0.000072	±	0.000009	2.06E-14	99.27%	20.33815	475.00	±	1.83	0.39%
au16.3k.mus.61a.txt	1.6	10	8.10676	±	0.00457	0.38311	±	0.00053	0.00491	±	0.00005	-0.00136	±	0.00094	0.000162	±	0.000010	5.68E-14	99.41%	21.03545	489.26	±	0.75	0.15%
au16.3k.mus.62a.txt	1.6	10	0.68073	±	0.00092	0.03216	±	0.00021	0.00044	±	0.00002	0.00207	±	0.00123	0.000036	±	0.000008	4.77E-15	98.47%	20.84115	485.30	±	3.71	0.76%
au16.3k.mus.63a.txt	1.6	10	2.19476	±	0.00265	0.10176	±	0.00020	0.00126	±	0.00002	0.00186	±	0.00110	0.000041	±	0.000011	1.54E-14	99.46%	21.45167	497.72	±	1.35	0.27%
au16.3k.mus.64a.txt	1.6	10	2.35868	±	0.00247	0.10495	±	0.00035	0.00129	±	0.00003	0.00105	±	0.00131	0.000104	±	0.000013	1.65E-14	98.70%	22.18226	512.48	±	1.98	0.39%
au16.3k.mus.65a.txt	1.6	10	1.11526	±	0.00067	0.05226	±	0.00011	0.00062	±	0.00003	-0.00120	±	0.00092	0.000036	±	0.000010	7.81E-15	99.06%	21.13599	491.31	±	1.68	0.34%
au16.3k.mus.66a.txt	1.6	10	1.34557	±	0.00113	0.06250	±	0.00026	0.00078	±	0.00003	0.00136	±	0.00135	0.000022	±	0.000010	9.42E-15	99.53%	21.42946	497.27	±	2.35	0.47%
au16.3k.mus.67a.txt	1.6	10	1.62845	±	0.00206	0.07612	±	0.00035	0.00098	±	0.00002	0.00046	±	0.00099	0.000004	±	0.000014	1.14E-14	99.93%	21.37761	496.22	±	2.66	0.54%
au16.3k.mus.68a.txt	1.6	10	4.43745	±	0.00185	0.20849	±	0.00055	0.00255	±	0.00003	-0.00092	±	0.00106	0.000077	±	0.000017	3.11E-14	99.49%	21.17509	492.11	±	1.44	0.29%
au16.3k.mus.70a.txt	1.6	10	1.03036	±	0.00182	0.04685	±	0.00014	0.00061	±	0.00002	-0.00059	±	0.00097	0.000099	±	0.000010	7.22E-15	97.16%	21.36481	495.96	±	2.29	0.46%
au16.3k.mus.71a.txt	1.6	10	0.97506	±	0.00097	0.04510	±	0.00013	0.00061	±	0.00002	-0.00142	±	0.00086	0.000054	±	0.000014	6.83E-15	98.36%	21.26340	493.90	±	2.57	0.52%
au16.3k.mus.72a.txt	1.6	10	2.26867	±	0.00220	0.10402	±	0.00037	0.00132	±	0.00002	0.00188	±	0.00120	0.000069	±	0.000010	1.59E-14	99.11%	21.61566	501.04	±	2.01	0.40%
au16.3k.mus.73a.txt	1.6	10	2.00838	±	0.00112	0.09430	±	0.00036	0.00120	±	0.00002	0.00148	±	0.00092	0.000028	±	0.000009	1.41E-14	99.59%	21.21013	492.82	±	2.02	0.41%
au16.3k.mus.74a.txt	1.6	10	1.63446	±	0.00191	0.07767	±	0.00040	0.00098	±	0.00002	0.00127	±	0.00105	0.000033	±	0.000009	1.14E-14	99.42%	20.92228	486.96	±	2.68	0.55%
au16.3k.mus.75a.txt	1.6	10	1.09818	±	0.00129	0.05111	±	0.00031	0.00061	±	0.00003	-0.00287	±	0.00036	0.000057	±	0.000017	7.69E-15	98.47%	21.15281	491.65	±	3.87	0.79%
au16.3k.mus.76a.txt	1.6	10	1.12979	±	0.00124	0.05098	±	0.00014	0.00064	±	0.00003	-0.00108	±	0.00096	0.000067	±	0.000018	7.91E-15	98.26%	21.77297	504.22	±	2.80	0.55%
au16.3k.mus.77a.txt	1.6	10	1.17603	±	0.00097	0.05414	±	0.00013	0.00069	±	0.00002	-0.00123	±	0.00100	0.000027	±	0.000017	8.24E-15	99.31%	21.56967	500.11	±	2.53	0.51%
au16.3k.mus.78a.txt	1.6	10	1.52118	±	0.00148	0.06943	±	0.00033	0.00084	±	0.00003	0.00036	±	0.00139	-0.000005	±	0.000016	1.07E-14	100.09%	21.90954	506.98	±	2.89	0.57%
au16.3k.mus.79a.txt	1.6	10	0.94352	±	0.00086	0.04457	±	0.00017	0.00054	±	0.00003	-0.00130	±	0.00095	0.000042	±	0.000012	6.61E-15	98.67%	20.88582	486.21	±	2.60	0.53%
au16.3k.mus.81a.txt	1.6	10	1.68971	±	0.00173	0.07869	±	0.00040	0.00094	±	0.00003	-0.00119	±	0.00071	0.000044	±	0.000012	1.18E-14	99.23%	21.30685	494.78	±	2.80	0.57%
au16.3k.mus.82a.txt	1.6	10	1.33166	±	0.00126	0.06199	±	0.00019	0.00079	±	0.00003	0.00070	±	0.00114	0.000056	±	0.000013	9.33E-15	98.76%	21.21490	492.91	±	2.14	0.43%
au16.3k.mus.83a.txt	1.6	10	1.90687	±	0.00179	0.08882	±	0.00020	0.00112	±	0.00003	-0.00184	±	0.00098	0.000031	±	0.000009	1.34E-14	99.51%	21.36254	495.91	±	1.37	0.28%
au16.3k.mus.84a.txt	1.6	10	1.23083	±	0.00141	0.05515	±	0.00012	0.00068	±	0.00002	0.00077	±	0.00097	0.000028	±	0.000008	8.62E-15	99.34%	22.17320	512.29	±	1.61	0.31%
au16.3k.mus.85a.txt	1.6	10	2.48609	±	0.00230	0.11472	±	0.00038	0.00143	±	0.00003	0.00102	±	0.00112	0.000046	±	0.000010	1.74E-14	99.46%	21.55425	499.80	±	1.84	0.37%
au16.3k.mus.86a.txt	1.6	10	0.69339	±	0.00113	0.03207	±	0.00011	0.00041	±	0.00002	0.00305	±	0.00078	0.000011	±	0.000008	4.86E-15	99.58%	21.52912	499.29	±	2.56	0.51%
au16.3k.mus.87a.txt	1.6	10	1.20247	±	0.00186	0.05558	±	0.00014	0.00070	±	0.00003	0.00016	±	0.00130	0.000007	±	0.000008	8.42E-15	99.82%	21.59612	500.65	±	1.80	0.36%
au16.3k.mus.88a.txt	1.6	10	1.04471	±	0.00124	0.04896	±	0.00013	0.00063	±	0.00002	-0.00242	±	0.00126	0.000045	±	0.000012	7.32E-15	98.74%	21.06512	489.87	±	2.18	0.45%
au16.3k.mus.89a.txt	1.6	10	1.21026	±	0.00127	0.05581	±	0.00030	0.00069	±	0.00003	0.00063	±	0.00147	0.000022	±	0.000012	8.48E-15	99.46%	21.56942	500.11	±	3.07	0.61%
au16.3k.mus.90a.txt	1.6	10	0.32321	±	0.00041	0.01498	±	0.00008	0.00022	±	0.00002	0.00266	±	0.00099	0.000011	±	0.000011	2.26E-15	99.05%	21.37358	496.14	±	5.83	1.17%
au16.3k.mus.91a.txt	1.6	10	2.61466	±	0.00242	0.12303	±	0.00046	0.00154	±	0.00003	-0.00075	±	0.00071	0.000078	±	0.000011	1.83E-14	99.12%	21.06451	489.85	±	2.01	0.41%
au16.3k.mus.92a.txt	1.6	10	1.21291	±	0.00154	0.05620	±	0.00038	0.00069	±	0.00002	0.00084	±	0.00097	0.000006	±	0.000010	8.49E-15	99.86%	21.55225	499.76	±	3.63	0.73%
au16.3k.mus.93a.txt	1.6	10	1.23501	±	0.00108	0.05624	±	0.00019	0.00070	±	0.00003	-0.00037	±	0.00138	0.000038	±	0.000010	8.65E-15	99.09%	21.75901	503.94	±	2.10	0.42%
au16.3k.mus.94a.txt	1.6	10	1.63858	±	0.00150	0.07589	±	0.00030	0.00091	±	0.00003	-0.00090	±	0.00161	-0.000005	±	0.000017	1.15E-14	100.08%	21.59153	500.56	±	2.54	0.51%
au16.3k.mus.95a.txt	1.6	10	0.67783	±	0.00110	0.03141	±	0.00013	0.00035	±	0.00003	0.00110	±	0.00101	0.000013	±	0.000009	4.75E-15	99.45%	21.46177	497.93	±	2.94	0.59%
au16.3k.mus.96a.txt	1.6	10	0.79785	±	0.00093	0.03583	±	0.00018	0.00048	±	0.00003	0.00180	±	0.00118	0.000040	±	0.000010	5.59E-15	98.53%	21.94112	507.62	±	3.20	0.63%
au16.3k.mus.97a.txt	1.6	10	0.92059	±	0.00128	0.04262	±	0.00013	0.00052	±	0.00002	-0.00147	±	0.00074	0.000023	±	0.000008	6.45E-15	99.27%	21.43746	497.43	±	2.10	0.42%
au16.3k.mus.98a.txt	1.6	10	0.90401	±	0.00105	0.04151	±	0.00012	0.00051	±	0.00003	-0.00151	±	0.00107	0.000056	±	0.000012	6.33E-15	98.18%	21.38038	496.28	±	2.53	0.51%
au16.3k.mus.99a.txt	1.6	10	0.92501	±	0.00166	0.04189	±	0.00016	0.00053	±	0.00003	0.00211	±	0.00099	0.000046	±	0.000011	6.48E-15	98.55%	21.76183	504.00	±	2.80	0.55%
au16.3k.mus.100a.txt	1.6	10	2.33733	±	0.00241	0.10567	±	0.00018	0.00126	±	0.00003	-0.00199	±	0.00097	0.000028	±	0.000011	1.64E-14	99.64%	22.03798	509.57	±	1.23	0.24%
														IH										
au16.3k.mus.1a.txt	###	20	0.42320	±	0.00065	0.01390	±	0.00008	0.00029	±	0.00002	0.00077	±	0.00084	0.000411	±	0.000010	2.96E-15	71.30%	21.70579	502.87	±	6.24	1.24%
au16.3k.mus.1b.txt	###	20	3.45695	±	0.00318	0.15923	±	0.00037	0.00209	±	0.00003	0.00050	±	0.00108	0.000255	±	0.000013	2.42E-14	97.82%	21.23745	493.37	±	1.37	0.28%
au16.3k.mus.1c.txt	###	20	6.09611	±	0.00485	0.28130	±	0.00086	0.00353	±	0.00004	0.00252	±	0.00101	0.000039	±	0.000010	4.27E-14	99.82%	21.63163	501.37	±	1.60	0.32%
au16.3k.mus.1d.txt	###	20	8.04052	±	0.00520	0.37299	±	0.00065	0.00467	±	0.00005	0.00127	±	0.00124	0.000032	±	0.000009	5.63E-14	99.88%	21.53210	499.35	±	0.94	0.19%
au16.3k.mus.1e.txt	###	20	14.48149	±	0.00756	0.67273	±	0.00081	0.00847	±	0.00006	0.00819	±	0.00089	0.000055	±	0.000013	1.01E-13	99.89%	21.50338	498.77	±	0.67	0.13%
au16.3k.mus.1f.txt	###	20	19.66545	±	0.00826	0.90542	±	0.00175	0.01176	±	0.00008	0.00534	±	0.00057	0.000254	±	0.000014	1.38E-13	99.62%	21.63747	501.49	±	1.00	0.20%
au16.3k.mus.1g.txt	###	20	0.43098	±	0.00061	0.01870	±	0.00017	0.00029	±	0.00002	0.00117	±	0.00136	0.000016	±	0.000010	3.02E-15	98.94%	22.79802	524.82	±	6.05	1.15%
au16.3k.mus.1h.txt	###	20	2.83642	±	0.00193	0.13245	±	0.00048	0.00160	±	0.00004	-0.00033	±	0.00126	0.000002	±	0.000008	1.99E-14	99.98%	21.41027	496.88	±	1.87	0.38%

APPENDIX 6(i): $^{40}Ar/^{39}Ar$ Age data of detrital muscovite from the northwestern Bengal Basin (IK-14)

Blank			7.43121		0.45754		0.00390		0.00472		0.000281							
Sample	P	t	40 V		39 V		38 V		37 V		36 V		Moles 40Ar*	%Rad	R	Age (Ma)		%-sd
au16.4a.mus.6a.txt	1.6	10	2.57311 ±	0.00317	0.01885 ±	0.00007	0.00041 ±	0.00002	0.00055 ±	0.00120	0.000541 ±	0.000012	1.80E-14	93.79%	128.00563	1918.18 ±	8.26	0.43%
au16.4a.mus.7a.txt	1.6	10	13.00473 ±	0.00924	0.57643 ±	0.00142	0.00726 ±	0.00005	0.01242 ±	0.00096	0.000487 ±	0.000018	9.11E-14	98.90%	22.31366	515.12 ±	1.35	0.26%
au16.4a.mus.8a.txt	1.6	10	9.67184 ±	0.00624	0.42751 ±	0.00073	0.00538 ±	0.00007	0.00240 ±	0.00166	0.000463 ±	0.000012	6.77E-14	98.59%	22.30455	514.93 ±	0.98	0.19%
au16.4a.mus.split.9a	1.6	10	17.92870 ±	0.00860	0.77999 ±	0.00130	0.00980 ±	0.00011	0.01091 ±	0.00139	0.000291 ±	0.000015	1.26E-13	99.53%	22.87700	526.39 ±	0.93	0.18%
au16.4a.mus.10a.txt	1.6	10	6.37024 ±	0.00746	0.23607 ±	0.00036	0.00297 ±	0.00005	0.00005 ±	0.00097	0.000135 ±	0.000012	4.46E-14	99.37%	26.81547	603.33 ±	1.22	0.20%
au16.4a.mus.11a.txt	1.6	10	13.21514 ±	0.00277	0.56346 ±	0.00108	0.00712 ±	0.00008	0.00803 ±	0.00099	0.000500 ±	0.000016	9.25E-14	98.89%	23.19278	532.68 ±	1.06	0.20%
au16.4a.mus.12a.txt	1.6	10	4.89846 ±	0.00238	0.18114 ±	0.00040	0.00223 ±	0.00003	-0.00137 ±	0.00089	0.000150 ±	0.000012	3.43E-14	99.10%	26.79747	602.98 ±	1.44	0.24%
au16.4a.mus.14a.txt	1.6	10	2.99414 ±	0.00215	0.11345 ±	0.00028	0.00321 ±	0.00003	0.00264 ±	0.00137	0.002171 ±	0.000018	2.10E-14	78.59%	20.74011	483.24 ±	1.93	0.40%
au16.4a.mus.15a.txt	1.6	10	6.00233 ±	0.00618	0.27040 ±	0.00074	0.00343 ±	0.00004	0.00211 ±	0.00069	0.000300 ±	0.000020	4.20E-14	98.52%	21.87028	506.19 ±	1.58	0.31%
au16.4a.mus.16a.txt	1.6	10	10.36474 ±	0.00601	0.46012 ±	0.00036	0.00586 ±	0.00005	0.00304 ±	0.00137	0.000665 ±	0.000018	7.26E-14	98.11%	22.10007	510.82 ±	0.57	0.11%
au16.4a.mus.17a.txt	1.6	10	3.67241 ±	0.00254	0.14229 ±	0.00031	0.00175 ±	0.00003	-0.00361 ±	0.00137	0.000047 ±	0.000010	2.57E-14	99.62%	25.70957	582.06 ±	1.41	0.24%
au16.4a.mus.18a.txt	1.6	10	7.43121 ±	0.00385	0.33216 ±	0.00048	0.00403 ±	0.00006	-0.00434 ±	0.00074	0.000256 ±	0.000010	5.20E-14	98.98%	22.14407	511.71 ±	0.82	0.16%
au16.4a.mus.19a.txt	1.6	10	7.71518 ±	0.00470	0.34524 ±	0.00070	0.00434 ±	0.00005	-0.00302 ±	0.00123	0.000528 ±	0.000012	5.40E-14	97.98%	21.89460	506.68 ±	1.12	0.22%
au16.4a.mus.20a.txt	1.6	10	11.04709 ±	0.00380	0.45754 ±	0.00106	0.00571 ±	0.00008	0.00472 ±	0.00060	0.000233 ±	0.000015	7.74E-14	99.38%	23.99513	548.57 ±	1.31	0.24%
au16.4a.mus.21a.txt	1.6	10	7.44559 ±	0.00505	0.35142 ±	0.00083	0.00433 ±	0.00005	-0.00244 ±	0.00093	0.000057 ±	0.000010	5.21E-14	99.77%	21.13862	491.36 ±	1.23	0.25%
au16.4a.mus.22a.txt	1.6	10	2.87839 ±	0.00276	0.12452 ±	0.00022	0.00156 ±	0.00002	-0.00005 ±	0.00142	0.000036 ±	0.000017	2.02E-14	99.63%	23.03126	529.47 ±	1.41	0.27%
au16.4a.mus.23a.txt	1.6	10	3.76540 ±	0.00273	0.15630 ±	0.00042	0.00189 ±	0.00004	0.00059 ±	0.00084	0.000138 ±	0.000010	2.64E-14	98.92%	23.83024	545.32 ±	1.60	0.29%
au16.4a.mus.24a.txt	1.6	10	7.53270 ±	0.00400	0.30818 ±	0.00072	0.00390 ±	0.00005	0.00080 ±	0.00117	0.000281 ±	0.000012	5.28E-14	98.90%	24.17317	552.08 ±	1.35	0.25%
au16.4a.mus.25a.txt	1.6	10	3.05638 ±	0.00316	0.12046 ±	0.00040	0.00178 ±	0.00003	0.00397 ±	0.00120	0.000590 ±	0.000016	2.14E-14	94.30%	23.92829	547.25 ±	2.20	0.40%
au16.4a.mus.26a.txt	1.6	10	1.36864 ±	0.00099	0.05657 ±	0.00025	0.00092 ±	0.00003	0.00173 ±	0.00082	0.000596 ±	0.000014	9.59E-15	87.15%	21.08494	490.27 ±	3.12	0.64%
au16.4a.mus.27a.txt	1.6	10	3.55335 ±	0.00277	0.15710 ±	0.00047	0.00204 ±	0.00004	0.00058 ±	0.00124	0.000099 ±	0.000016	2.49E-14	99.17%	22.43116	517.47 ±	1.75	0.34%
au16.4a.mus.28a.txt	1.6	10	1.95046 ±	0.00229	0.08519 ±	0.00022	0.00122 ±	0.00005	0.00066 ±	0.00122	0.000055 ±	0.000012	1.37E-14	99.16%	22.70526	522.96 ±	1.81	0.35%
au16.4a.mus.29a.txt	1.6	10	2.61601 ±	0.00254	0.10110 ±	0.00023	0.00140 ±	0.00004	0.00083 ±	0.00117	0.000173 ±	0.000010	1.83E-14	98.05%	25.37126	575.50 ±	1.58	0.27%
au16.4a.mus.30a.txt	1.6	10	2.52867 ±	0.00261	0.11374 ±	0.00043	0.00146 ±	0.00003	0.00292 ±	0.00147	0.000131 ±	0.000009	1.77E-14	98.47%	21.89295	506.65 ±	2.09	0.41%
au16.4a.mus.31a.txt	1.6	10	3.86735 ±	0.00412	0.14797 ±	0.00033	0.00189 ±	0.00004	0.00272 ±	0.00152	0.000137 ±	0.000010	2.71E-14	98.96%	25.86311	585.02 ±	1.54	0.26%
au16.4a.mus.33a.txt	1.6	10	6.15197 ±	0.00308	0.28123 ±	0.00038	0.00353 ±	0.00003	-0.00331 ±	0.00101	0.000323 ±	0.000011	4.31E-14	98.45%	21.53386	499.39 ±	0.78	0.16%
au16.4a.mus.34a.txt	1.6	10	5.65532 ±	0.00372	0.26721 ±	0.00082	0.00338 ±	0.00004	-0.00269 ±	0.00118	0.000091 ±	0.000010	3.96E-14	99.53%	21.06295	489.82 ±	1.56	0.32%
au16.4a.mus.35a.txt	1.6	10	3.18085 ±	0.00233	0.12821 ±	0.00037	0.00160 ±	0.00003	-0.00180 ±	0.00108	0.000079 ±	0.000009	2.23E-14	99.26%	24.62610	560.97 ±	1.75	0.31%
au16.4a.mus.36a.txt	1.6	10	2.76648 ±	0.00297	0.10105 ±	0.00032	0.00129 ±	0.00003	-0.00250 ±	0.00088	0.000097 ±	0.000010	1.94E-14	98.96%	27.09045	608.58 ±	2.15	0.35%
au16.4a.mus.37a.txt	1.6	10	1.40965 ±	0.00182	0.06093 ±	0.00016	0.00076 ±	0.00003	-0.00256 ±	0.00057	0.000028 ±	0.000010	9.87E-15	99.40%	22.99424	528.73 ±	1.90	0.36%
au16.4a.mus.38a.txt	1.6	10	0.03897 ±	0.00049	0.00166 ±	0.00006	0.00000 ±	0.00002	0.00197 ±	0.00115	0.000009 ±	0.000010	2.73E-16	93.58%	21.97479	508.30 ±	44.84	8.82%
au16.4a.mus.39a.txt	1.6	10	1.66253 ±	0.00147	0.06821 ±	0.00013	0.00087 ±	0.00003	-0.00134 ±	0.00162	0.000070 ±	0.000011	1.16E-14	98.76%	24.07064	550.06 ±	1.58	0.29%
au16.4a.mus.40a.txt	1.6	10	6.46966 ±	0.00242	0.24766 ±	0.00056	0.00313 ±	0.00003	0.00022 ±	0.00094	0.000075 ±	0.000011	4.53E-14	99.66%	26.03383	588.32 ±	1.38	0.24%
au16.4a.mus.39a.txt	1.6	10	1.66253 ±	0.00147	0.06821 ±	0.00013	0.00087 ±	0.00003	-0.00134 ±	0.00162	0.000070 ±	0.000011	1.16E-14	98.76%	24.07064	550.06 ±	1.58	0.29%
au16.4a.mus.42a.txt	1.6	10	0.07441 ±	0.00038	0.00104 ±	0.00004	0.00002 ±	0.00002	-0.00088 ±	0.00092	0.000004 ±	0.000010	5.21E-16	98.41%	70.05060	1283.96 ±	76.19	5.93%
au16.4a.mus.43a.txt	1.6	10	0.71389 ±	0.00134	0.02645 ±	0.00010	0.00034 ±	0.00001	0.00270 ±	0.00099	0.000045 ±	0.000009	5.00E-15	98.15%	26.49044	597.10 ±	3.36	0.56%
au16.4a.mus.44a.txt	1.6	10	0.06261 ±	0.00059	0.00338 ±	0.00006	0.00008 ±	0.00002	0.00662 ±	0.00068	0.000070 ±	0.000008	4.38E-16	67.66%	12.5652	307.8895 ±	19.25458	6.25%
au16.4a.mus.45a.txt	1.6	10	1.41195 ±	0.00124	0.06201 ±	0.00025	0.00075 ±	0.00002	0.00233 ±	0.00082	0.000030 ±	0.000010	9.89E-15	99.39%	22.63320	521.52 ±	2.40	0.46%
au16.4a.mus.46a.txt	1.6	10	4.97951 ±	0.00432	0.20248 ±	0.00057	0.00254 ±	0.00003	0.00368 ±	0.00123	0.000131 ±	0.000019	3.49E-14	99.23%	24.40331	556.60 ±	1.76	0.32%
au16.4a.mus.47a.txt	1.6	10	0.45956 ±	0.00088	0.02272 ±	0.00012	0.00040 ±	0.00002	0.00347 ±	0.00096	0.000326 ±	0.000014	3.22E-15	79.08%	15.99622	383.57 ±	5.08	1.33%
au16.4a.mus.48a.txt	1.6	10	2.92421 ±	0.00381	0.11867 ±	0.00012	0.00154 ±	0.00002	-0.00520 ±	0.00181	0.000185 ±	0.000012	2.05E-14	98.13%	24.17708	552.15 ±	1.14	0.21%
au16.4a.mus.48a.txt	1.6	10	2.92421 ±	0.00381	0.11867 ±	0.00012	0.00154 ±	0.00002	-0.00520 ±	0.00181	0.000185 ±	0.000012	2.05E-14	98.13%	24.17708	552.15 ±	1.14	0.21%
au16.4a.mus.50a.txt	1.6	10	5.82361 ±	0.00369	0.25900 ±	0.00083	0.00323 ±	0.00005	-0.00005 ±	0.00064	0.000091 ±	0.000011	4.08E-14	99.54%	22.38178	516.48 ±	1.72	0.33%
au16.4a.mus.51a.txt	1.6	10	7.77282 ±	0.00122	0.35132 ±	0.00082	0.00433 ±	0.00006	-0.00094 ±	0.00135	0.000081 ±	0.000012	5.44E-14	99.69%	22.05609	509.94 ±	1.22	0.24%
au16.4a.mus.52a.txt	1.6	10	0.00735 ±	0.00028	0.00015 ±	0.00005	-0.00002 ±	0.00002	-0.00116 ±	0.00147	0.000018 ±	0.000011	5.15E-17	27.19%	13.00977	317.88 ±	741.13	233.15%
au16.4a.mus.53a.txt	1.6	10	0.03409 ±	0.00029	0.00053 ±	0.00004	0.00002 ±	0.00002	-0.00095 ±	0.00082	0.000096 ±	0.000009	2.39E-16	16.98%	10.71223	265.66 ±	202.79	76.33%
au16.4a.mus.54a.txt	1.6	10	0.46856 ±	0.00060	0.01895 ±	0.00008	0.00043 ±	0.00003	0.00158 ±	0.00135	0.000286 ±	0.000013	3.28E-15	81.98%	20.27518	473.71 ±	5.27	1.11%
au16.4a.mus.55a.txt	1.6	10	2.46091 ±	0.00218	0.09455 ±	0.00024	0.00118 ±	0.00004	0.00122 ±	0.00116	0.000087 ±	0.000011	1.72E-14	98.96%	25.75854	583.00 ±	1.77	0.30%
au16.4a.mus.56a.txt	1.6	10	1.53124 ±	0.00177	0.06209 ±	0.00017	0.00078 ±	0.00002	0.00324 ±	0.00097	0.000040 ±	0.000012	1.07E-14	99.25%	24.47889	558.08 ±	2.11	0.38%
au16.4a.mus.57a.txt	1.6	10	1.85723 ±	0.00147	0.08290 ±	0.00034	0.00103 ±	0.00002	0.00237 ±	0.00106	0.000065 ±	0.000012	1.30E-14	98.97%	22.17309	512.29 ±	2.37	0.46%

APPENDIX 6(ii): $^{40}Ar/^{39}Ar$ Age data of detrital muscovite from the northwestern Bengal Basin (IK-14)

Blank			0.55571			0.02182			0.00049			0.00088			0.000064									
Sample	P	t	40 V			39 V			38 V			37 V			36 V			Moles 40Ar*	%Rad	R		Age (Ma)		%-sd
au16.4a.mus.58a.txt	1.6	10	0.66123	±	0.00069	0.02775	±	0.00011	0.00033	±	0.00002	0.00283	±	0.00094	0.000055	±	0.000012	4.63E-15	97.56%	23.24922	533.81	±	3.68	0.69%
au16.4a.mus.59a.txt	1.6	10	0.05844	±	0.00030	0.00254	±	0.00005	0.00005	±	0.00002	0.00257	±	0.00089	0.000018	±	0.000009	4.09E-16	91.02%	20.93563	487.23	±	26.97	5.53%
au16.4a.mus.60a.txt	1.6	10	1.72482	±	0.00143	0.06427	±	0.00015	0.00083	±	0.00003	0.00339	±	0.00135	0.000002	±	0.000010	1.21E-14	99.98%	26.83361	603.68	±	1.80	0.30%
au16.4a.mus.61a.txt	1.6	10	0.07101	±	0.00039	0.00198	±	0.00004	0.00001	±	0.00002	-0.00032	±	0.00142	0.000044	±	0.000011	4.97E-16	81.62%	29.32151	650.63	±	41.94	6.45%
au16.4a.mus.62a.txt	1.6	10	1.71775	±	0.00178	0.07624	±	0.00020	0.00096	±	0.00002	0.00151	±	0.00064	-0.000009	±	0.000020	1.20E-14	100.17%	22.53320	519.52	±	2.32	0.45%
au16.4a.mus.63a.txt	1.6	10	0.13119	±	0.00055	0.00578	±	0.00004	0.00009	±	0.00002	0.00345	±	0.00087	0.000020	±	0.000010	9.19E-16	95.65%	21.70269	502.80	±	12.51	2.49%
au16.4a.mus.64a.txt	1.6	10	3.01917	±	0.00190	0.12938	±	0.00052	0.00176	±	0.00005	0.00455	±	0.00121	0.000099	±	0.000011	2.11E-14	99.04%	23.11142	531.07	±	2.27	0.43%
au16.4a.mus.65a.txt	1.6	10	0.55571	±	0.00091	0.02404	±	0.00019	0.00033	±	0.00002	0.00244	±	0.00114	-0.000052	±	0.000015	3.89E-15	102.82%	23.12698	531.38	±	6.07	1.14%
au16.4a.mus.66a.txt	1.6	10	0.67273	±	0.00096	0.02292	±	0.00010	0.00029	±	0.00002	0.00220	±	0.00083	0.000053	±	0.000010	4.71E-15	97.72%	28.68060	638.65	±	4.28	0.67%
au16.4a.mus.67a.txt	1.6	10	0.52497	±	0.00091	0.02182	±	0.00007	0.00030	±	0.00002	-0.00134	±	0.00097	0.000014	±	0.000021	3.68E-15	99.22%	23.86743	546.05	±	6.92	1.27%
au16.4a.mus.68a.txt	1.6	10	2.37983	±	0.00258	0.09159	±	0.00019	0.00117	±	0.00004	0.00218	±	0.00101	0.000069	±	0.000011	1.67E-14	99.16%	25.76464	583.12	±	1.58	0.27%
au16.4a.mus.69a.txt	1.6	10	0.54775	±	0.00117	0.02361	±	0.00008	0.00022	±	0.00002	-0.00399	±	0.00079	0.000087	±	0.000016	3.84E-15	95.30%	22.09076	510.63	±	5.01	0.98%
au16.4a.mus.70a.txt	1.6	10	0.57841	±	0.00078	0.02603	±	0.00016	0.00033	±	0.00002	-0.00043	±	0.00090	0.000053	±	0.000015	4.05E-15	97.29%	21.61243	500.98	±	5.20	1.04%
au16.4a.mus.71a.txt	1.6	10	2.75526	±	0.00253	0.10112	±	0.00018	0.00126	±	0.00003	-0.00198	±	0.00086	0.000156	±	0.000016	1.93E-14	98.32%	26.78978	602.84	±	1.63	0.27%
au16.4a.mus.72a.txt	1.6	10	1.97184	±	0.00159	0.08706	±	0.00022	0.00104	±	0.00003	-0.00237	±	0.00094	0.000064	±	0.000016	1.38E-14	99.04%	22.42809	517.41	±	1.89	0.37%
au16.4a.mus.73a.txt	1.6	10	0.05903	±	0.00040	0.00312	±	0.00004	0.00005	±	0.00002	-0.00154	±	0.00087	0.000072	±	0.000016	4.13E-16	64.19%	12.10230	297.43	±	38.83	13.05%
au16.4a.mus.75a.txt	1.6	10	1.03755	±	0.00091	0.03565	±	0.00018	0.00049	±	0.00003	-0.00190	±	0.00084	0.000122	±	0.000010	7.27E-15	96.53%	28.09163	627.57	±	3.76	0.60%
au16.4a.mus.76a.txt	1.6	10	2.35224	±	0.00175	0.08625	±	0.00040	0.00094	±	0.00005	0.00088	±	0.00071	0.000031	±	0.000009	1.65E-14	99.61%	27.16890	610.08	±	2.94	0.48%
au16.4a.mus.77a.txt	1.6	10	0.89350	±	0.00127	0.04058	±	0.00032	0.00050	±	0.00003	-0.00085	±	0.00118	0.000055	±	0.000010	6.26E-15	98.20%	21.61688	501.07	±	4.37	0.87%
au16.4a.mus.78a.txt	1.6	10	6.02933	±	0.00304	0.26337	±	0.00060	0.00331	±	0.00004	0.00065	±	0.00112	-0.000004	±	0.000015	4.22E-14	100.02%	22.89300	526.71	±	1.30	0.25%
au16.4a.mus.79a.txt	1.6	10	1.59795	±	0.00115	0.07204	±	0.00046	0.00085	±	0.00003	-0.00257	±	0.00076	0.000040	±	0.000010	1.12E-14	99.26%	22.01249	509.06	±	3.43	0.67%
au16.4a.mus.81a.txt	1.6	10	0.65837	±	0.00095	0.02908	±	0.00011	0.00038	±	0.00002	0.00174	±	0.00102	0.000047	±	0.000010	4.61E-15	97.91%	22.16563	512.14	±	3.20	0.62%
au16.4a.mus.82a.txt	1.6	10	1.43342	±	0.00139	0.06524	±	0.00033	0.00080	±	0.00002	-0.00048	±	0.00140	0.000018	±	0.000010	1.00E-14	99.64%	21.88904	506.57	±	2.79	0.55%
au16.4a.mus.83a.txt	1.6	10	0.79669	±	0.00131	0.03512	±	0.00013	0.00043	±	0.00002	0.00066	±	0.00117	0.000033	±	0.000011	5.58E-15	98.79%	22.41258	517.10	±	3.02	0.58%
au16.4a.mus.84a.txt	1.6	10	1.68440	±	0.00197	0.06750	±	0.00015	0.00082	±	0.00003	-0.00032	±	0.00066	0.000067	±	0.000011	1.18E-14	98.83%	24.66289	561.69	±	1.83	0.33%
au16.4a.mus.85a.txt	1.6	10	0.61840	±	0.00132	0.02706	±	0.00014	0.00037	±	0.00001	-0.00459	±	0.00088	0.000039	±	0.000019	4.33E-15	98.11%	22.40259	516.90	±	5.67	1.10%
au16.4a.mus.86a.txt	1.6	10	0.14410	±	0.00041	0.00610	±	0.00008	0.00009	±	0.00002	-0.00022	±	0.00079	0.000022	±	0.000010	1.01E-15	95.59%	22.57539	520.36	±	13.52	2.60%
au16.4a.mus.87a.txt	1.6	10	0.13588	±	0.00043	0.00259	±	0.00005	0.00011	±	0.00002	-0.00183	±	0.00072	0.000271	±	0.000011	9.52E-16	41.14%	21.47684	498.23	±	40.14	8.06%
au16.4a.mus.89a.txt	1.6	10	1.12485	±	0.00150	0.05235	±	0.00018	0.00066	±	0.00003	-0.00241	±	0.00081	0.000045	±	0.000009	7.88E-15	98.82%	21.22947	493.21	±	2.18	0.44%
au16.4a.mus.90a.txt	1.6	10	0.93034	±	0.00099	0.03994	±	0.00011	0.00047	±	0.00002	0.00071	±	0.00069	0.000042	±	0.000011	6.52E-15	98.68%	22.98646	528.58	±	2.36	0.45%
au16.4a.mus.91a.txt	1.6	10	2.04314	±	0.00127	0.09105	±	0.00024	0.00109	±	0.00003	0.00038	±	0.00116	0.000077	±	0.000010	1.43E-14	98.89%	22.19079	512.65	±	1.57	0.31%
au16.4a.mus.92a.txt	1.6	10	0.72039	±	0.00144	0.03116	±	0.00014	0.00038	±	0.00002	0.00306	±	0.00166	-0.000005	±	0.000009	5.05E-15	100.23%	23.13083	531.45	±	3.34	0.63%
au16.4a.mus.93a.txt	1.6	10	0.36024	±	0.00056	0.01446	±	0.00007	0.00019	±	0.00002	0.00073	±	0.00101	0.000102	±	0.000010	2.52E-15	91.62%	22.82190	525.29	±	5.59	1.06%
au16.4a.mus.94a.txt	1.6	10	4.89028	±	0.00242	0.17748	±	0.00081	0.00229	±	0.00002	0.00115	±	0.00130	0.000684	±	0.000014	3.42E-14	95.87%	26.41575	595.67	±	2.89	0.49%
au16.4a.mus.95a.txt	1.6	10	0.42102	±	0.00063	0.01637	±	0.00008	0.00019	±	0.00002	0.00272	±	0.00101	0.000006	±	0.000009	2.95E-15	99.64%	25.62988	580.51	±	4.70	0.81%
au16.4a.mus.96a.txt	1.6	10	0.67522	±	0.00121	0.02823	±	0.00011	0.00035	±	0.00002	0.00144	±	0.00099	0.000059	±	0.000012	4.73E-15	97.45%	23.31179	535.05	±	3.66	0.68%
au16.4a.mus.97a.txt	1.6	10	0.73199	±	0.00082	0.02590	±	0.00012	0.00031	±	0.00002	0.00115	±	0.00080	0.000015	±	0.000010	5.13E-15	99.40%	28.09511	627.64	±	4.04	0.64%
au16.4a.mus.98a.txt	1.6	10	0.32969	±	0.00045	0.01367	±	0.00010	0.00017	±	0.00002	0.00018	±	0.00084	0.000003	±	0.000011	2.31E-15	99.69%	24.05120	549.68	±	6.64	1.21%
au16.4a.mus.99a.txt	1.6	10	1.82174	±	0.00189	0.08262	±	0.00031	0.00106	±	0.00002	0.00030	±	0.00140	0.000053	±	0.000011	1.28E-14	99.14%	21.85984	505.98	±	2.18	0.43%
au16.4a.mus.100a.txt	1.6	10	0.23747	±	0.00045	0.00918	±	0.00004	0.00007	±	0.00004	0.00168	±	0.00101	0.000155	±	0.000011	1.66E-15	80.82%	20.91162	486.74	±	8.98	1.84%
au16.4a.mus.103a.txt	1.6	10	0.48828	±	0.00074	0.02128	±	0.00011	0.00028	±	0.00002	-0.00216	±	0.00118	0.000022	±	0.000010	3.42E-15	98.67%	22.63317	521.52	±	4.42	0.85%
au16.4a.mus.104a.txt	1.6	10	2.29727	±	0.00162	0.10180	±	0.00039	0.00134	±	0.00004	-0.00034	±	0.00128	0.000075	±	0.000011	1.61E-14	99.03%	22.34725	515.79	±	2.14	0.41%
au16.4a.mus.105a.txt	1.6	10	1.62859	±	0.00196	0.05399	±	0.00019	0.00069	±	0.00002	-0.00159	±	0.00096	0.000013	±	0.000011	1.14E-14	99.76%	30.09204	664.93	±	2.82	0.42%
au16.4a.mus.106a.txt	1.6	10	0.24665	±	0.00027	0.01050	±	0.00006	0.00015	±	0.00002	-0.00005	±	0.00165	0.000026	±	0.000011	1.73E-15	96.94%	22.76583	524.17	±	7.58	1.45%
au16.4a.mus.107a.txt	1.6	10	0.00577	±	0.00025	0.00011	±	0.00004	0.00000	±	0.00002	-0.00235	±	0.00099	0.000018	±	0.000010	4.04E-17	7.82%	2.38750	62.69	±	1015.19	1619.43%
au16.4a.mus.01a.txt	1.6	10	2.98232	±	0.00206	0.12858	±	0.00045	0.00165	±	0.00003	0.00046	±	0.00084	0.000193	±	0.000012	2.09E-14	98.09%	22.75183	523.89	±	2.00	0.38%
au16.4a.mus.02a.txt	1.6	10	0.05095	±	0.00038	0.00193	±	0.00004	0.00001	±	0.00002	-0.00186	±	0.00089	0.000031	±	0.000010	3.57E-16	81.76%	21.44848	497.66	±	38.38	7.71%
au16.4a.mus.03a.txt	1.6	10	0.30503	±	0.00042	0.01350	±	0.00007	0.00016	±	0.00003	-0.00332	±	0.00102	0.000022	±	0.000009	2.14E-15	97.85%	22.07848	510.39	±	5.47	1.07%
au16.4a.mus.05a.txt	1.6	10	1.44307	±	0.00175	0.05693	±	0.00022	0.00071	±	0.00002	-0.00059	±	0.00142	0.000006	±	0.000010	1.01E-14	99.88%	25.31827	574.47	±	2.57	0.45%

APPENDIX 7: Photomicrographs of detrital muscovite grains analyzed for argon datin.

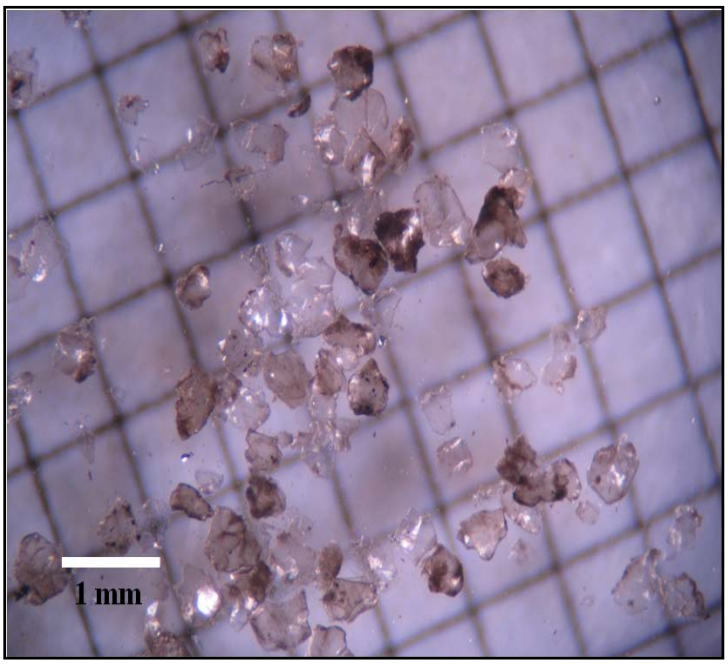

Sample IK 02 (Well GDH 46, Gondwanan Group, Khalashpir, northwestern Bengal Basin)

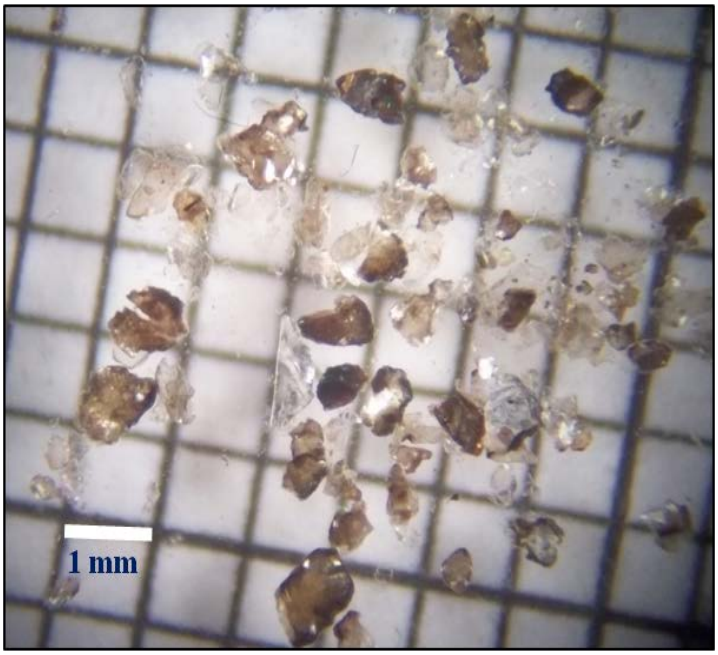

Sample IK 14 (Well GDH 46, Gondwanan Group, Khalashpir, northwestern Bengal Basin)